Article:

Lebedeva, MA, Chamberlain, TW and Khlobystov, AN (2015) Harnessing the Synergistic and Complementary Properties of Fullerene and Transition-Metal Compounds for Nanomaterial Applications. Chemical Reviews, 115 (20). 11301 - 11351. ISSN 0009-2665

https://doi.org/10.1021/acs.chemrev.5b00005

Harnessing the synergistic and complementary properties of fullerene and transition metal compounds for nanomaterial applications.

Maria A. Lebedeva[a], Thomas W. Chamberlain[a], and Andrei N. Khlobystov*[a,b].

[a]School of Chemistry, University of Nottingham, Nottingham, NG7 2RD, UK

[b]Nottingham Nanotechnology & Nanoscience Centre, University of Nottingham, University Park, Nottingham, NG7 2RD, UK.

Email: Andrei N. Khlobystov – andrei.khlobystov@nottingham.ac.uk

Contents

1. Introduction.

C_{60} fullerene is an icosahedral shaped nanosized molecule and is a useful building block to form various ordered functional nanostructures due to its size, shape and physicochemical properties. To date fullerenes have found application in various fields such as the preparation of novel materials for molecular electronic devices and sensors,[1] spintronic[2] and photovoltaic[3] devices, liquid crystalline mesomorphic materials[4] and protective films[5] as well as materials for medical applications such as drug delivery,[6] imaging,[7] photodynamic[8] and radiotherapy.[9] Chemical functionalisation of the fullerene cage can be easily achieved allowing the introduction of various functional groups which can both help to control and manipulate the fullerene molecules and tune the properties of the resulting hybrid compounds.[10] The combination of fullerene cages with transition metal complexes which are known to possess a variety of functional properties such as electron donating and electron accepting capacity, intense light absorption, magnetism and catalytic activity is a diverse strategy which can enhance and tune the properties of the resulting fullerene-containing compound. This route allows the formation of materials which display hybrid properties whilst retaining the characteristic features of the individual building blocks.

C_{60}, the most abundant fullerene, is an electron deficient polyolefin, spherical in shape with a crystallographic diameter of 0.7 nm and van der Waals diameter of 1 nm (Figure 1, top). It has a triply degenerate low-lying LUMO (Figure 1, bottom) and hence is an excellent electron acceptor able to accommodate up to 6 electrons per molecule.[11] The electronic spectra of C_{60} fullerene show several strong absorptions between 190 and 410 nm as well as some forbidden transitions in the visible region.[12] Due to its excellent light-harvesting ability C_{60} fullerene can be easily photoexcited at different wavelengths forming a singlet excited state ($^1C_{60}$*) which then relaxes into the triplet excited state ($^3C_{60}$*), both of which exhibit characteristic absorption spectra.[13]

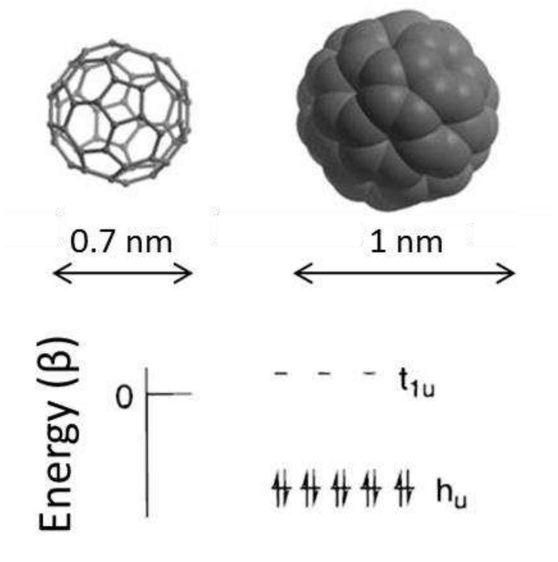

Figure 1. Crystallographic and van der Waals dimensions and molecular orbital diagram of C_{60} fullerene, illustrating its nanoscopic size and electron accepting ability respectively.[14]

Transition metal complexes which generally tend to be good electron donors and also excellent light acceptors are ideal candidates to combine with the fullerene cage to form photoactive donor-acceptor (D-A) dyads for green energy production. A number of studies have been conducted to estimate the performance of fullerene-transition metal complexes as elements for solar cell fabrication. To estimate the potential of such compounds for artificial photosynthesis devices photoinduced processes in these compounds are investigated using transient absorption and time-resolved infrared (TRIR) spectroscopies, and the lifetimes of charge separated states are compared. A number of reviews describe different types of fullerene-containing D-A dyads, including some transition metal complexes of fullerenes.[15]

Being a large polyunsaturated molecule, C_{60} fullerene possesses a large spherical π-electron surface which is likely to engage in π-π stacking interactions with various polyaromatic hydrocarbons and extended carbon supports, self-assembling into well-ordered 1D, 2D and 3D supramolecular arrays.[16,17] This ability can be utilised to order and deposit fullerene-tagged molecules, including transition metal complexes as 2D networks on surfaces or as quasi-1D chains in narrow carbon containers and form heterogeneous systems which retain the individual properties of the transition metal complex. For instance, functional monolayers from carbon nanostructures including fullerenes, carbon nanotubes and graphene, showed potential as novel materials for energy conversion.[18]

Combining C_{60} and transition metals in one molecule can yield novel compounds which exhibit the properties of the individual building blocks as well as hybrid properties due to intramolecular fullerene-transition metal interactions. These compounds have potential for application in various fields, depending on the nature of transition metal and the way the fullerene and the transition metal are connected. This review summarises this class of compounds with specific emphasis on the properties and potential applications of the individual compounds.

1.1. Classification of fullerene-transition metal hybrids.

There are numerous ways in which to combine fullerene cages with transition metal centres. Uncoordinated individual metal atoms or ions and small metal containing clusters can be trapped inside the fullerene cage during the fullerene formation process to form endohedral metallofullerenes. These are elegant structures with high symmetry and have well-defined but externally inaccessible metal centres. The range of metals that can be trapped inside the fullerene cage is limited to Group I-III metals such as scandium and the lanthanides, which makes endohedral fullerenes ideal for preparation of functional materials for applications as MRI contrasting agents and as electron-accepting blocks in photovoltaic devices. This class of compounds has been extensively reviewed recently.[19]

The addition of metal centres or metal containing functional groups to the outside of the fullerene cage to form exohedral metal-fullerene systems is a more versatile approach and allows a wide range of transition metals to be attached to the fullerene cage using relatively straightforward synthetic methodologies. It has resulted in the preparation of a wide range of systems combining one or more fullerene cage/cages with transition metal centres. A review by M. D. Meijer, et al describes in detail the structures reported up to 2001.[20] In this review we summarise the advances in this area in the past decade, focusing primarily on the functional properties and applications of these exciting systems.

It is possible to classify exohedrally functionalised fullerenes into three major groups based on the type of bonding between the fullerene cage and the metal containing moiety. These are 1) organometallic compounds in which the metal is attached directly to carbon atoms of the fullerene cage; 2) systems in which the metal centre is coordinated to a metal binding moiety attached to the fullerene cage using covalent or non-covalent interactions and 3) cocrystallates, host-guest inclusion complexes and fulleride salts in which pristine fullerene cages and metal species are bound by non-covalent interactions such as van der Waals or electrostatic forces.

2. Organometallic fullerene-metal complexes.

C_{60} and the rest of the fullerene family are electron deficient polyolefins and can act as metal binding ligands coordinating transition metals in different binding modes directly to the carbon cage. Examples of the various C_{60} metal binding modes are presented in Figure 2.

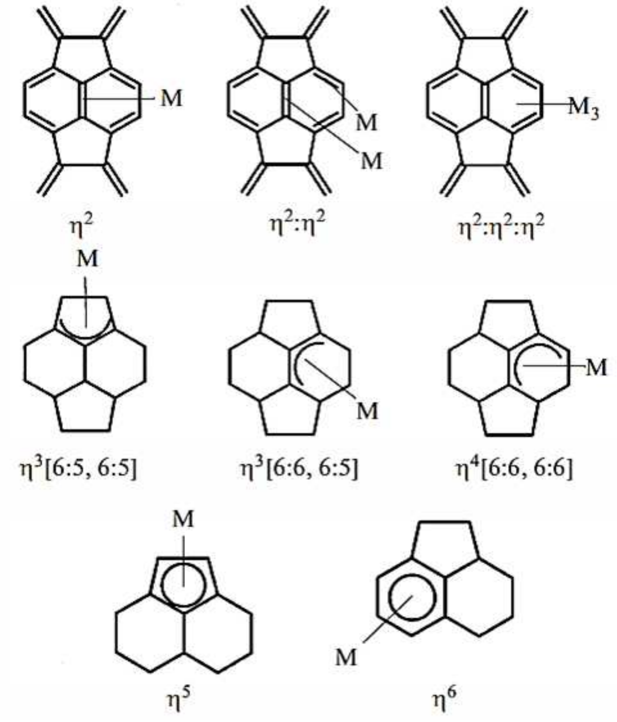

Figure 2. Possible metal binding modes of fullerene.[21,22] Reprinted with permission from ref 22. Copyright 2010 Springer.

A number of complexes of this type have been synthesised and characterised incorporating a wide range of heavy, mainly second and third row transition metals attached to the fullerene cage (Table 1).

Table 1. Organometallic compounds of C_{60} and higher fullerenes.

Fullerene	Metal	Binding mode	C_{60}:M ratio	Properties/comments	Ref.
C_{60}	Ru^0	η^1	1:2	-	23
C_{60}	Co^0	η^2	2:2	Paramagnetic at room temperature, diamagnetic at low temperatures	24
C_{60}	Co^0	η^2	2:2	-	25
C_{60}	Ni^0	η^2	$(1:1)_\infty$	Diamagnetic linear coordination polymer	26
C_{60}, C_{70}	Ni^0	η^2	1:1	-	27, 28
C_{60}	Mo^0	η^2	2:1	Electronic communication between two fullerenes in the ground state	29
C_{60}	Mo^0, W^0	η^2	2:1	Electronic communication between two fullerenes in the ground state	30
C_{60}	Rh_6 cluster	η^2	2:6	Strong electronic communication between two fullerenes in the ground state	31
C_{60}	Rh^I, Ir^I	η^2	1:1	Optically active complexes with enantiomeric ligands	32

C_{60}, C_{70}	Rh^I, Pd^0	η^2	1:1	Catalysts for acetylenic bond hydrogenation	33
C_{60}	Pd^0	η^2	1:1	Catalyst for hydrogenation of acetylenic alcohols	34
C_{60}, C_{70}	Pd^0	η^2	1:1	Redox activity	35, 36
C_{60}	Pd^0; Pt^0	η^2	2:2	-	37
C_{60}; open cage C_{60}	W^0	η^2	1:1	Catalyst for alkyne-alkyne coupling and alkyne scission induction	38
C_{60}	W^0	η^2	1:1	Catalyst for C-H bond activation	39
$Sc_2C_2@C_{82}$	Re^0	η^2	1:3	-	40
C_{60}	Os^0	η^2	1:3	Nanotube encapsulation	41, 42
C_{60}	Os^0	η^2	1:3	Redox activity	43
C_{60}	Pt^0	η^2	1:1	Ab initio binding energy calculations	44
$Li^+@C_{60}$	Pt^0, Ir^I	η^2	1:1	-	45
C_{60}	Ir_4 cluster	η^1, η^1, η^2, η^2	2:4	Electronic communication between the two fullerenes in the ground state	46
C_{60}	Cu^I, Ag^I, Au^I	η^1/η^3; η^2/η^3; η^5	1:1	-	47
C_{60}	Au^I	η^1/η^3; η^2	1:1	-	48
$C_{64}H_3$	Os_3 cluster	η^4	1:1	-	49
C_{60}	Cr^{III}, Cr^{II}, Mo^{II}, Mo^{IV}	η^5	1:1	-	50
C_{60}	Fe^{II}	η^5	1:1	Monolayer on a silicon oxide surface for organic field effect transistors (OFET)	51
C_{60}	Fe^{II}	η^5	1:1	Monolayer on Au(111) electrodes studied by in situ electrochemical STM	52
C_{60}	Fe^{II}	η^5	1:2	Redox activity, electronic communication between two metal centres	53
C_{60}	Fe^{II}	η^5	1:1	Redox activity	54
C_{60}	Fe^{II}	η^5	1:1	Liquid crystalline properties	55
C_{60}	Fe^{II}	η^5	1:1 1:2	Photoinduced charge transfer with lifetimes of 20-30 ps; shorter for double-decker complex	56
C_{60}	Fe^{II}, Co^I, Ru^{II}, Re^I	η^5	1:1	-	57
C_{60}	Fe^{II}, Ru^{II}	η^5	1:1	-	58
C_{60}	Fe^{II}, Ru^{II}	η^5	1:1	Chemical functionalisation of the cyclopentadienyl ligand	59
C_{60}	Fe^{II}, Ru^{II}	η^5	1:1	Photoinduced charge transfer with lifetimes of 30 ps for Fe; no charge transfer for Ru	60
C_{60}	Fe^{II}, Ru^{II}	η^5	1:1	Self-assembled monolayers (SAM) on indium tin oxide (ITO); bidirectional photocurrent upon irradiation	61
C_{70}	Fe^{II}, Ru^{II}	η^5	1:2 1:3	Redox activity; electronic communication between the metal atoms	62
C_{60}	Co^{III}	η^5	1:1 2:2	Stabilisation of aromatic four-membered rings	63
C_{60}	Co^{III}	η^5	2:2	Tetrathiafulvallene (TTF) as additional electron donor; photoinduced charge separation with lifetimes of 36-65 ps; non-linear optical properties	64

C_{60}, C_{70}	Zn_2	η^5	1:2 2:2	Theoretical study	65
C_{60}	Ru^{II}, Pd^{II}	η^5	1:1	-	66
C_{60}	Ru^{II}	η^5	1:1	Catalysts for isomerisation of 1-decene into internal decenes	67
C_{60}	Rh^{II}	η^5	1:1	-	68
C_{60}	Re^{I}	η^5	1:1	Redox activity	69
C_{60}	Pd^0; Fe^{II}	η^2; Metallocene[a]	1:1:1	Redox activity	70
C_{60}. C_{70}	Pd^0, Pt^0; Fe^{II}	η^2; Metallocene[a]	1:1:1	-	71
C_{60}	Fe^{II}	Metallocene[a]	1:1	Redox activity; fluorescence quenching by electron transfer and energy transfer processes	72
C_{60}	Fe^{II}	Metallocene[a]	1:1	Redox activity; fluorescence quenching by electron transfer and energy transfer processes	73
C_{60}	Fe^{II}	Metallocene[a]	1:1	Liquid crystalline properties; photoinduced charge separation with lifetimes of 490-560 ns	74
C_{60}	Fe^{II}	Metallocene[a]	1:1	Redox activity; photoinduced charge separation with lifetimes of 0.1-50 ns	75
C_{60}	Fe^{II}	Metallocene[a]	1:4 2:4	Redox activity; no ground state electronic communication	76
C_{60}	Fe^{II}	Metallocene[a]	1:2 1:4	Liquid crystalline properties; redox activity; fluorescence quenching	77
C_{60}, Open cage C_{60}	Fe^{II}	Metallocene[a]	1:1	Redox activity	78
C_{60}	Fe^{II}	Metallocene[a]	1:4	Redox activity; electrocatalyst for hydrogen peroxide reduction	79
C_{60}	Fe^{II}	Metallocene[a]	1:1	Redox activity; fluorescence quenching; Cu^{2+} sensor	80
$Sc_3N@C_{80}$	Fe^{II}	Metallocene[a]	1:1	Redox activity; charge separated state with 84-128 ps lifetime	81
C_{60}	Fe^{II}	Metallocene[a]	1:2	Excitation wavelength dependent ultrafast photoinduced charge transfer (CT) with 12-88 ps lifetimes	82
C_{60}	Fe^{II}	Metallocene[a]	1:1	Photoinduced charge separation with lifetimes of 26-50 ns	83
C_{60}	Fe^{II}	Metallocene[a]	1:1	Liquid crystalline properties; photoinduced processes	84
C_{60}	Fe^{II}	Metallocene[a]	1:1	Triphenyl amine and BODIPY as chromophores; photoinduced charge separation with lifetimes of 416 ps	85
C_{60}	Fe^{II}	Metallocene[a]	1:1	Photoinduced charge separation with lifetimes of 94 μs; spatially separated radical-ion pair (RIP)	86
C_{60}	Fe^{II}	Metallocene[a]	1:2 1:6 1:12	Photoinduced charge separation with lifetimes of 45-127 ps for 1:2 complex; no charge transfer in 1:12 complex	87
C_{60}	Fe^{II}	Metallocene[a]	1:1	Ferrocene-naphthalenediimide-fullerene triad; photoinduced charge separation with lifetime of 935 ps	88
C_{60}	Fe^{II}	Metallocene[a]	1:1	Two-electrode energy storage device fabricated and tested	89
C_{60}	Fe^{II}	Metallocene[a]	1:1	BODIPY as chromophore; photoinduced charge separation with lifetime of 500 ps	90

C_{60}	Fe^{II}	Metallocene[a]	2:1	Redox activity; fluorescence quenching	91
C_{60}	Fe^{II}, Ru^{II}	Metallocene[a]	1:1	Redox activity; fluorescence quenching; photoinduced charge separation with lifetime of 100 ns for ruthenocene dyad, no charge transfer in ferrocene dyad Fc	92
C_{60}	Fe^{II}, Ru^{II}	Metallocene[a]	1:1 2:1	Redox activity	93

[a] Metallocene covalently attached to the fullerene cage via a linker group.

It is clear from Table 1 that a large number of transition metals can be attached to the fullerene cage in order to form organometallic compounds such as Ni, Co, Cu and Fe from the first row, Mo, Ru, Rh, Pd and Ag from the second row and W, Re, Os, Ir, Pt and Au from the third row of the transition metal block of the periodic table. The metal centres predominantly form η^2 or η^5 complexes however there are a few notable exceptions which form η^1,[23] η^3 and η^4 complexes (Figure 3, compounds **2-3**).[46-49] The overlap between the π-system of the fullerene cage and the d-orbitals of the transition metal determines the properties of these systems and results in strong electronic coupling between the two components of these complexes. The strength of these interactions has been extensively probed by electrochemical techniques, absorption and emission spectroscopy and photophysical methods.

The metals which can be attached in a η^2 fashion to the [5,6] or [6,6] bond of the fullerene cage consist mainly of the zero-valent second and third row transition metals or metal clusters such as W,[30,38,39] Mo,[29] Pd,[34-36] Pt,[37,44] Rh,[31,33] Ir,[32] Re,[40] and Os[41,42,43] with only Co[24,25] and Ni[26-28] represented from the first row. An example of a 1:1 fullerene-metal complex is presented in Figure 3, showing an Ir complex containing an enantiomeric phosphine ligand resulting in an optically active compound.[32] Late transition metals reported to be attached in the η^2 fashion are typically catalytically active showing activity in various reactions, for example both Pd and Rh fullerene complexes are observed to promote acetylenic bond hydrogenation,[33,34] and a W fullerene complex was found to induce interligand alkyne-alkyne coupling and alkyne scission reactions[38] as well as C-H bond activation and C-C bond formation[39] which suggests potential application in catalytic alkyne oligomerisation and metathesis reactions. Such compounds also possess rich electrochemical properties showing several reduction and oxidation waves in cyclic voltammetry corresponding to fullerene cage based reductions and metal-based oxidations. These systems are fully conjugated due to the nature of the fullerene-metal bond, which allows strong ground-state electronic communications between the different parts of the complex. This has been demonstrated for so-called dumbbell type structures which contain two fullerene cages connected via either a single metal atom such as Mo[29,30] or W[30] or a metal cluster such as Ir_4[46] or Rh_6[31] (Figure 3, compounds **4** and **5**). Cyclic voltammetry is dominated by the sequential fullerene cage reductions, and demonstrates a shift of the reduction potential for the addition of a second electron towards more negative values for such complexes.

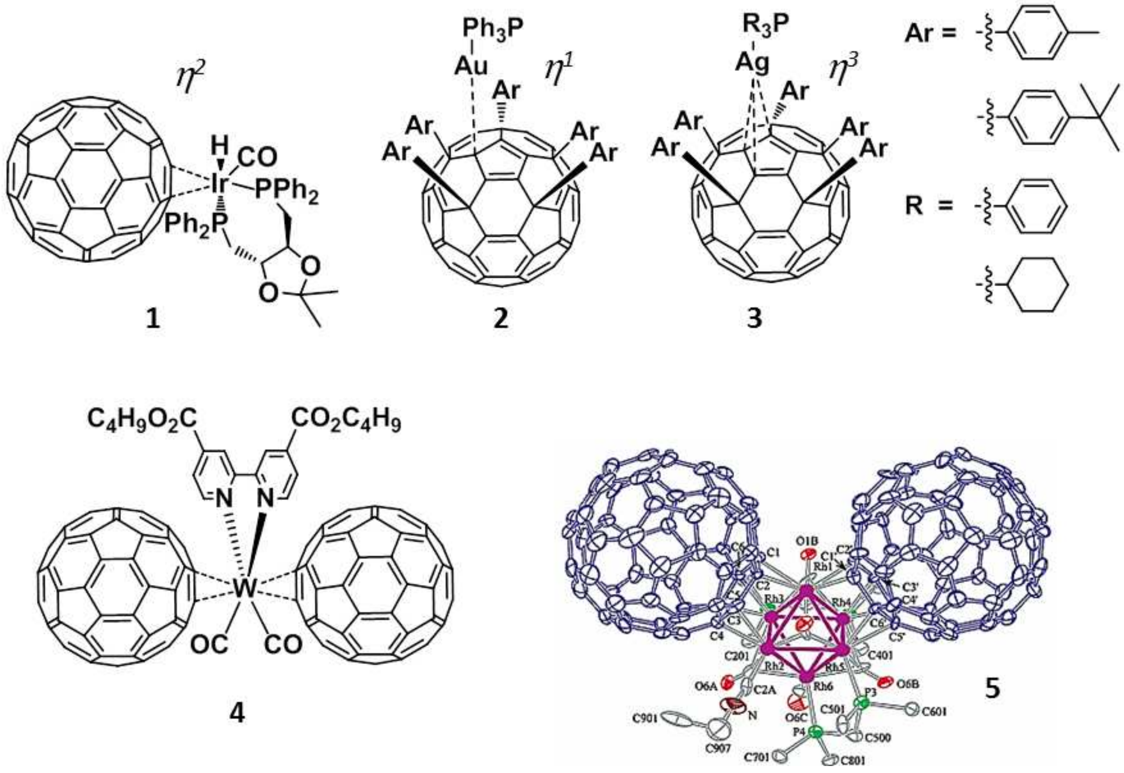

Figure 3. Examples of an η^2 Ir complex (**1**),[32] a η^1 Au complex (**2**), a η^3 Ag complex (**3**)[47] and two dumbbell structures in which two fullerene cages are connected via a W atom (**4**)[30] and a Rh_6 cluster (**5**).[31] Reprinted with permission from ref 32, Copyright 2011 Elsevier; ref 47, Copyright 2011 American Chemical Society; ref 30, Copyright 2002 Royal Society of Chemistry; and ref 31, Copyright 2002 American Chemical Society.

η^5 complexes of fullerenes, or so-called buckymetallocenes, allow the coordination of metal centres in different non-zero oxidation states to the centre of the five-membered ring of the fullerene cage (Figure 4, compounds **6-10**). Metals that can be coordinated in this fashion are typically the smaller first and second row transition metals such as Fe,[51-62] Co,[57,63,64] Cr,[50] Ru,[58-62,66,67] Pd,[66] Mo,[50] and Rh,[68] however, a few examples of Re[57,69] from the third row have also been reported. Additional ligands around the metal centre, usually represented by cyclopentadienyl, carbonyl or alkyl groups, can be chemically functionalised, as has been demonstrated for the cyclopentadienyl Fe and Ru buckymetallocenes,[59] to yield useful molecular building blocks. These compounds possess rich electrochemistry, especially in the oxidation region as metallocenes such as ferrocene, cobaltocene and ruthenocene are known to be good electron donors. The combination of such metal centres with the excellent electron accepting ability of C_{60} fullerenes introduces the possibility of creating donor-acceptor arrays capable of photoinduced energy and electron transfer processes forming $C_{60}^{\cdot-}$-$D^{\cdot+}$ radical ion pairs (RIP). This has resulted in these systems being suggested as potential materials for artificial photosynthetic devices and has been thoroughly investigated.[56,60,64]

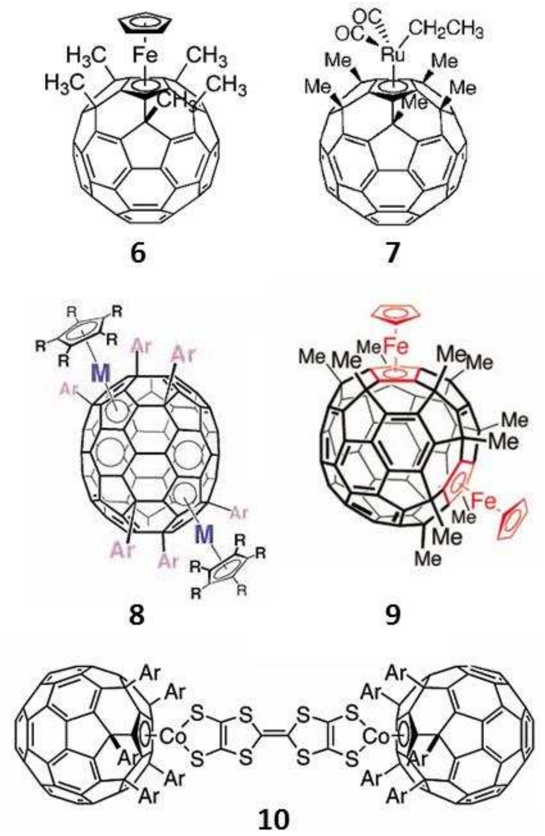
6 7

8 9

10

Figure 4. η^5 complexes of C_{60} with Fe and Ru (**6**, **7**),[67] double-decker η^5 complexes of C_{60} and C_{70} with Fe (**8**, **9**, M=Fe, Ru)[62,56] and a dumbbell type compound linked via two η^5-Co moieties and tetrathiafulvallene (**10**).[64] Reprinted with permission from ref 67, Copyright 2007 WILEY-VCH Verlag GmbH & Co. KGaA, Weinheim; ref 56, Copyright 2008 American Chemical Society; ref 62, Copyright 2009 WILEY-VCH Verlag GmbH & Co. KGaA, Weinheim; and ref 64, Copyright 2009 American Chemical Society.

Cyclic voltammetry of these bucky ferrocene systems typically shows three quasi-reversible reduction processes corresponding to the addition of electrons to the fullerene cage at approximately -1.3, -1.9 and -2.3 V respectively and a quasi-reversible or irreversible metal based oxidation in the region of 0.5-0.6 V vs. Fc^+/Fc.[54] The addition of a second and third Fe or Ru metal centre can be achieved to form so-called double-decker systems, and the relative configuration of the metal centres can be precisely controlled using a carefully designed organic tether.[62,53,56] These systems exhibit strong ground state electronic communication between the metal centres which results in a shift in the potential of the second and third metal based oxidations towards more positive values and at the same time causes a shift in the fullerene cage based reductions towards more negative potentials. Moreover, these compounds possess excellent photophysical properties, with the Fe complexes found to form photoinduced $C_{60}^{\cdot -}$-Fe^{III}Cp (where Cp is cyclopentadiene) charge separated states, however such separation is relatively short lived with lifetimes of ~30 ps due to strong metal-C_{60} electronic coupling.[56,60] Such charge separation was not observed in similar Ru containing systems which was attributed to the poorer electron donating properties of ruthenocene compared to ferrocene.[60] Attaching a strong electron donor, tetrathiafulvalene (TTF), to the fullerene cage via a fully conjugated cobaltocene type linker resulted in a system with a short lived $C_{60}^{\cdot -}$-CoCp-TTF$^{\cdot +}$charge separated state of 35-65 ps. This was attributed to strong electronic communication between the constituent parts of the molecule causing fast charge separation but also fast charge recombination processes.[64] The exciting properties of these systems make them potential candidates for various molecular electronic devices, and a few examples of such devices have been already reported, including an organic field effect transistor (OFET) containing monolayers of bucky ferrocene on a silicon oxide surface,[51] and a photoswitch containing self-assembled monolayer (SAM) of single iron atom doped fullerenes on indium tin oxide (ITO).[61] The catalytic properties of these systems have also been investigated with a Ru containing fullerene complex found to be an efficient catalyst for the isomerisation of 1-decene into internal decenes.[67]

To improve the photoinduced charge separation properties of bucky ferrocenes and to avoid fast charge recombination non-conjugated or partially-conjugated linkers have been utilised to separate the ferrocene and fullerene moieties. This has resulted in the formation of the whole new class of organometallic fullerene-metallocene compounds (Figure 5).

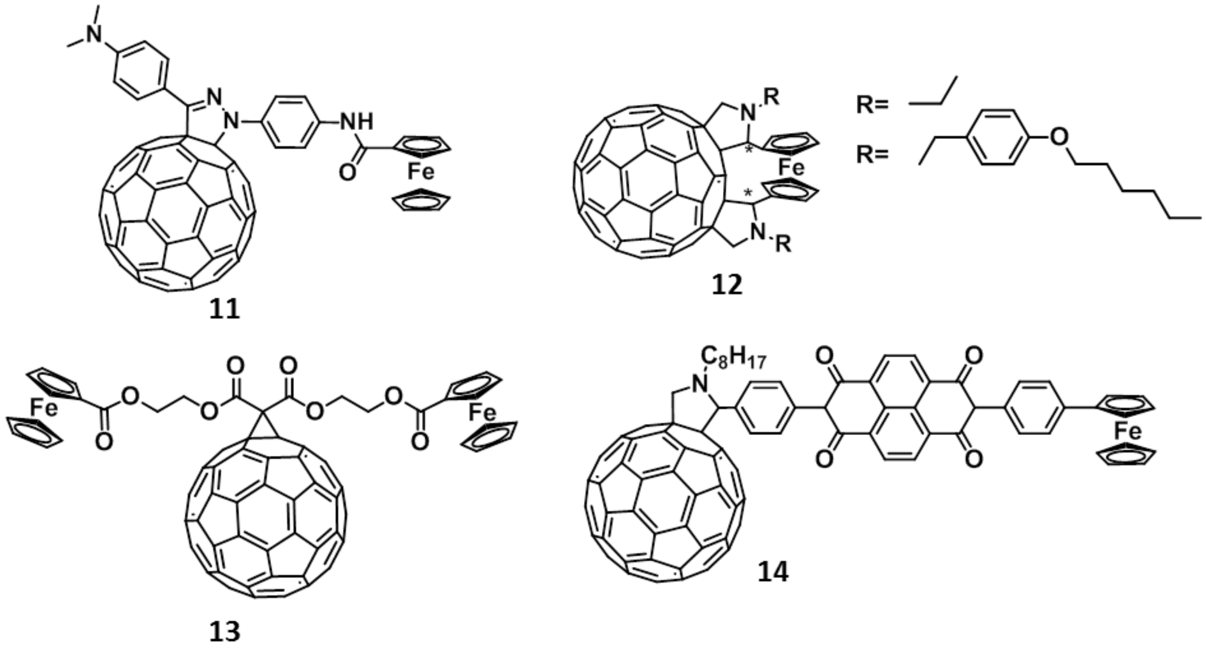

Figure 5. Examples of C_{60}-ferrocene containing species (**11**,[83] **12**,[93] **13**,[87] and **14**[88]), in which the ferrocene is attached to the fullerene cage via various bridging groups. Reprinted with permission from ref 83, Copyright 2006 Royal Society of Chemistry; ref 93, Copyright 2013 Royal Society of Chemistry; ref 87, Copyright 2009 American Chemical Society; and ref 88, Copyright 2011 American Chemical Society.

Attaching the metallocene centre/s to the fullerene cage via a linker group has a drastic effect on the properties of the molecule. When the conjugation between the fullerene cage and the metal centre is disrupted by one or more sp^3 hybridised carbon atoms of the linker this results in the minimising of intramolecular electronic communications in the ground state.[70-93] Cyclic voltammetry shows only negligible changes in the $E_{1/2}$ potential of the first, second and third recuctions of the fullerene cage in the presence or absence of ferrocene unit as well as no shift in the $E_{1/2}$ of the ferrocene unit oxidation process in the presence or absence of the fullerene cage.[73] Furthermore, cyclic voltammetry of dumbbell shaped bisfullerene species in which ferrocene (Figure 6, compounds **15**, **16**) or a ferrocene containing cluster are attached via pyrrolidine groups bridged between two fullerene cages (Figure 6, compound **17**), shows no ground-state intramolecular electronic communication between the fullerene units: the addition of the first and second electrons to the fullerene cages are observed to occur simultaneously at identical potentials.[76,91]

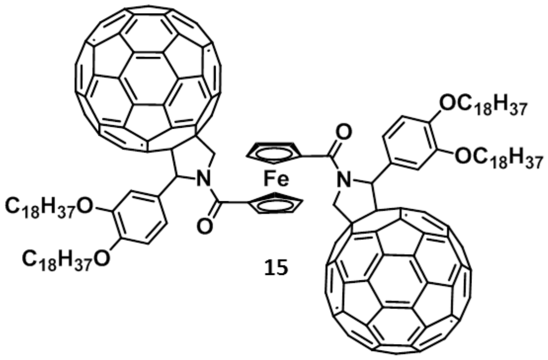

15

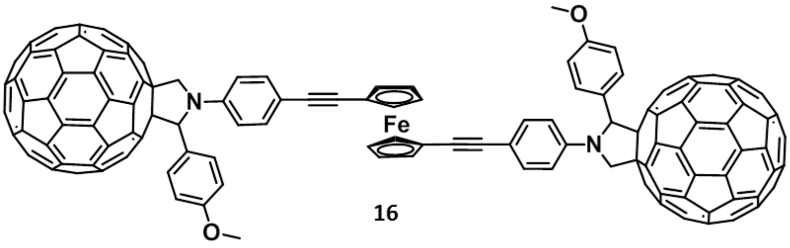

16

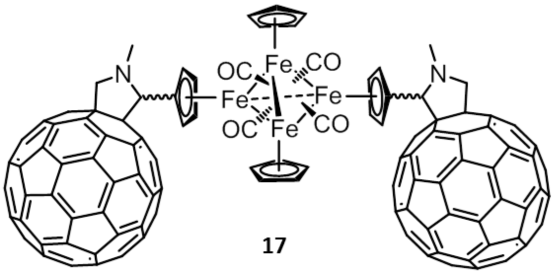

17

Figure 6. Structures of ferrocene-bridged C_{60}-dumbbells containing non-conjugated fullerpopyrrolidine linkers (**15** and **16**[91]), and a tetrairon cluster $Cp_4Fe_4(CO)_4$ bridged bisfullerene (**17**[76]). Reprinted with permission from ref 91, Copyright 2012 Royal Society of Chemistry; ref 76, Copyright 2013 Royal Society of Chemistry.

However, excited state communication is still present in this type of compound as observed by the effective quenching of the fluorescence of the fullerene singlet by the ferrocene moiety.[77,92] The mechanism of such quenching is however still a subject of debate and is suggested to occur either by electron transfer from the ferrocene moiety to the fullerene singlet state, or by energy transfer from the triplet state of the fullerene to the ferrocene unit.[73] As well as a good electron donor, ferrocene is also a good energy acceptor with a triplet energy of only 1.16 eV compared to 1.50 eV for $^{3}C_{60}^{*}$,[94] however both the ferrocene cation and ferrocene triplet posses no significant absorbtion or emission signatures, and can only be detected by indirect measurements, therefore it is difficult to distinguish between the formation of a charge-separated RIP and a ferrocene triplet. Nevertheless, examples of the generation of radical-ion pairs upon photoecitation have been reported for fullerene-ferrocene dyads with various linker (Figure 7, compounds **18**-**23**) with lifetimes ranging from hundreds of picoseconds[81,82,87] to several nanoseconds[83,92] and even microseconds.[86] This is several orders of magnitude longer than those observed for the fully conjugated fullerene containing donor-acceptor systems due to the presence of a significantly slower charge recombination step. This makes compounds of this type potential candidates for use in molecular electronics, artificial photosynthesis and energy storage devices.[89]

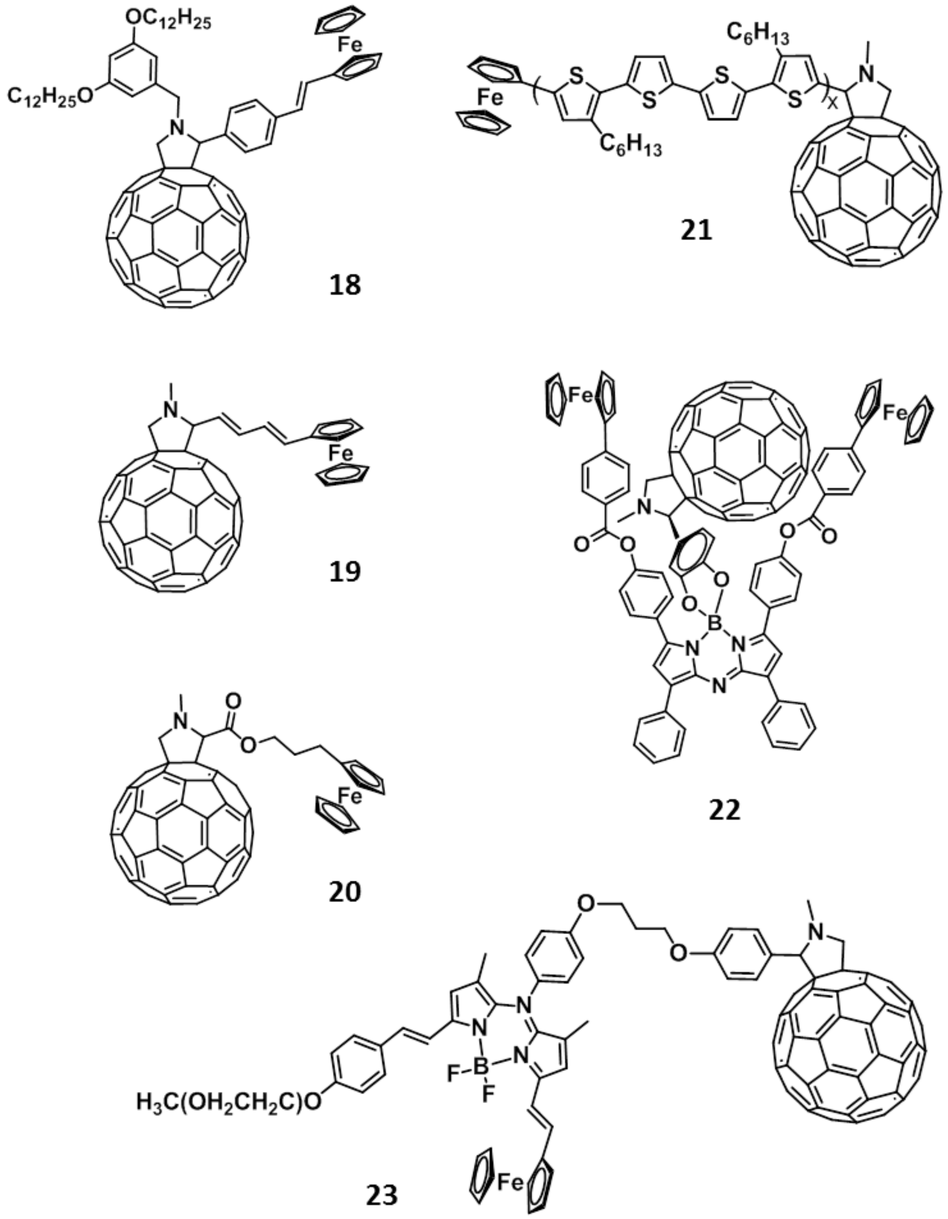

Figure 7. Examples of C_{60}-ferrocene dyads linked via non-conjugated or partially-conjugated linkers such as phenylenevinylene (**18),**[73] polyvinylene (**19**),[72] ester (**20)**,[72] oligothiophene (**21)**,[75] and BODIPY containing C_{60}-ferrocene composites (**22**[82] and **23**[90]). Reprinted with permission from ref 73, Copyright 2008 Royal Society of Chemistry; ref 72, Copyright 1997 American Chemical Society; ref 75, Copyright 2006 American Chemical Society; ref 82, Copyright 2013 WILEY-VCH Verlag GmbH & Co. KGaA, Weinheim; ref 90, Copyright 2012 WILEY-VCH Verlag GmbH & Co. KGaA, Weinheim.

Fullerene-ferrocene dyads can be incorporated into functional materials with a range of useful properties. For example, a C_{60}-ferrocene composite has been shown to be an effective electrocatalyst for hydrogen peroxide reduction,[79] and therefore can be incorporated into electrochemical H_2O_2 sensor devices. Furthermore, liquid crystalline properties can be introduced into these systems by adding bulky chains to the side of the molecule which, combined with the presence of the metallocene moiety, makes these compounds interesting functional materials (Figure 8, compounds **24** and **25**).[74,77,84] Such dendritic fullerene-ferrocene dyads were found to form smectic A layers, and exhibit electrochemical properties consistent with the individual components. Furthermore, light-induced charge-transfer processes have also been detected with the formation of charge-separated states which have lifetimes of up to 560 ns,[74] which makes these materials valuable candidates for the development of supramolecular switches.

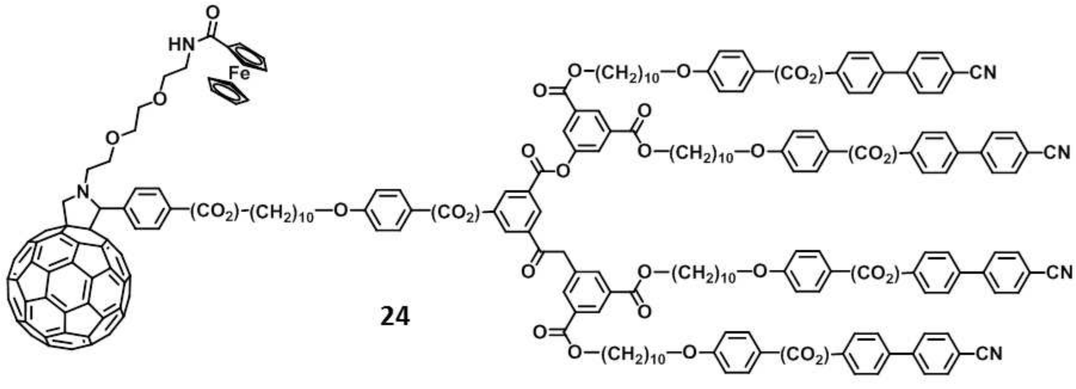

24

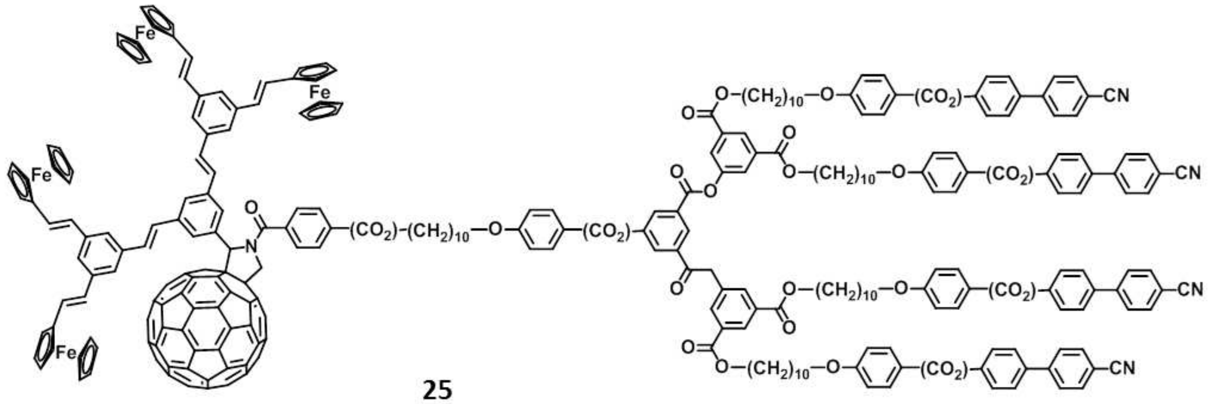

25

Figure 8. Examples of dendritic C_{60}-ferrocene dyds exhibiting liquid-crystalline properties (**24**[74] and **25**[77]). Reprinted with permission from ref 74, Copyright 2004 Royal Society of Chemistry; ref 77, Copyright 2006 Elsevier.

3. Fullerene containing metal coordination complexes.

The development of fullerene based organic chemistry has led to the covalent attachment of a variety of different metal coordinating moieties to fullerene cages. This has enabled the coordination of a wealth of different transition metals to fullerenes and has led to the formation of numerous stable and versatile systems with tuneable properties. Different metal binding moieties can be used to stabilise a wide range of transition metals in various oxidation states, whilst the geometry of the metal centre can be precisely controlled by the choice of the metal binding group. Additionally, the fullerene to metal separation can be adjusted by the careful choice of covalent linker introducing a mechanism to control intramolecular interactions within these systems.

A number of metal binding moieties have been attached to the fullerene cage either covalently or using non-covalent supramolecular interactions.

3.1. Metal binding groups covalently attached to the fullerene cage.

3.1.1. N-donor ligands.

The majority of reported metal coordinating ligands attached to the fullerene cage are N-donors and can be classified by the number of coordination sites as monodentate (pyridine, imidazole), bidentate (bipyridine, diazafluorene, dipyrrin), tridentate (terpyridine) and tetradentate (porphyrin and phthalocyanine) ligands which result in the formation of square-pyrimidal, octahedral or square-planar complexes respectively.

3.1.1.1. Monodentate N-donor ligands.

A large number of examples of fullerenes functionalised with monodentate N-donor ligands such as various pyridine and imidazole derivatives attached via pyrrolidine, imidazole, cyclopropane or cyclohexene linkers have been reported (Figure 9, Table 2). Pyridine and imidazole functional groups are known to coordinate to the axial position of square planar transition metal complexes such as substituted porphyrins and phthalocyanines forming supramolecular dyad and polyad systems with square pyramidal or square bipyramidal metal centres (Scheme 1), the first example of the coordination of a pyridine-functionalised fullerene being reported in 1999.[95] Table 2 summarises the structures of coordination compounds formed by pyridyl or imidazole functionalised fullerenes and different transition metal containing moieties reported since then and details the formation process and the resultant properties of the complexes.

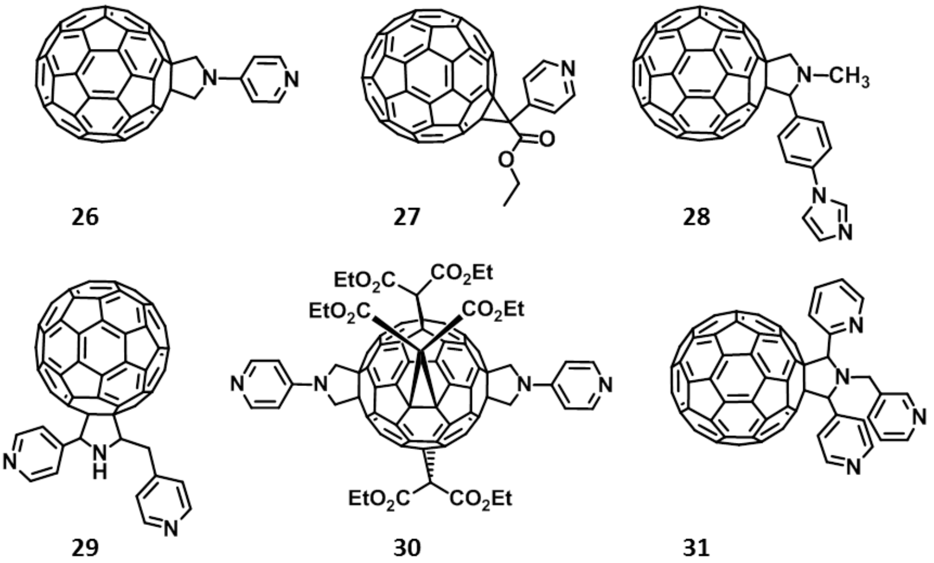

Figure 9. Examples of C_{60} fullerene functionalised with monodentate N-donor ligands, such as a 4-pyridyl group attached via pyrrolidine (**26**[96]) or cyclopropane (**27**[95]) linkers, an imidazole group (**28**),[97] two 4-pyridyl groups on the same pyrrolidine linker (**29**),[98] two spatially separatated 4-pyridyl groups (**30**),[99] and three pyridyl binding groups on the same pyrrolidine linker (**31**).[100] Reprinted with permission from ref 96, Copyright 2010 WILEY-VCH Verlag GmbH & Co. KGaA, Weinheim; ref 95, Copyright 1999 Royal Society of Chemistry; ref 97, Copyright 2014 American Chemical Society; ref 98, Copyright 2014

WILEY-VCH Verlag GmbH & Co. KGaA, Weinheim; ref 99, Copyright 2009 American Chemical Society; ref 100, Copyright 2008 WILEY-VCH Verlag GmbH & Co. KGaA, Weinheim.

Table 2. Complexes of monodentate N-donor C_{60} containing ligands.

Fullerene cage	Metal and ancillary ligand	Ligand on the fullerene	C_{60}:M ratio[a]	Additional chromophore	Binding constant (K_a, M^{-1})	Lifetime of charge separated state	Ref.
C_{60}	Eu^{III}	2-Pyridyl, 3-Pyridyl	1:1	-	-	-	100
C_{60}	Zn, Co and Mn Porphyrin	3-Pyridyl	1:1 1:2	-	$8.4x10^4$ in cyclohexane	-	101
C_{60}	Zn Porphyrin	3-Pyridyl	1:1	-	4.4-$8.5x10^4$ in toluene	-	102
C_{60}	Ag^I	3-Pyridyl, 4-Pyridyl	1:1	-	-	-	103
C_{60}	Cd^{II}	4-Pyridyl	1:2	-	-	-	104
C_{60}	Fe Porphyrin	4-Pyridyl	1:1	H_2 Porphyrin	1.2-$3.2x10^3$ in ODCB	38 ns; 20 μs	105
C_{60}	Zn Porphyrin	4-Pyridyl	1:1		$3.6x10^3$ in C_6D_6	-	95
C_{60}	Zn Porphyrin	4-Pyridyl	1:1	-	2.3-$2.4x10^4$ in $CHCl_3$	-	106
C_{60}	Zn Porphyrin	4-Pyridyl	1:2	Zn Phthalocyanine	1.7 $x10^5$ in ODCB	1.7 ns	107
C_{60}	Zn Porphyrin	4-Pyridyl	1:2	-	$7.3x10^4$ in 1,2-difluorobenzene	230 ps	108
C_{60}	Zn Porphyrin	4-Pyridyl	1:2 2:4	H_2 Porphyrin	$1.8x10^5$ in ODCB	160-170 ns	109
C_{60}	Zn Porphyrin	4-Pyridyl	1:1	-	1.4-$7.4x10^4$ in ODCB	-	110
C_{60}	Zn Porphyrin	4-Pyridyl	1:1 1:2 1:6	-	$1.3x10^3$-$3.2x10^5$ in CH_2Cl_2	-	111
C_{60}	Zn Porphyrin	4-Pyridyl	1:1	Perylenediimide	$3.4x10^6$ in ODCB	1 ns; 3.8 ns	112
C_{60}	Zn Porphyrin	4-Pyridyl	1:2	Azabodipy	$1.9x10^5$ in ODCB	5.5 ns	113
C_{60}	Zn Porphyrin	4-Pyridyl	1:3	Zn phthalocyanine	$1.2x10^5$ in ODCB	Not specified	98
C_{60}	Zn Porphyrin	4-Pyridyl	1:6	-	$1.5x10^4$ in toluene	Not specified	114
C_{60}	Zn Porphyrin	4-Pyridyl	1:1	-	$0.94x10^4$; $1.8x10^4$; $2.0x10^4$ in chlorobenzene	250-1076 ps in chlorobenzene	115
C_{60}	Zn Porphyrin macroring	4-Pyridyl	1:9	-	$3x10^8$ in benzonitrile	-	116
C_{60}	Zn Porphyrin macroring	4-Pyridyl	1:9	-	$8x10^7$ in benzonitrile	-	117

C_{60}	Zn Porphyrin macroring	4-Pyridyl	1:9	-	$1x10^7$-$3x10^8$ in benzonitrile	-	118
La@C_{82}	Zn Porphyrin	4-Pyridyl	1:1	-	$8.9x10^3$ in ODCB	-	119
La_2@C_{80}					$2.4x10^4$ in ODCB	-	
C_{60}	Zn, Pd Porphyrin	4-Pyridyl	1:2	Zn Phthalocyanine	1.0-$3.4x10^6$ in toluene	1.1-1.9 ns	120
C_{60}	Zn Azulenocyanine	4-Pyridyl	1:1	-	-	0.78 ns	121
C_{60}	Zn Phthalocyanine	4-Pyridyl	1:1	BODIPY	$1.7x10^6$ in toluene	39.9 ns	96
C_{60}	Ru (bipyridine)$_2$	4-Pyridyl	1:1	-	-	-	122
C_{60}	Ru Phthalocyanine	4-Pyridyl	1:1 2:1 1:2	-	-	130-170 ns	99
C_{60}	Zn Porphyrin	Imidazole; 4-pyridyl	1:1	-	$1.2x10^4$-$1.2x10^5$ in CH_2Cl_2	1-4 ns	97
C_{60}	Zn Porphyrin	Imidazole	1:1	H_2 Porphyrin	-	100 ns	123
C_{60}	Zn Porphyrin	Imidazole	1:1	Triphenylamine, BODIPY	3.6-$4.6x10^3$ in ODCB	-	124
C_{60}	Zn Porphyrin	Imidazole	1:1	Triphenyl amine, Subphthalocyanine	$1.0x10^4$ in toluene	6.6 μs	125
C_{60}	Zn Porphyrin	Imidazole	1:1	-	-	-	126
C_{60}	Zn Porphyrin	Imidazole	1:1	-	$2.8x10^4$ in ODCB	4 μs	127
C_{60}	Zn Porphyrin	Imidazole	1:1 n:12	-	$7.4x10^3$ in CH_2Cl_2	300 ns	128
C_{60}	Zn Porphyrin	Imidazole	1:1	BODIPY	$1.7x10^4$ in ODCB	-	129
C_{60}	Zn Porphyrin	Imidazole	1:1	1, 2 or 4 BODIPY	$3.9x10^3$-$3.0x10^4$ in ODCB	4 ns	130
C_{60}	Zn Phthalocyanine	Imidazole	1:1	-	$6.2x10^4$ in toluene	-	131
C_{60}	Zn Phthalocyanine	Imidazole	1:1	4 Carbazole units	$7.7x10^5$ in ODCB	60 ns	132

[a] Includes all metal centres in the molecule.

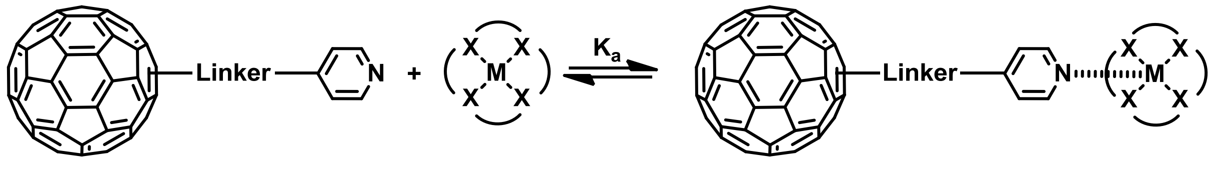

Scheme 1. Coordination of the fullerene containing pyridyl ligand to the axial position of the square planar metal complex.

One, two or three pyridine groups can be easily attached to the C_{60} cage via pyrrolidine or cyclopropane ring formation reactions to form stable and soluble ligands. The coordination chemistry of these molecules has been extensively studied, predominantly monitoring the association of the fullerene ligand in solution with a variety of square planar porphyrin and phthalocynine transition metal complexes using absorption and emission spectroscopy techniques. By far the most commonly used metal complex is Zn porphyrin due to the fact that it is a good electron donor and introduces the possibility of creating charge separated states upon photoexcitation, however examples of Fe, Ru, Co and Mn complexes have also been reported. Formation constants for these coordination complexes vary in the range of $1.2 \times 10^3 - 3 \times 10^8$ M^{-1} indicating strong coordination bonding and the high stability of such systems (Scheme 1). Fullerene ligands bearing one pyridine group have been shown to form 1:1 C_{60} : transition metal complexes when coordinated to monoporphyrin or phthalocyanine moieties (Figure 10, **32-33**).[95,96,102,105,106,110,115,119,121] Whilst examples of two pyridyl fullerene molecules coordinating to one metal porphyrin moiety are rare (Figure 10, compound **36**),[99] the introduction of a second pyridyl group to the same fullerene ligand allows it to coordinate to two metallated porphyrins or phthalocyanines forming 1:2 fullerene:metal complexes (Figure 10, **34**).[101,107-109,111,113,120] Fullerene functionalised with three pyridyl units was successfully combined with Eu(III) to form a 1:1 complex, however, only one pyridyl group participated in metal coordination (Figure 10, compound **35**).[100]

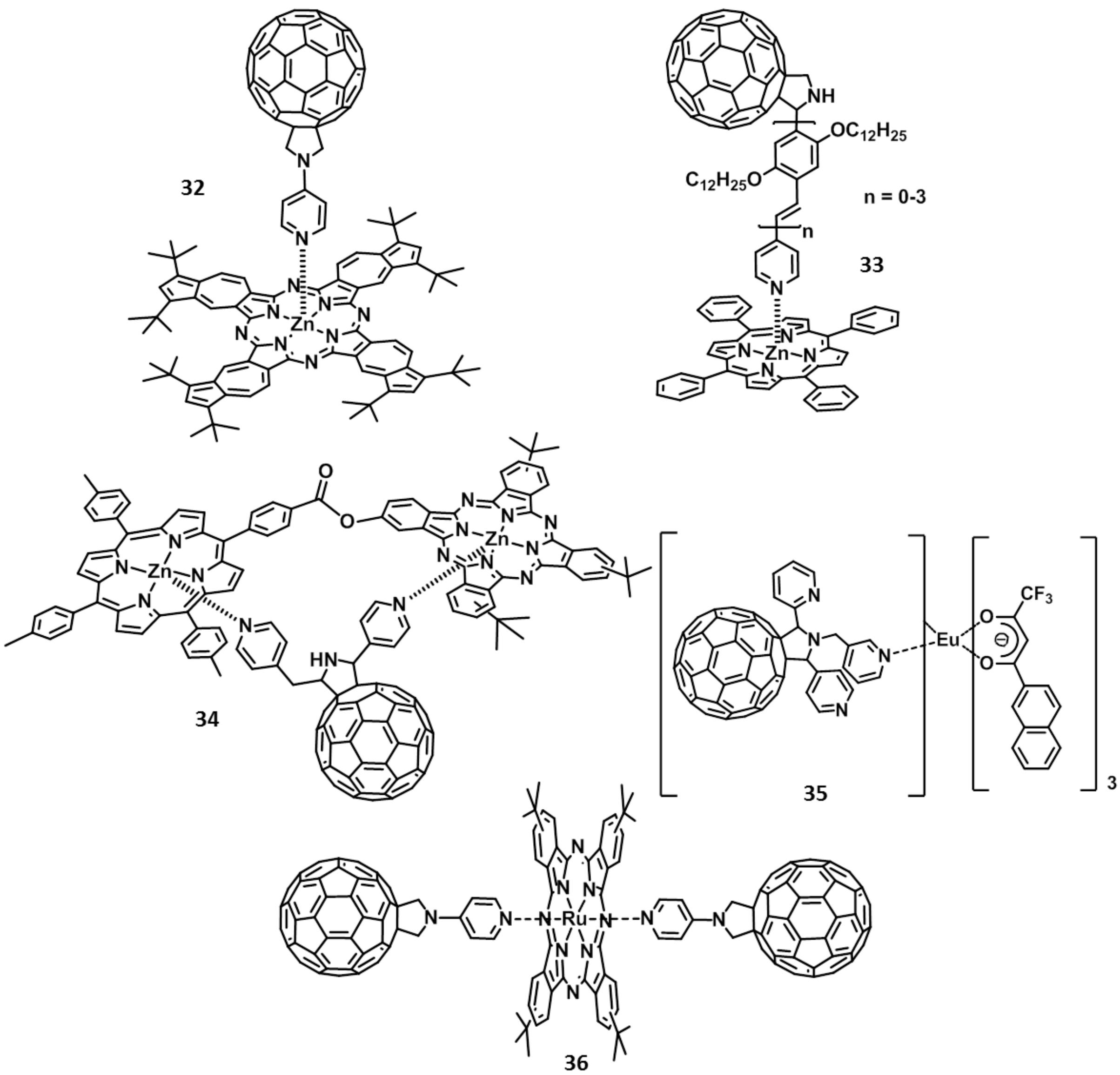

32

33

34

35

36

Figure 10. Examples of 1:1 C_{60}Py:Zn(Phthalocyanine) (**32**),[121] 1:1 C_{60}Py:Zn(Porphyrin) (**33**),[115] 1:2 C_{60}Py:Zn(Porphyrin)-Zn(Phthalocyanine) (**34**)[107] complexes, a $C_{60}(Py)_3$-Eu(III) complex (**35**),[100] and a 2:1 C_{60}Py:Ru(Porphyrin)-C_{60}Py (**36**).[99] Reprinted with permission from ref 121, Copyright 2012 Royal Society of Chemistry; ref 115, Copyright 2015 Royal Society of Chemistry; ref 99, Copyright 2009 American Chemical Society; ref 107, Copyright 2013 Royal Society of Chemistry; and ref 100, Copyright 2008 WILEY-VCH Verlag GmbH & Co. KGaA, Weinheim.

Coordination of these ligands with metal ions such as Ag^+ or Cd^{2+} leads to the formation of dimeric species or quasi one-dimensional coordination polymers,[103] or two-dimensional metal-organic frameworks (MOFs)[104] respectively (Figure 11). Such fullerene-linked

MOFs show potential for hydrogen storage, as has been recently demonstrated by the DFT study of the 2D network built upon the $Ca_{32}C_{60}$-node and p-dihydroxybenzene linker which was estimated to be able to bind molecular hydrogen in the range of 8.0-9.2 %.[133]

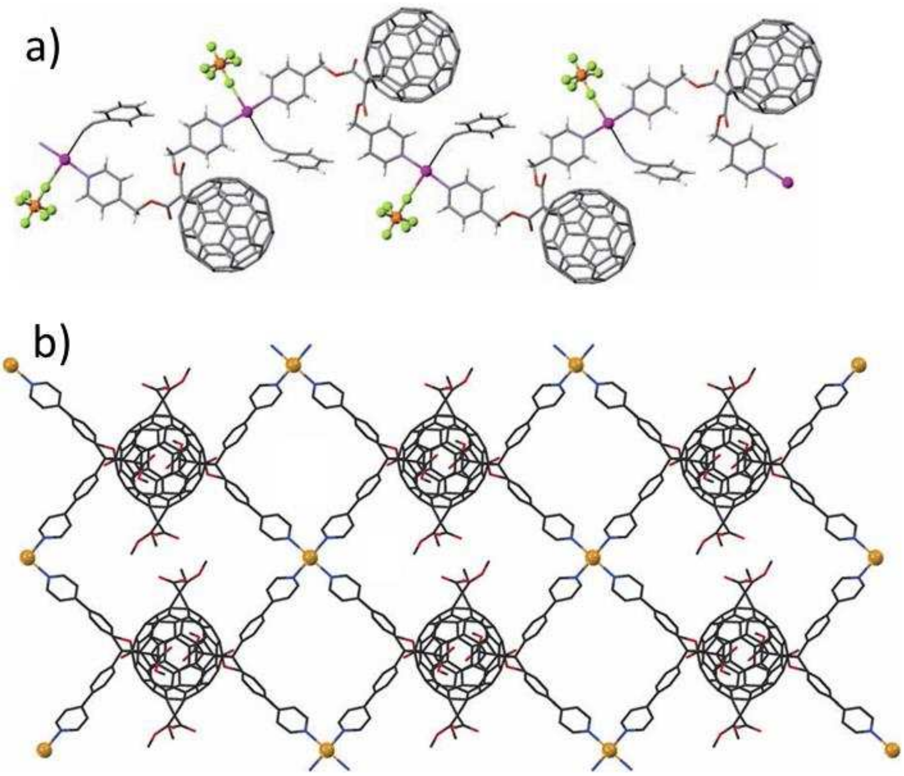

Figure 11. a) 1D coordination polymer built by binding Ag^+ with a C_{60}-bispyridine monoadduct[103] and b) 2D network based on a C_{60}-bispyridine bisadduct and Cd^{2+}.[104] Reprinted with permission from ref 103, Copyright 2007 WILEY-VCH Verlag GmbH & Co. KGaA, Weinheim; and ref 104, Copyright 2014 WILEY-VCH Verlag GmbH & Co. KGaA, Weinheim.

Incorporating more than two metal containing units and one C_{60} cage has been achieved by coordination of a tripod-like functionalised C_{60} bearing three pyridyl groups in addition to a porphyrin macroring containing nine Zn porphyrin units (Figure 12, structures **37-39**).[116-118] Formation constants for 1:1 C_{60}-metal complexes are generally slightly lower (between $1.2 \times 10^3 - 8.5 \times 10^4$ M^{-1}) than those of the 1:2 complexes (between $7.3 \times 10^4 - 3.4 \times 10^6$ M^{-1}) in which two transition metal centres are both coordinated to the fullerene containing bis-pyridyl ligands (Figure 10, compound **34**). The highest association constant values are achieved for the tripod-like tris-pyridyl ligands coordinated to three out of nine Zn porphyrins of the macroring (between $1\text{x}10^7$-$3\text{x}10^8$ M^{-1}) (Figure 12).

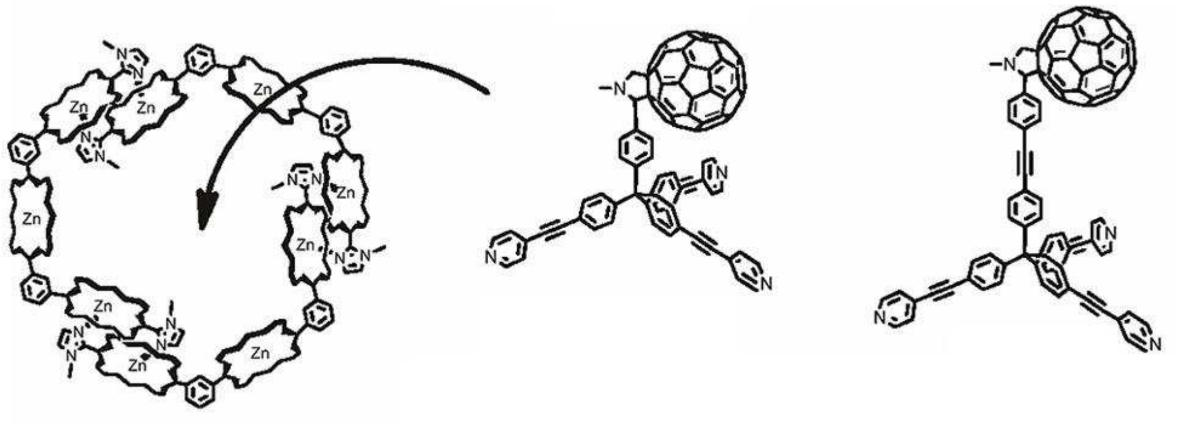

37 **38** **39**

Figure 12. Examples of tripodal C_{60}-tris-pyridyl ligands (**38** and **39**) able to self-assemble with Zn porphyrin macrorings (**37**).[116-118] Reprinted with permission from ref 118, Copyright 2011 American Chemical Society.

The resultant properties of these systems are generally determined by the characteristic features of the individual moieties, such as the electron accepting ability of the fullerene cage, and light-absorbing and electron donating properties of the Zn porphyrin moiety. This results in these systems being ideally suited to form charge separated states upon photoexcitation with relatively long lifetimes ranging from ps to μs. Thus, 1:1 and 1:2 C_{60}:Zn porphyrin complexes are observed to form charge separated states with 230 ps[108] and 780 ps[121] lifetimes respectively. Interestingly, spatial separation of the pyridyl binding group and C_{60} by several phenylenevenylene units (Structure **33**, Figure 10) results in decrease of the radical-ion pair lifetime from 991 ps to 259 ps due to significant increase in reorganisation energy from 0.74 to 0.91 eV.[115] Endohedral La@C_{82} and La_2@C_{80} fullerene containing pyridyl ligands coordinated to a Zn porphyrin show similar charge separation and charge recombination kinetics to those of the C_{60} fullerene derivatives.[101,119] Ru phthalocyanine systems, which are better electron donors than the equivalent Zn complexes, result in the formation of longer lived charge separated species with lifetimes of 130-170 ns.[99] The mechanism, dynamics and kinetics of photoinduced processes in these systems are discussed in detail in the review by El-Khouly et al.[134]

Additional components can be also introduced into these supramolecular systems which can act as either electron donors, electron acceptors, or energy acceptors (chromophores), thus allowing the creation of artificial antenna-reaction centre type complexes (Scheme 2). Examples of the introduction of groups such as boron-dipyrromethene (BODIPY), azaBODIPY, perylene diimine (PDI), free base porphyrin (H_2 porphyrin) or a second Zn porphyrin or Zn phthlocyanine moiety have also been reported (Figure 13). This second component acts as a chromophore resulting in an efficient energy migration to the Zn porphyrin or Zn phthalocyanine unit followed by photoinduced electron transfer to the fullerene moiety to yield a charge-separated state with good quantum yield. Thus, incorporation of perylenediimine (PDI) into the ZnPorphyrin-C_{60}Py dyad (Figure 13, structure **40**) increases the lifetime of the resulting radical-ion pair to 3.8 ns compared to only 1 ns in the absence of PDI.[112] Incorporation of another unbound Zn porphyrin into the C_{60}:Zn porphyrin/Zn phthalocyanine assembly (Figure 13, structure **41**) is reported to extend the lifetime up to 1.9 ns,[120] whilst attaching an azaBODIPY or BODIPY moiety to the Zn porphyrin ring increases the lifetime of charge separated species further to 5.5 ns[113] and 39.9 ns[96] respectively (Figure 13, structure **42**). Attempts have been made to incorporate this azaBODIPY-ZnPorphyrin$_2$-C_{60}Py tetrad into a photoelectrochemical cell and an incident photon-to-current conversion efficiency of up to 17 % has been reported.[113] Furthermore, in the presence of the free-base porphyrin, the $C_{60}^{\cdot -}$-Zn(Porphyrin)$^{\cdot +}$ radical ion pair does not decay for up to 170 ns.[109] Interestingly, a free-base H_2Porphyrin incorporated into a C_{60}Py-Fe^{III}(Cl)(Porphyrin) dyad (Figure 13, compound **43**) acts as an electron donor resulting in a

H_2Porphyrin$^{\cdot+}$- C_{60}Py$^{\cdot-}$-Fe^{III}(Cl)Porphyrin RIP with a lifetime of 38 ns, which then exhibits evidence of an electron shift from C_{60} to the ferric porphyrin unit with the formation of H_2Porphyrin$^{\cdot+}$-C_{60}Py–Fe^{II}(Cl)Porphyrin with the lifetime of nearly 20 µs.[105] In contrast, the 1:9 complex, in which the fullerene is combined with the Zn porphyrin macroring containing 9 electron donating units, did not result in the formation of a long lived charge separated state suggesting that the charge recombination rate was similar to that of the charge separation.[116]

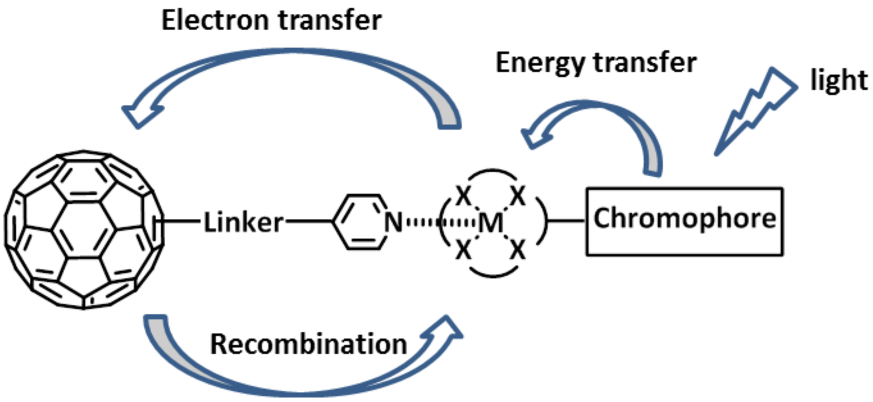

Scheme 2. Schematic representation of the photophysical processes in a fullerene containing pyridine ligand coordinated to the axial position of the square planar metal complex containing a chromophore unit.

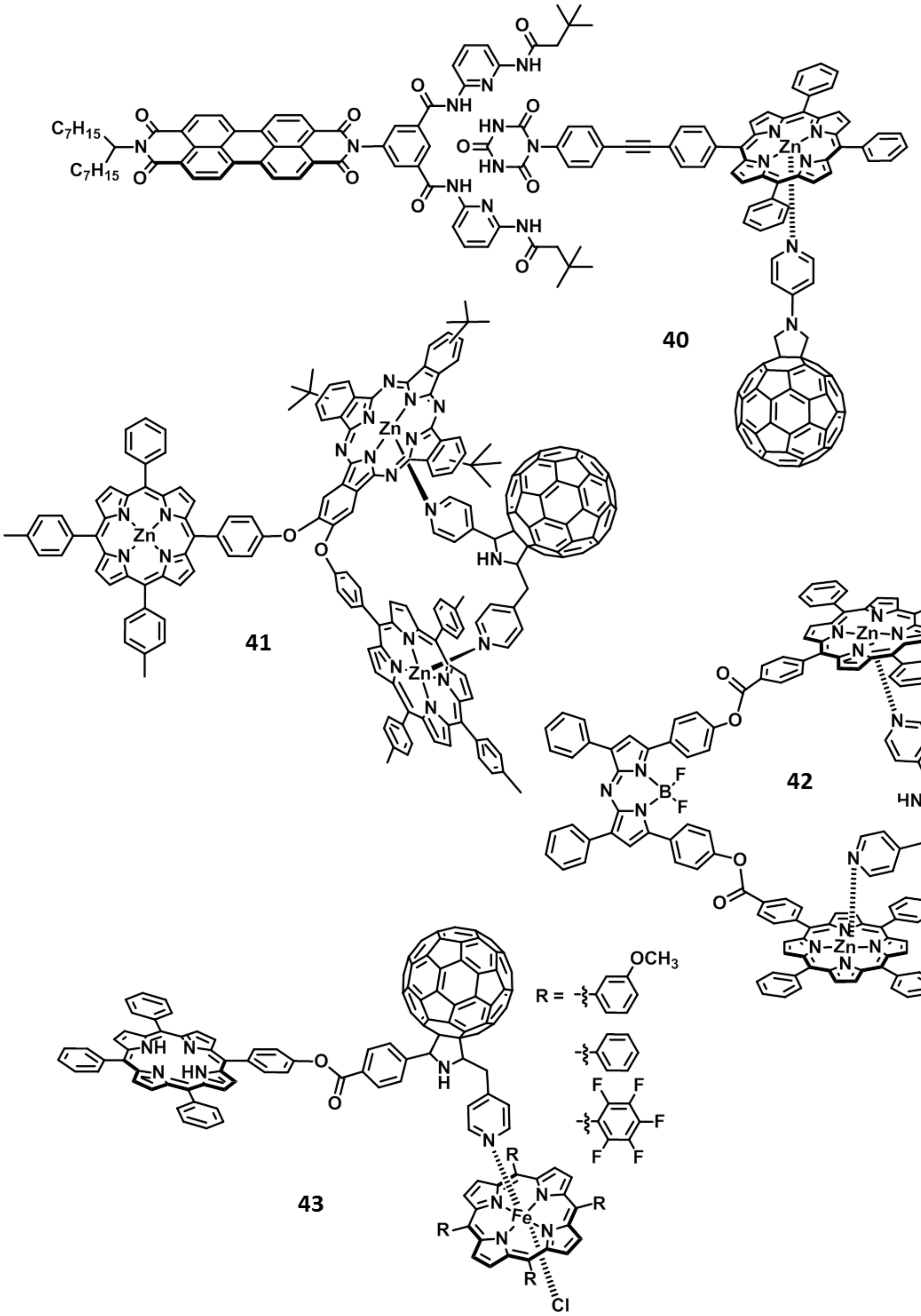

Figure 13. Examples of incorporating chromophore units into C_{60}Py-M(Porphyrin) and C_{60}Py-M(Phthalocyanine) dyads showing non-covalent attachment of perylenediimine unit (**40**[112]), an unbound Zn(Porphyrin) unit (**41**[98]), azaBODIPY unit (**42**[113]), and a free-base porphyrin attached to the C_{60}-Fe^{III}(Cl)Porphyrin (**43**[105]). Reprinted with permission from ref 98, Copyright 2014 WILEY-VCH Verlag GmbH & Co. KGaA, Weinheim; ref 113,

Copyright 2012 American Chemical Society; ref 105, Copyright 2007 American Chemical Society.

The metal coordinating ability of the imidazole functionalised fullerene are in the same range as those of the pyridyl functionalised C_{60}, with the formation constants for the 1:1 fullerene : metal complexes varying from 3.6×10^{3}– 7.7×10^{5} M^{-1},[123-132] a typical example of such dyad shown in Figure 14 (structure **44**). The photophysical properties of imidazole bridged complexes with Zn(Porphyrin) or Zn(Phthalocyanine) are also similar to those of the pyridyl bridged complexes, with long-lived charge separated ion pairs observed upon introduction of a chromophore to the system. Thus, in the presence of a BODIPY moiety a lifetime of 4 ns was achieved as a result of efficient energy transfer from the BODIPY moiety to the ZnPorphyrin followed by electron transfer to the fullerene cage (Figure 14, structure **45**), however, further introduction of additional BODIPY moieties led to a decrease in the solubility of these systems.[129,130] The addition of four carbazole moieties led to an increase in the lifetime to 60 ns whilst H_2(Porphyrin) enabled the formation of the ion pair with a 100 ns lifetime.[123] Finally, the introduction of triphenyl amine and subphthalocyanine (SubPc) moieties into Zn(Porphyrin) (Figure 14, structure **46**) resulted in the longest radical ion pair lifetime of 6.6 μs.[125]

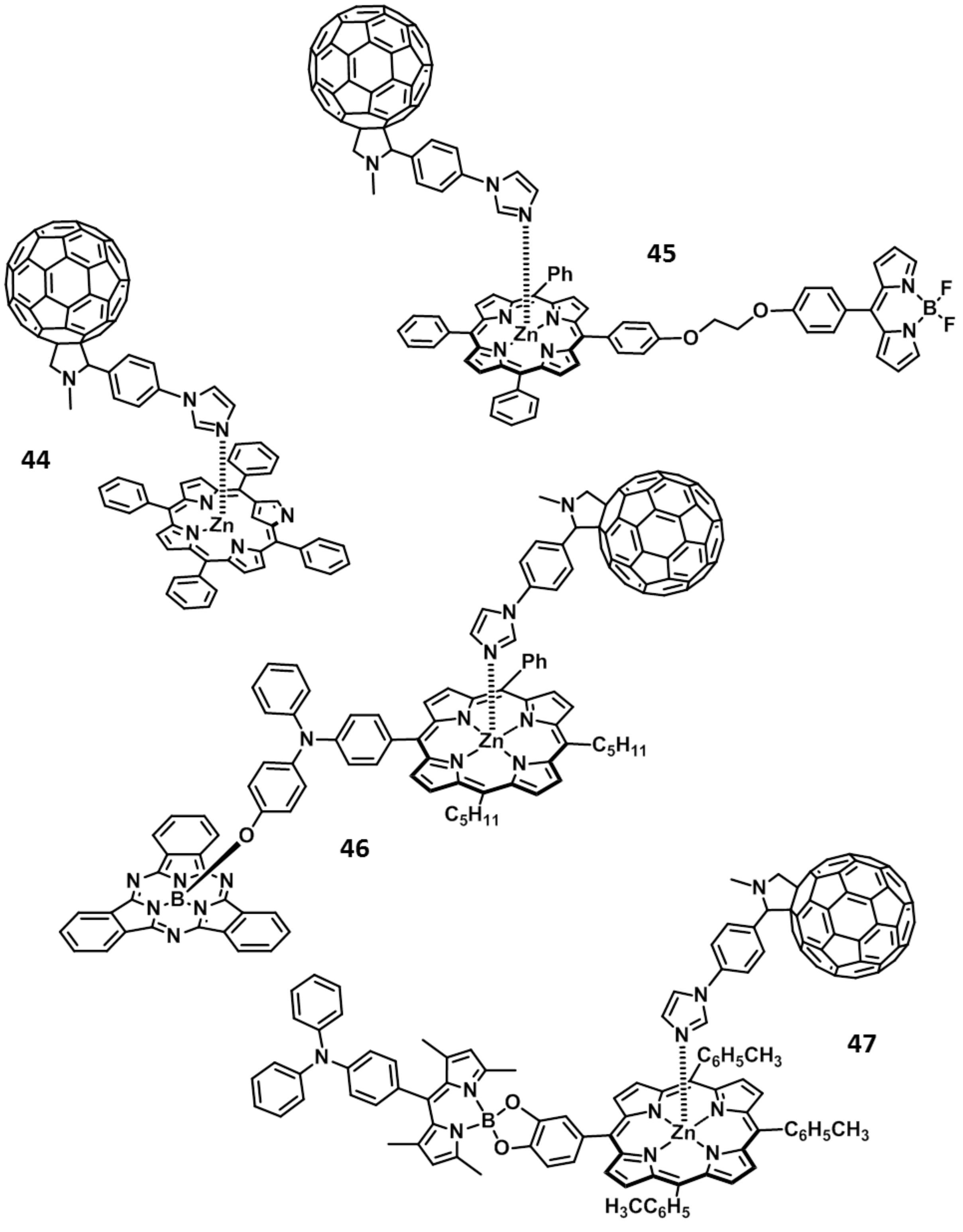

Figure 14. Examples of a C_{60}Imidazole-Zn N-Confused Porphyrin supramolecular dyad (**44**[127]), and C_{60}Imidazole-ZnPorhyrin complexes containing BODIPY (**45**[129]), subphthalocyanine (**46**[125]) and triphenylamine-BODIPY (**47**[124]) chromophores. Reprinted with permission from ref 127, Copyright 2006 American Chemical Society; ref

129, Copyright 2004 American Chemical Society; ref 125, Copyright 2010 WILEY-VCH Verlag GmbH & Co. KGaA, Weinheim; ref 124, Copyright 2012 WILEY-VCH Verlag GmbH & Co. KGaA, Weinheim.

3.1.1.2. Chelating bidentate and tridentate N-donor ligands.

A range of bidentate and tridentate N-donor ligands have been chemically attached to the C_{60} fullerene cage, including 2,2'-bipyridine (bipy), 1,10-phenanthroline (phen), diazafluorene, dipyrromethene (dipyrrin, dipy) and terpyridine (terpy) which can all bind a limited range of transition metals forming octahedral charged complexes incorporating inorganic counter ions. The summary of such compounds published in the last decade is presented in Table 3.

Table 3. Complexes of bidentate and tridentate N-donor C_{60} containing ligands.

Fullerene cage	Metal	Ligand on the fullerene	C_{60}:M ratio	Properties	Luminescence quantum yield (Φ)	Type of photo induced process	Lifetime of excited /charge separated state	Ref
C_{60}	Ru^{II}	Bipyridine	1:1	Luminescence; incorporation into Zr phosphate matrix; solid state luminescence	$0.09x10^{-4}$ /CH_2Cl_2 $0.03\ x10^{-4}$ /CH_3CN	-	-	135
C_{60}	Ru^{II}	Bipyridine	1:1	Luminescence; incorporation into Zr phosphate matrix; solid state luminescence	$0.83\ x10^{-4}$ /CH_2Cl_2 $0.21\ x10^{-4}$ /CH_3CN	-	-	
C_{60}	Ru^{II}	Bipyridine	1:1	Luminescence; ultrafast light-induced processes	$1.44x10^{-4}$/ CH_2Cl_2, toluene	CT	$\tau_{1/2}$ 210 ns in CH_2Cl_2	136
C_{60}	Ru^{II}	Bipyridine	1:1	Luminescence; ultrafast light-induced processes	$0.14x10^{-4}$ /CH_2Cl_2 $0.07x10^{-4}$ /CH_3CN	ET	0.27 ns	137
C_{60}	Ru^{II}	Bipyridine	1:1	-	-	-	-	138
C_{60}	Ru^{II}	Pyrazolino Pyridine	1:1	Luminescence; ultrafast light-induced processes	$1x10^{-4}$ /CH_3CN	ET	28 μs	139
	Ru^{II}	Bipyridine	1:1		$2x10^{-4}$ /CH_3CN	ET	1.3μs	
	Ru^{II}	Bipyridine	1:1		$<<1x10^{-4}$ /CH_3CN	ET	42 μs	

C_{60}	Ru^{II}	Bipyridine	1:1	Luminescence; ultrafast light-induced processes	-	ET	20 µs	140
	Ru^{II}	Bipyridine	1:1		-	ET		
	Ru^{II}	Bipyridine	1:1		-	ET		
C_{60}	Ru^{II}	Bipyridine	1:1	Ultrafast light-induced processes	-	ET	13 µs	141
C_{60}	Ru^{II}	Bipyridine	1:1	Amphiphilic C_{60} derivative for incorporation in Langmuir films	-	-	-	142
C_{60}	Ru^{II}	Bipyridine	2:1	-	-	-	-	143
C_{60}	Ru^{II}	Bipyridine	1:2	Luminescence; ultrafast light-induced processes	0.73 /CH_2Cl_2, CH_3CN	ET unfavoured	22 ns	144
	Ru^{II}	Bipyridine	1:1		0.11 /CH_2Cl_2, CH_3CN	ET favoured	30 ns	
C_{60}	Ru^{II}	Bipyridine	2:1	Luminescence; ultrafast light-induced processes	0.009	Competitive CT and ET	Up to 2.74 µs	145
	Re^{I}	Bipyridine	2:1		0.026	Competitive CT and ET	Up to 10.4 µs	
C_{60}	Ru^{II}	Bipyridine	1:1	Luminescence; ultrafast light-induced processes	$0.07x10^{-2}$/ CH_2Cl_2	CT and ET	18 µs	146
	Re^{I}	Bipyridine	1:1		$0.02x10^{-2}$/ CH_2Cl_2	CT and ET	14.9 µs	
C_{60}	Ru^{II}	Bipyridine	1:1		$7.2x10^{-4}$/ CH_2Cl_2, $2x10^{-4}$/ CH_3CN	ET	-	147
	Re^{I}	Bipyridine	1:1		$4.4x10^{-5}$/ CH_2Cl_2	ET	629 ns	
C_{60}	Re^{I}	Bipyridine	2:1	Amphiphilic C_{60} derivative for incorporation in Langmuir films	-	-	-	148
C_{60}	Re^{I}	Bipyridine	2:1	Luminescence	0.01	-	-	149
C_{60}	Cd^{II}	Bipyridine	1:1	Delivery of metal to SWNT	-	-	-	150
C_{60}	Pt^{II}	Bipyridine	1:1	Ultrafast light-induced charge transfer	-	CT	56-331 ps; 98-178 ns	151 152
C_{60}	Cu^{I}	Phenanthroline	2:1	Luminescence; ultrafast light-induced processes	-	CT and ET	-	153
C_{60}	Cu^{I}	Phenanthroline	2:2	Luminescence; ultrafast light-induced processes	$5.1x10^{-4}$/ CH_2Cl_2	CT and ET	-	154
C_{60}	Cu^{I}	Phenanthroline	1:1	Luminescence; ultrafast light-induced processes	-	ET	-	155
C_{60}	Zn^{II}	Dipyrrin	2:1	Luminescence; ultrafast light-induced processes	$2-6x10^{-4}$	CT	990-1516 ps	156

C_{60}	Ru^{II}	Diazafluorene	1:1	Second order non-linear optical (NLO) chromophore	-	-	-	157
C_{60}	Ir^{III}	Diazafluorene	1:1	Second order NLO chromophore	-	-	-	158
C_{60}	Re^{I}	Pyridazine	1:2	Redox activity; ultrafast light-induced processes	-	CT	τ 105 ps	159
C_{60}	Cu^{II}	N,N'-Dimethyl ethylenediamine	1:1	Paramagnetism	-	-	-	160
C_{60}	Fe^{II}, Co^{II}	Terpyridine	2:1	Photophysical and optical limiting properties	Non-luminescent	ET	-	161
C_{60}	Ru^{II}	Terpyridine	1:1	Redox activity	-	-	-	162
C_{60}	Ru^{II}	Terpyridine	1:1	Redox activity	-	-		163
C_{60}	Ru^{II}	Terpyridine	1:1	Photophysical properties	-	CT	-	164
C_{60}	Ru^{II}	Terpyridine	1:1	-	-	-	-	137
C_{60} open cage	Ru^{II}	Terpyridine	1:1	-	-	-	-	165
C_{60} open cage	Ru^{II}	Terpyridine	1:1	Optical limiting properties	-	-	-	166

[a] ET = Energy transfer, CT = charge transfer.

The majority of reported systems utilise 2,2'-bipyridine as a metal binding moiety which enables the coordination of second and third row transition metals such as Ru, Cd, Re and Pt respectively. Octahedrally coordinated Ru complexes are usually obtained from $Ru(bipy)_2Cl_2$ via substitution of the chloride ligands with a third C_{60} derivatised 2,2'-bipyridine ligand (Figure 15, **48** and **49**).[135-138,140] This process can be assisted by using Ag^{I} cations which bind to the displaced Cl^- anions.[139] Re complexes are typically obtained via the substitution of two carbonyl groups of $Re(CO)_5Cl$ with a C_{60} derivatised 2,2'-bipyridine ligand resulting in the formation of octahedral Re^{I} complexes.[148, 149] Both methods result in the formation of 1:1 fullerene-transition metal complexes. To attach two fullerene cages per Ru or Re centre a dumbbell shaped 2,2'-bipyridine ligand, in which two fullerene cages are appended to different sides of a bipyridine moiety, was synthesised and subsequently combined with the appropriate transition metal centre using the approach outlined above

(Figure 15, **51**).[143,145,148,149] A rare example of two Ru centres attached to the same fullerene cage was achieved by covalently attaching a metal binding moiety containing two spatially separated bipyridine units to the fullerene cage and subsequently reacting it with two equivalents of the Ru precursor (Figure 15, **52**).[144] Pt(II) centre can also be incorporated to the fullerene cage by ligand substitution of two DMSO groups in $(DMSO)_2PtCl_2$ complex with the C_{60}-bipyridine ligand. The two chloride ligands can then be replaced with acetylide groups containg various functional units such as phenyl, phenothiazine[151] or carbazole[152] groups (Figure 15, **50**). The only reported example of an octahedral Cd-C_{60} complex was obtained via substitution of the four water molecules of $Cd(NO_3)_2$ tetrahydrate with two bidentate 2,2'-bipyridine moieties covalently attached to the fullerene cage (Figure 15, **53**).[150]

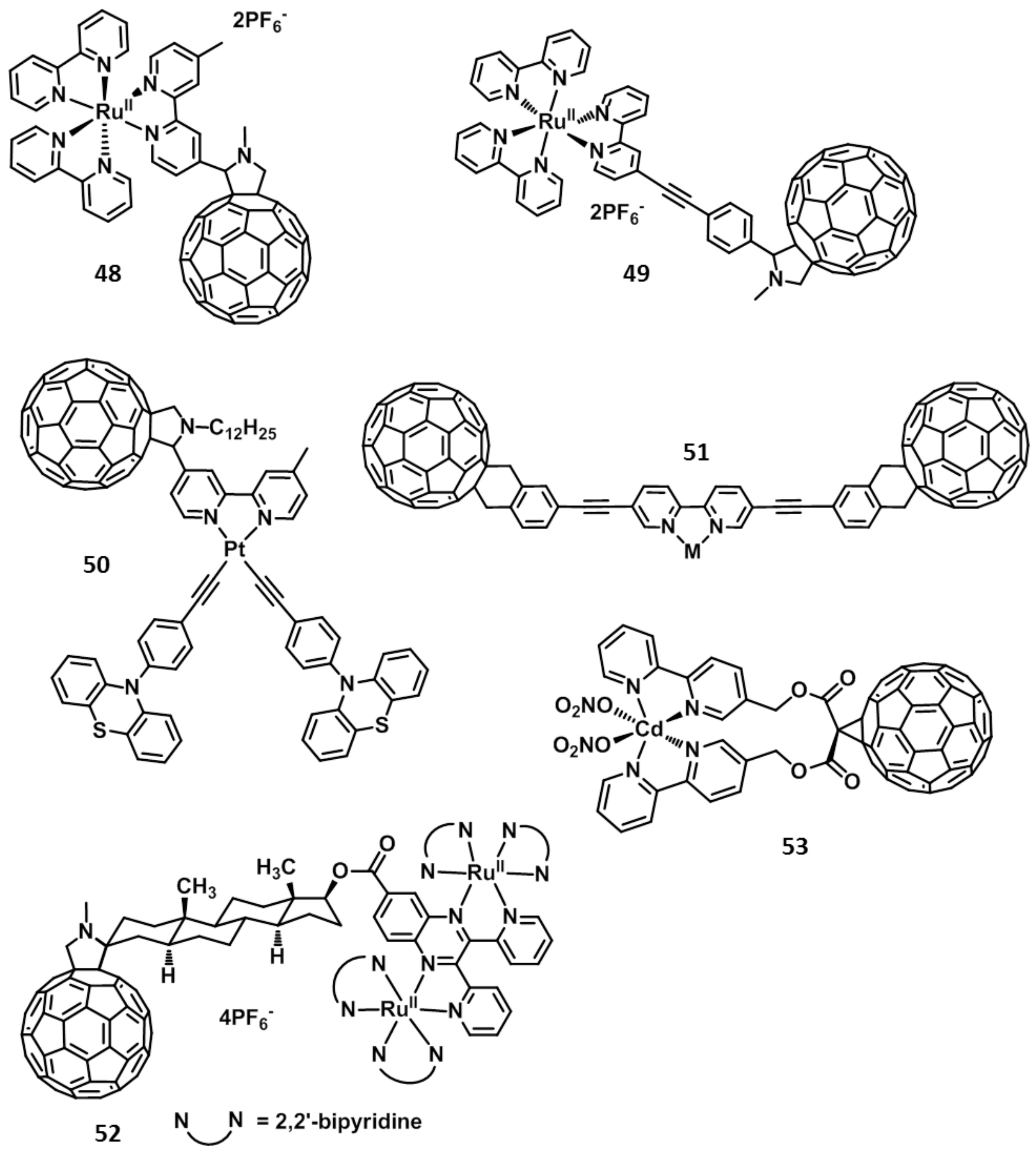

Figure 15. Examples of C_{60}-bipy-Ru dyads in which the fullerene cage and the metal are in close proximity (**48**)[139] and separated by a rigid spacer (**49**),[141] a C_{60}-bipy-Pt-$(PTZ)_2$ complex where PTZ = phenothiazine (**50**),[151] a dumbbell shape C_{60}-bipyM-C_{60} triad where M=$Re(CO)_3Cl$ and M=$Ru(bipy)_2[PF_6]_2$ (**51**),[145] a dinuclear C_{60}-$(Ru)_2$ complex (**52**),[144] and a C_{60}-$(bipy)_2$Cd complex (**53**).[150] Reprinted with permission from ref 139, Copyright 2008 American Chemical Society; ref 141, Copyright 2006 Royal Society of Chemistry; ref 151, Copyright 2014 American Chemical Society; ref 145, Copyright 2013 Elsevier; ref 144,

Copyright 2001 WILEY-VCH Verlag GmbH & Co. KGaA, Weinheim; ref 150, Copyright 2011 Royal Society of Chemistry.

In general the properties of C_{60}-bipyridine-metal complexes are simply a superposition of the properties of the individual moieties with little evidence of any electronic interactions in the ground state. As expected such complexes are good chromophores, able to absorb light in the whole range of the UV/vis spectrum through either the fullerene cage or the metal bipyridine moiety. The complexes also possess rich electrochemistry, typically showing three quasi reversible reductions of the fullerene cage, a reduction of the bipyridine moiety and at least one oxidation process localised on the metal centre (either Ru^{3+}/Ru^{2+} or Re^{2+}/Re^{1+}) at potentials of over +1 V vs. a SCE.

In contrast, the excited state properties of these systems display a strong degree of interaction between the fullerene cage and the metal moiety. The nature of these interactions has been studied in depth using luminescence-based spectroscopies. Individually both fullerene and the bipyridine metal moieties of the C_{60}-Ru and C_{60}-Re dyads are luminescent exhibiting a fluorescence band for the functionalised fullerene at 720 nm and a band associated with metal to ligand chare transfer (MLCT) between the Ru-bipy and Re-bipy in the 600-700 nm range. However when combined within dyad systems the fluorescence of the metal-bipy moiety is efficiently quenched by the presence of the fullerene cage showing luminescence quantum yields (Φ) in the order of 10^{-4} for C_{60}-Ru complexes. C_{60}-Re dyads are observed to exhibit an even higher degree of quenching (up to 4.4×10^{-5}).[147] Further investigations of the excited state properties of C_{60}-Ru dyads revealed that the ^{3}MLCT excited state of such systems is long-lived and is potentially capable of generating a charge-separated state (via either an electron, or charge transfer process, Table 3) which competes with the formation of a fullerene based triplet state (a triplet-triplet energy transfer process, Table 3). However, the majority of reported systems do not exhibit any features corresponding to the formation of a charge separated state, instead only the formation of long-lived fullerene-based triplet excited states with lifetimes of up to 40 μs are observed. Similar observations were reported for systems in which the fullerene and metal bipyridine moieties are either in close proximity or linked by a flexible group. In contrast, systems in which the fullerene and metal chromophore are connected with longer and more rigid linkers revealed competition between two possible decay pathways and report indirect evidence of the formation of a radical-ion pair, a result of charge transfer, as well as formation of fullerene triplet states.[145,146] C_{60}-Ru dyads were also observed to form charge separated states with relatively long lifetimes in the order of hundreds of ns [136] which was confirmed experimentally through the observation of a transient absorption band at 1040 nm corresponding to C_{60}^{-}. C_{60}-Pt dyads exhibit evidence of formation of charge-separated radical-ion pair with the lifetimes in the ns range for the dyad containing phenothiazine donor[151] and in the ps range for the dyad containg carbazole donor groups[152] which both also decay to the ground state via the formation of fullerene triplets.

Though the majority of C_{60}-Ru and C_{60}-Ru systems do not form charge separated states which is required for light harvesting device applications, they still possess excellent photophysical properties which have resulted in the preparation of a number of novel organic-inorganic hybrid materials. Thus, C_{60}-Ru dyads incorporated within a Zr phosphonate matrix exhibits luminescent properties in the solid state.[135] Additionally, a few examples of amphiphilic C_{60}-Ru derivatives have been synthesised (Figure 16, **54** and **55**) and successfully incorporated into Langmuir films and are of potential interest for technological applications as preparation of photovoltaic devices requires the efficient incorporation of the photoactive compound into thin films.[142,148]

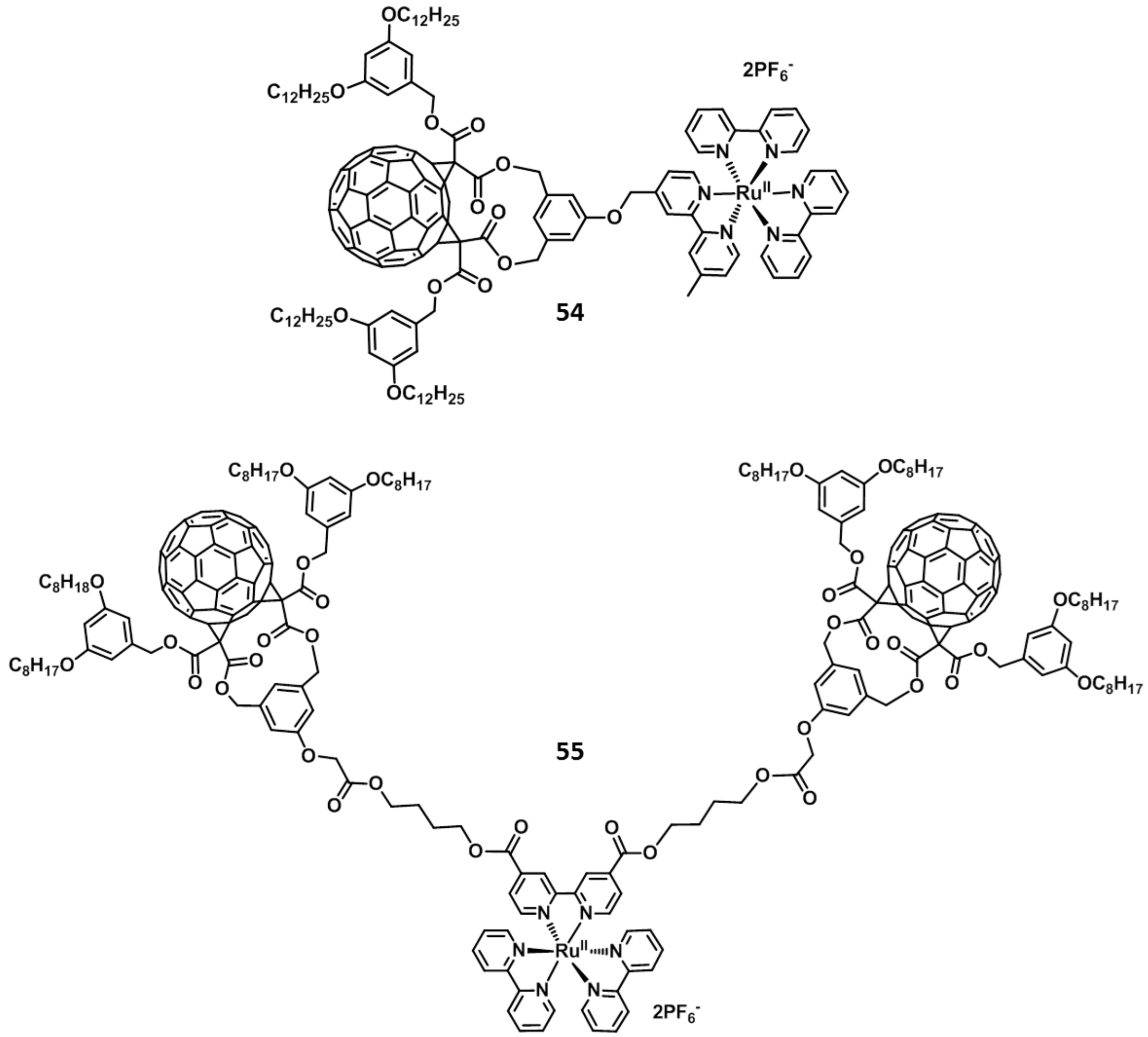

Figure 16. Examples of amphiphilic C_{60}-bipy-Ru complexes (**54**, **55**).[142,148] Reprinted with permission from ref 142, Copyright 2005 Elsevier; ref 148, Copyright 2007 WILEY-VCH Verlag GmbH & Co. KGaA, Weinheim.

The attachment of 1,10-phenanthroline binding moieties to the fullerene cage enables the coordination of Cu^{I} ions to form a variety of polyads with various fullerene:metal ratios including one fullerene cage and one copper centre (Figure 17, **56**), two fullerene cages and one copper centre (Figure 17, **57**) or two fullerene cages and two copper centres (Figure 17, **58**). All of these complexes are prepared via substitution of acetonitrile ligands in $[Cu(CH_3CN)_4]BF_4$ by phenanthroline derivatised fullerene ligands.[153-155] These supramolecular systems possess interesting photochemical properties showing effective luminescence quenching of the MLCT band of the phenanthroline Cu centres by the fullerene moiety. Photoexcitation of the C_{60}-Cu system generates an excited state which decays via competitive charge transfer and electron transfer processes forming C_{60}^{-}-Cu^{2+} radical ion pairs and longer lived fullerene triplets.

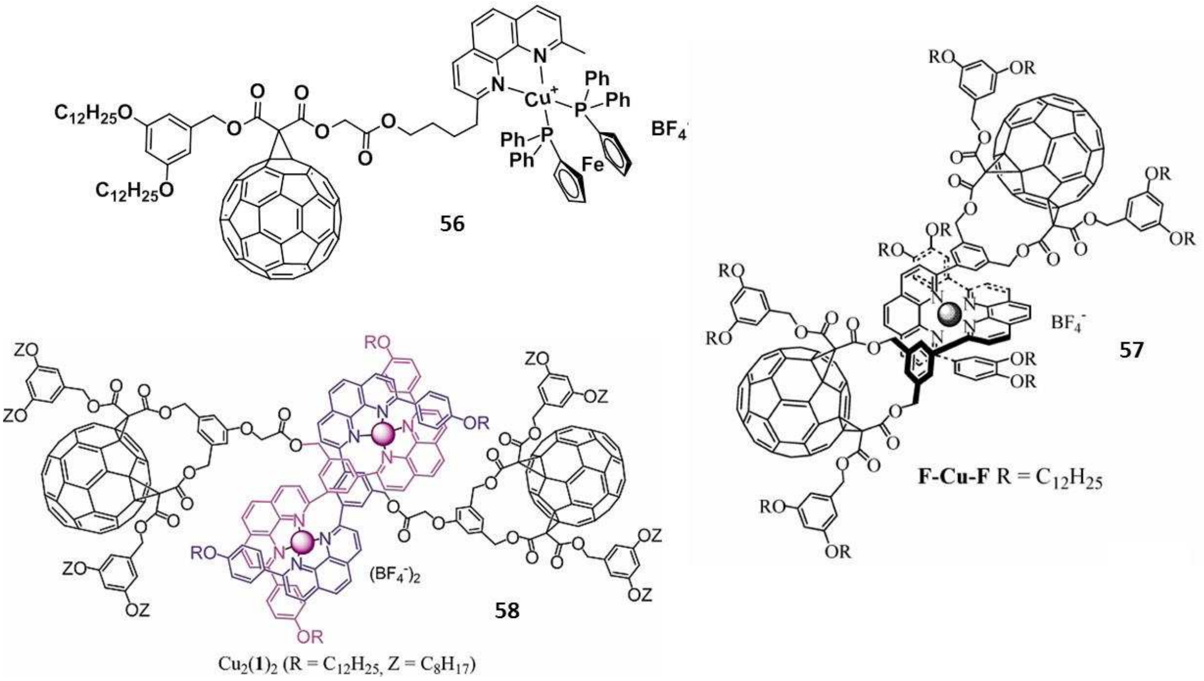

Figure 17. Examples of C_{60}(Phen)-Cu complexes containg containing one fullerene cage and one Cu centre (**56**),[155] two fullerene cages and one (**57**)[153] or two Cu centres (**58**).[154] Reprinted with permission from ref 155, Copyright 2008 American Chemical Society; ref 153, Copyright 2003 American Chemical Society; ref 154, Copyright 2004 Royal Society of Chemistry.

Other N-donor bidentate ligands have also been utilised including a dipyrromethane functionalised C_{60} fullerene which was reported to form a dumbbell shaped complex with Zn in a 2:1 fullerene-metal ratio (Figure 18, **59**). This complex not only exhibited excellent electrochemical, light absorbing and luminescent properties but was also found to form a charge separated state with a lifetime of 990-1516 ps depending on the solvent.[156] N,N’-dimethylethylenediamine has also been attached to a fullerene cage enabling the coordination of Cu^{II} ions generating a magnetically active Cu complex with exhibits a strong

EPR signal (Figure 18, **60**).[160] The diazafluorene metal binding moiety has also been appended to the fullerene cage allowing the coordination of both Ru[157] (Figure 18, **61**) or Ir[158] (Figure 18, **62**) centres both in octahedral geometries. These compounds were found to exhibit interesting second order NLO properties and hence are potential candidates for optoelectronic devices. Finally, an example of C_{60}-pyridazine ligand has also been reported which form a dinuclear complex with Re (Figure 18, **63**) exhibiting a photoinduced electron transfer with the time constant of 105 ps which then decays to the ground state via formation of a fullerene triplet.[159]

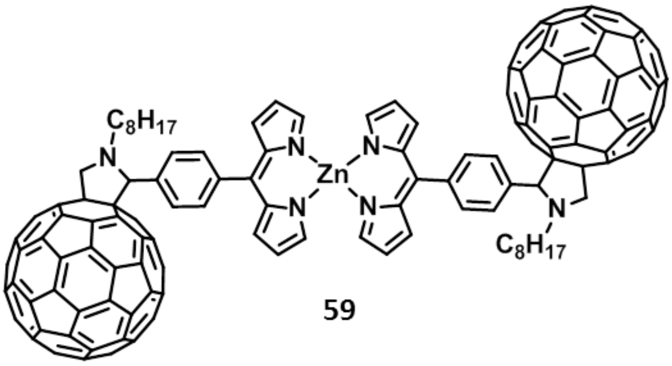

59

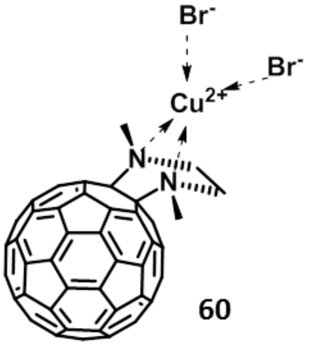

60

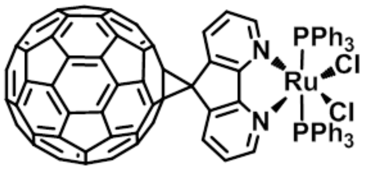

61

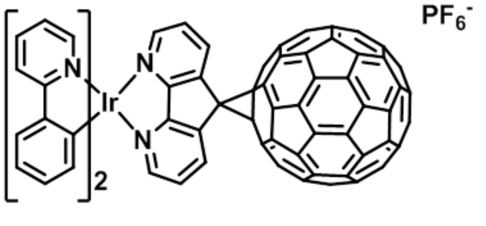

62

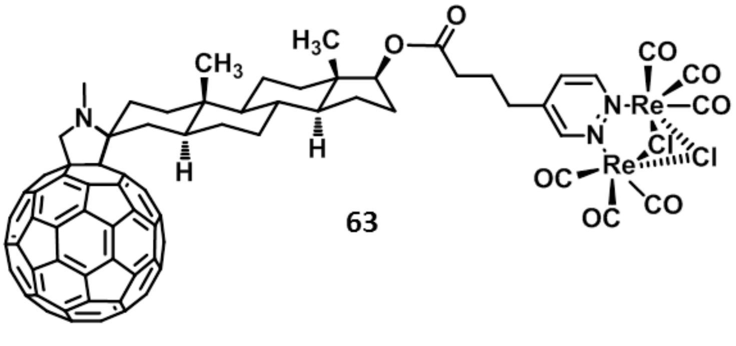

63

Figure 18. A dumbbell complex of a dipyrromethane functionalised C_{60} and Zn (**59**[156]), a Cu complex of a N,N'-dimethylethylenediamine functionalised C_{60} (**60**[160]), and Ru^{II} C_{60}-diazafluorene (**61**)[157] and Ir^{III} C_{60}-diazafluorene (**62**) complexes,[158] and C_{60}-pyridazine-Re_2 complex.[159] Reprinted with permission from ref 156, Copyright 2009 WILEY-VCH Verlag GmbH & Co. KGaA, Weinheim; ref 160, Copyright 2004 Elsevier; 157, Copyright 2010 Royal Society of Chemistry; and ref 158, Copyright 2012 Elsevier; ref 159, Copyright 2015 Royal Society of Chemistry.

Examples of tridentate terpyridine ligands covalently attached to the fullerene cage are less abundant than bipyridine examples however have been reported, first by Diederich and Constable in 1996 and 1998,[162,163] followed by a significant number of other reports. These ligands form analogous ruthenium complexes when prepared from Ru^{III} salts via in situ reduction of the metal centre in the presence of Ag^{I} to form Ru^{II} complexes (Figure 19, **64**).[164,165] These Ru containing compounds were found to possess photochemical properties similar to those of the bipyridine coordinated compounds and form photoexcited states with the potential for charge separation.[164] In addition, Ru open cage C_{60}-fulleroid dyads (Figure 19, **66**) possesses excellent optical limiting properties.[166] Fe^{II} and Co^{II} triads containing two C_{60}-tepryridine ligands coordinated around one metal centre (Figure 19, **65**) have also been reported and though they exhibit limited solubility in common organic solvents this did not preclude the investigation of their photochemical properties. The Fe-terpyridine complex was found to be non-luminescent which was attributed to a very short excited state lifetime which also precluded formation of any charge-separated states upon photoexcitation.[161]

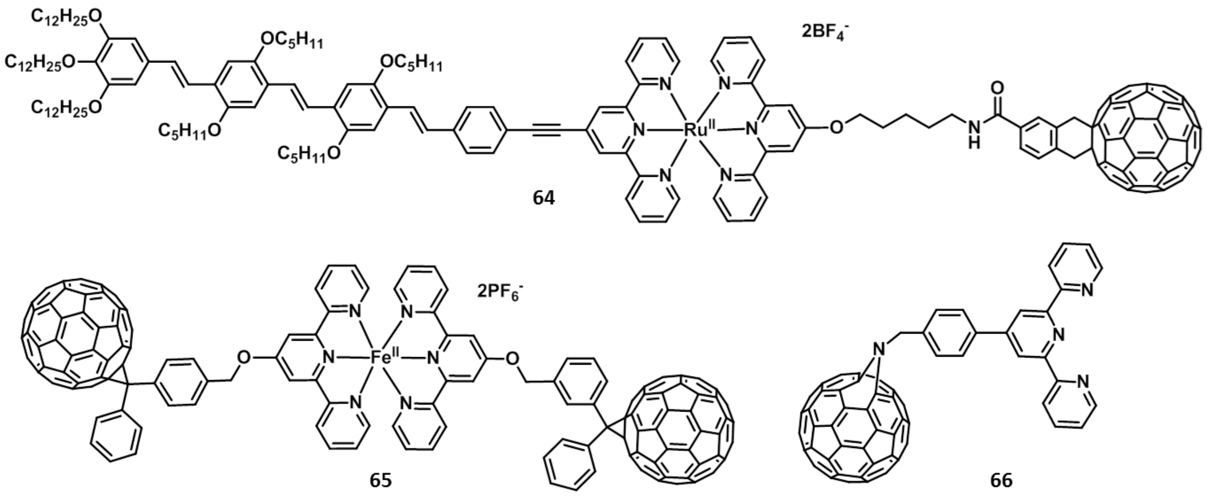

Figure 19. Examples of a C_{60}-terpyridine-Ru dyad (**64**[164]), (C_{60}-terpyridine)$_2$Fe triad (**65** where M=Fe[161]), and an open cage C_{60}-terpyridine ligand (**66**).[165,166] Reprinted with permission from ref 164, Copyright 2002 Elsevier; ref 161, Copyright 2002 Elsevier; and ref 166, Copyright 2003 Springer.

3.1.1.3. Tetradentate N-donor ligands.

Tetradentate metal binding moieties such as porphyrin and phthalocyanine have also been covalently attached to the fullerene cage via multi-step synthetic methodologies. Preparation of these systems is usually non-facile as it requires the synthesis of asymmetric porphyrin/phthalocyanine precursors, however, a number of such molecules have been reported, predominantly containing a coordinated Zn^{II} centre as the resultant systems are very stable and possess interesting properties. Co^{II}, Cu^{II}, Mg^{II} , Ni^{II}, Pd^{II} and Pt^{II} porphyrin-fullerene complexes have also been reported.[167,169,206] In general these complexes are square planar and capable of coordinating solvent molecules to the axial position providing a route to tune the properties of the metal complex. Other metal centres incorporated within C_{60}-porphyrin/phthalocyanine complexes include: square pyramidal Fe^{III}, Mn^{III} and Al^{III} complexes in which the additional ligand in the axial position of the metal complex can be utilised to stabilise the systems,[169,204,205] a square bipyramidal Sn^{IV} complex is which two axial ligands are coordinated to the metal atom,[207,208] a Ti^{IV} phthalocyanine system containing two additional ligands on the same side of the plane,[210] and Lanthanide metals such as Sm, Eu and Lu which form double-decker sandwich type complexes.[217] All of these are summarised in Table 4.

Table 4. Porphyrin and phthalocyanine derivatised fullerene containing metal complexes.

Fullerene cage	Metal	Ligand on the fullerene	C_{60}:M ratio	Lifetime of charge-separated state/other properties	Chromophore	Ref.
C_{60}	Mg^{II}	Porphyrin	1:2	-	-	167
C_{60}	Mn^{III}	Porphyrin	1:1	-	-	168
C_{60}	Mn^{III} Fe^{III} Co^{II} Ni^{II} Cu^{II} Zn^{II}	Porphyrin	1:1	35-118 ps 20-25 ps 762-1713 ps 105-205 ps 520-588 ps 409-678 ps	-	169
C_{60}	Co^{II}, Zn^{II}	Porphyrin	1:1	860 ps in THF, 560 ns in benzonitrile	-	170
$N@C_{60}$	Cu^{II}	Porphyrin	1:1	-	-	171
C_{60}	Zn^{II}	Porphyrin	1:1 2:2 2:3 2:4	-	-	172
C_{60}	Zn^{II}	Porphyrin	2:2	Fullerene to porphyrin ET vs porphyrin to fullerene CT	-	173
C_{60}	Zn^{II}	Porphyrin	1:1 2:1 2:2 2:3 2:4	Fullerene to porphyrin ET	-	174, 175
C_{60}	Zn^{II}	Porphyrin	1:1	Formation of highly stable micro-vesicles	-	176
C_{60}	Zn^{II}	Porphyrin	1:1	90 ps	-	177
C_{60}	Zn^{II}	Porphyrin	1:1	60 ps	-	178
C_{60}	Zn^{II}	Porphyrin	1:1	35-130 ps	-	179
C_{60}, C_{70}	Zn^{II}	Porphyrin	2:1	100 ns	-	180
C_{60}	Zn^{II}	Porphyrin	1:1	445-1990 ns	-	181
C_{60}	Zn^{II}	Porphyrin	1:1	418-844 ns	-	182
C_{60}	Zn^{II}	Porphyrin	1:1	555-714 ns	-	183
C_{60}	Zn^{II}	Porphyrin	1:1	-	-	184
C_{60}	Zn^{II}	Porphyrin	1:1 1:2	1 μs; 286 ns	-	185
C_{60}	Zn^{II}	Porphyrin	1:1	2 μs	Triphenyl amine	186
C_{60}	Zn^{II}	Porphyrin	1:1	8.5 μs; 1 μs	Ferrocene;	187

					triphenylamine	
C_{60}	Zn^{II}	Porphyrin	1:1	7.5 μs	Ferrocene	188
C_{60}	Zn^{II}	Porphyrin	1:1	0.38 s	Ferrocene, H_2 Porphyrin	189
C_{60}	Zn^{II}	Porphyrin	1:1	-	-	190
C_{60}	Zn^{II}	Porphyrin	1:1	-	-	191
C_{60}	Zn^{II}	Porphyrin	1:1	260 μs, 630 μs (triplet CS states)	Ferrocene	192
C_{60}	Zn^{II}	Porphyrin	2:1	Not investigated	-	193
C_{60}	Zn^{II}	Porphyrin	1:6	0.2-0.65 ns; temperature dependant	Porphyrin	194
C_{60}	Zn^{II}	Porphyrin	1:1	Self-assemble into NT; photoconductivity	-	195
C_{60}	Zn^{II}	Porphyrin	1:1	145-435 ns	-	196
C_{60}	Zn^{II}	Porphyrin	1:1	-	-	197
C_{60}	Zn^{II}	Porphyrin	1:1 1:2 1:4	0.64 ns, 7.1 ns, 7.8 ns; small distance dependance	Ferrocene	198
C_{60}	Zn^{II}; Os_3 cluster	Porphyrin	1:4	SAM on ITO based photochemical cell with 29 % efficiency	BODIPY	199
C_{60}	Zn^{II}; Os_3 cluster	Porphyrin	1:4	SAM on ITO based photochemical cell	Ferrocene	200
$La_2@C_{80}$; $Sc_3N@C_{80}$	Zn^{II}	Porphyrin	1:1	170-230 ps; 62-108 ps; 42-49 ps	-	201
$Sc_3N@C_{80}$	Zn^{II}	Porphyrin	1:1	1-3.2 μs	-	202
$Ce_2@C_{80}$	Zn^{II}	Porphyrin	1:1	55-115 ps	-	203
C_{60}	Al^{III}	Porphyrin	1:1	39-100 ns	Phenothiazine	204
C_{60}	Al^{III}	Porphyrin	1:1	17 ns	Ferrocene	205
C_{60}	Pd^{II}, Pt^{II}	Porphyrin	1:1	Energy transfer processes	-	206
C_{60}	Sn^{IV}	Porphyrin	2:1	-	-	207
C_{60}	Sn^{IV}	Porphyrin	1:1	Formation of nanowires	-	208
C_{60}	Zn^{II}, Ni^{II}	Porphyrin, Phthalocyanine	1:2 2:3	168-3000 ps; 1-2 ns; 0.5-1.6 ns	H_2 Porphyrin	209
C_{60}	Ti^{IV}	Phthalocyanine	1:1	1.74 μs	-	210
C_{60}	Cu^{II}	Phthalocyanine	1:1	-	-	211
C_{60}	Zn^{II}	Phthalocyanine	1:1	-	-	212
C_{60}	Zn^{II}	Phthalocyanine	1:1	-	-	213
C_{60}	Zn^{II}	Phthalocyanine	1:1	220-5530 ps	-	214
C_{60}	Zn^{II}	Phthalocyanine	1:1	-	-	215
C_{60}	Zn^{II}	Phthalocyanine	1:1	30 ns	-	216
C_{60}	Zn^{II}	Phthalocyanine	1:1	-	-	121
C_{60}	Sm^{III}, Eu^{III}, Lu^{III}	Phthalocyanine	1:1	>3 ns	-	217
C_{60}	Fe^{II},	Tribenzotetraaza	1:1	-	-	218

	Co^{II}	chlorin				

The properties of fullerene-porphyrin/phthalocyanine systems combine the individual features of the fullerene and metal containing moieties which results in systems capable of absorbing light across the whole UV, visible and NIR spectrum. The electron accepting properties of the fullerene cage and electron donating properties of the metal containing moiety combine to create systems capable of reversibly accepting and donating electrons readily. The fluorescence of the metal porphyrin moiety is quenched by the fullerene cage indicating electronic interactions between the two units in the excited state. Above all, these systems possess unique photophysical properties forming charge separated species upon photoexcitation with variable lifetimes, see Table 4.

The lifetimes of the charge separated states depend primarily on the distance between the metal porphyrin moiety and the fullerene cage. In systems where the two units are separated by short linkers charge separated states are either not observed as in the case of azulenocyanine-Zn (Figure 20, compound **69)**[121] or are relatively short lived with the reported lifetimes in the 60-90 picosecond range (Figure 20, compound **67**, **68**).[177-178] This is attributed to energy wasting charge recombination processes that can easily occur in these systems. The same trend is observed in C_{60}-Zn(Phthalocyanine) systems[212,213] and is also observed for the systems in which the metalloporphyrin unit is attached via bis-functionalisation of the fullerene cage (Figure 21). In this case despite relatively long chain linkers the metalloporphyrin unit is still located a short distance, several Å, from the fullerene cage which is determined by the sterical restrictions imposed by the method of functionalisation.[169,170,179] Thus, such ZnPorphyrin complexes shows formation of charge-separated species with the lifetime of 35-130 ps (Figure 21, **70**).[179] Similar observations have been reported for other metals, including Cu^{II}, Fe^{III}, Co^{II}, Mn^{III}, and Ni^{II}, showing the shortest lifetimes for Fe^{III} (20-25 ps) and Mn^{III} porphyrins (35-118 ps) and the longest lifetimes for Zn^{II} (409-768 ps) and Co^{II} porphyrins (762-1713 ps) (Figure 21, **71**).[169] On the contrary, Pd^{II} and Pt^{II} porphyrin-C_{60} dyads exhibited no evidence of charge-separated state formation but triplet energy transfer processes only.[206] Interestingly, these lifetimes are solvent dependant, for example the Co-C_{60}-porphyrin complex has a charge separated state lifetime of 890 ps in tetrahydrofuran but 560 ns in benzonitrile (Figure 21, **72**). This is attributed to axial coordination of the solvent molecule which affects the stability of the oxidised state of the metal centre.[170]

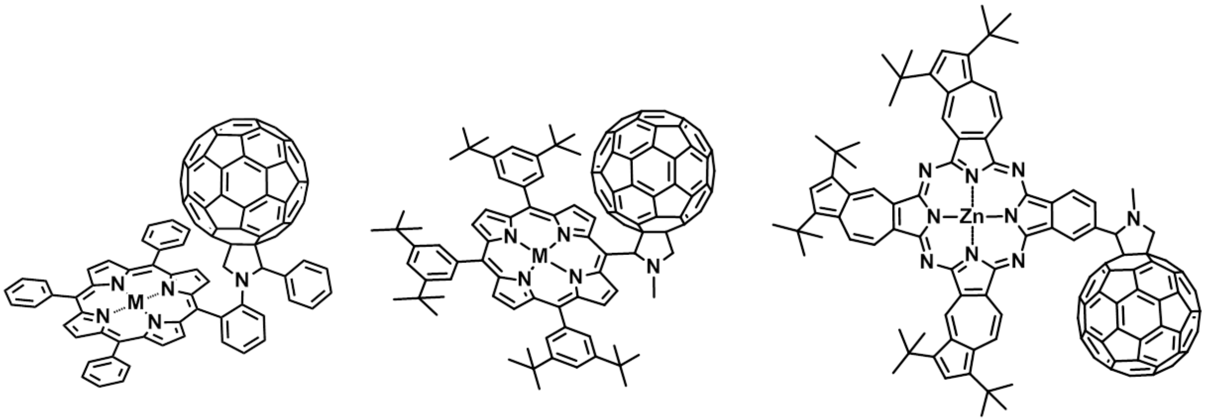

67 **68** **69**

Figure 20. Zn porphyrin complexes covalently linked in close proximity to the C_{60} fullerene cage (**67)**, where M=Zn,[177] (**68)**, where M=Zn,[178] and (**69)**.[121] Reprinted with permission from ref 177, Copyright 2012 WILEY-VCH Verlag GmbH & Co. KGaA, Weinheim; ref 178, Copyright 2003 American Chemical Society; and ref 121, Copyright 2012 Royal Society of Chemistry.

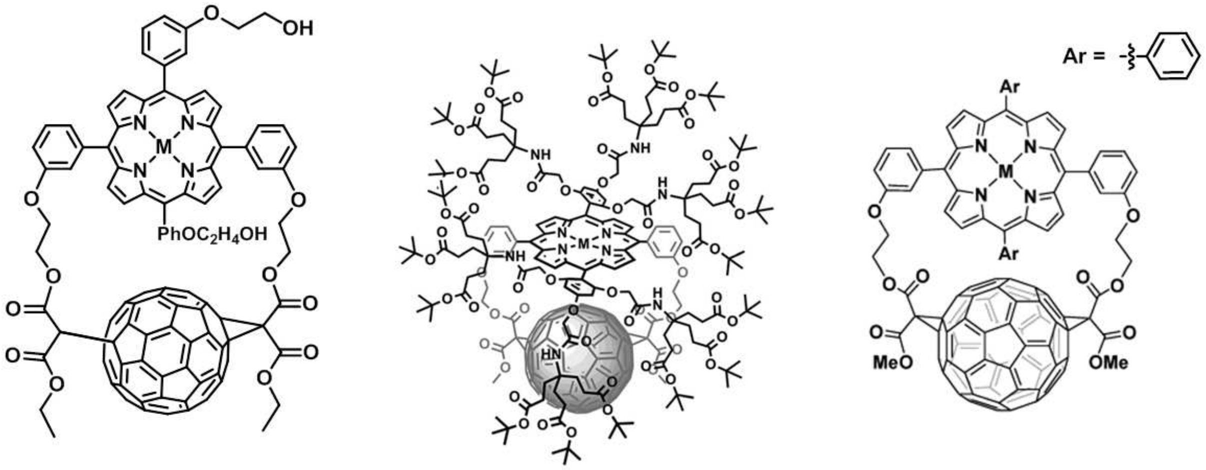

70 **71** **72**

Figure 21. Metalloporphyrins covalently linked in close proximity to the C_{60} fullerene cage by bis(cyclopropane) functionalisation (**70),**[179] (**71**), where M=Cu, Fe, Co, Mn and Ni,[169] and (**72**), where M=Zn and Co.[170]. Reprinted with permission from ref 179, Copyright 2011 American Chemical Society; ref 169, Copyright 2012 WILEY-VCH Verlag GmbH & Co. KGaA, Weinheim; ref 170, Copyright 2004 American Chemical Society.

Systems which contain oligoporphyrins, either triply fused (Figure 22, **73**) or linked sequentially in meso,meso-positions (Figure 22, **74**) attached in close proximity to the C_{60} have also been reported.[172-175] These systems have exceptional multicharge storage capacity due to the large number of electrons that can be reversibly exchanged, and show weak ground-state prophyrin-porhyrin and porphyrin-fullerene interactions. Excited state properties differ between the triply fused porphyrin dimers (**73**) and meso,meso-linked diporphyrins (**74**). Despite being a better electron donor, triply fused porphyrin dimers are also very good energy acceptors with low-lying short-lived siglet excited states, and favour C_{60} to porphyrin energy transfer processes in **73**, whereas **74** exhibits more traditional porphyrin to fullerene charge transfer processes.[173,175]

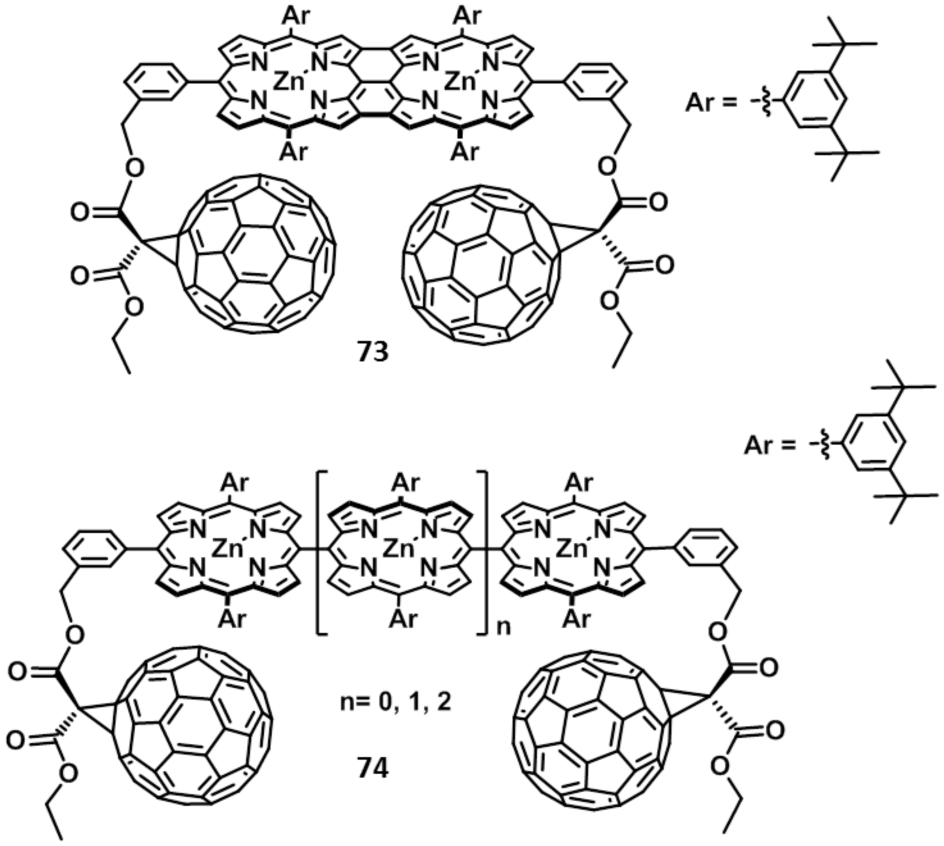

Figure 22. Triply fused porphyrin dimer (**73**)[173] and meso,meso-linked oligoporphyrins (**74)**[175] containing fullerene dumbbells. Reprinted with permission from ref 173, Copyright 2003 WILEY-VCH Verlag GmbH & Co. KGaA, Weinheim; ref 174, Copyright 2005 WILEY-VCH Verlag GmbH & Co. KGaA, Weinheim.

A variety of attempts to improve the stability of charge-separated radical ion pairs have been reported in which the length and the nature of the spacer between the fullerene cage and the metal containing moiety were varied. Systematic variation of the linker length resulted in an increase in the lifetimes of the charge-separated states up to the hundreds of nanoseconds range,[182,185,209,214,216] and an increase in the radical ion pairs lifetimes from 555 to 714 ns[183] and from 445 ns to 1190 ns[181] (Figure 23, **75**, **76**). The nature of the bridging group was also shown to play an important role. Thus, utilisation of rigid conjugated wires such as carbon-bridged oligo-p-phenylenevenylenes (Figure 23, **77**) showed an 840-fold increase in the electron transfer rates compared with equivalent flexible molecular bridges.[184] A lifetime of 100 ns was reported for systems containing both C_{60} and C_{70}

fullerene cages as a result of a negative charge shift from the C_{60} to the C_{70} cage, this resulted in a longer distance between the charges in the $C_{70}^{\cdot -}$-C_{60}-Zn(Porphyrin)$^{\cdot +}$ radical-ion pair (Figure 23, **78**).[180]

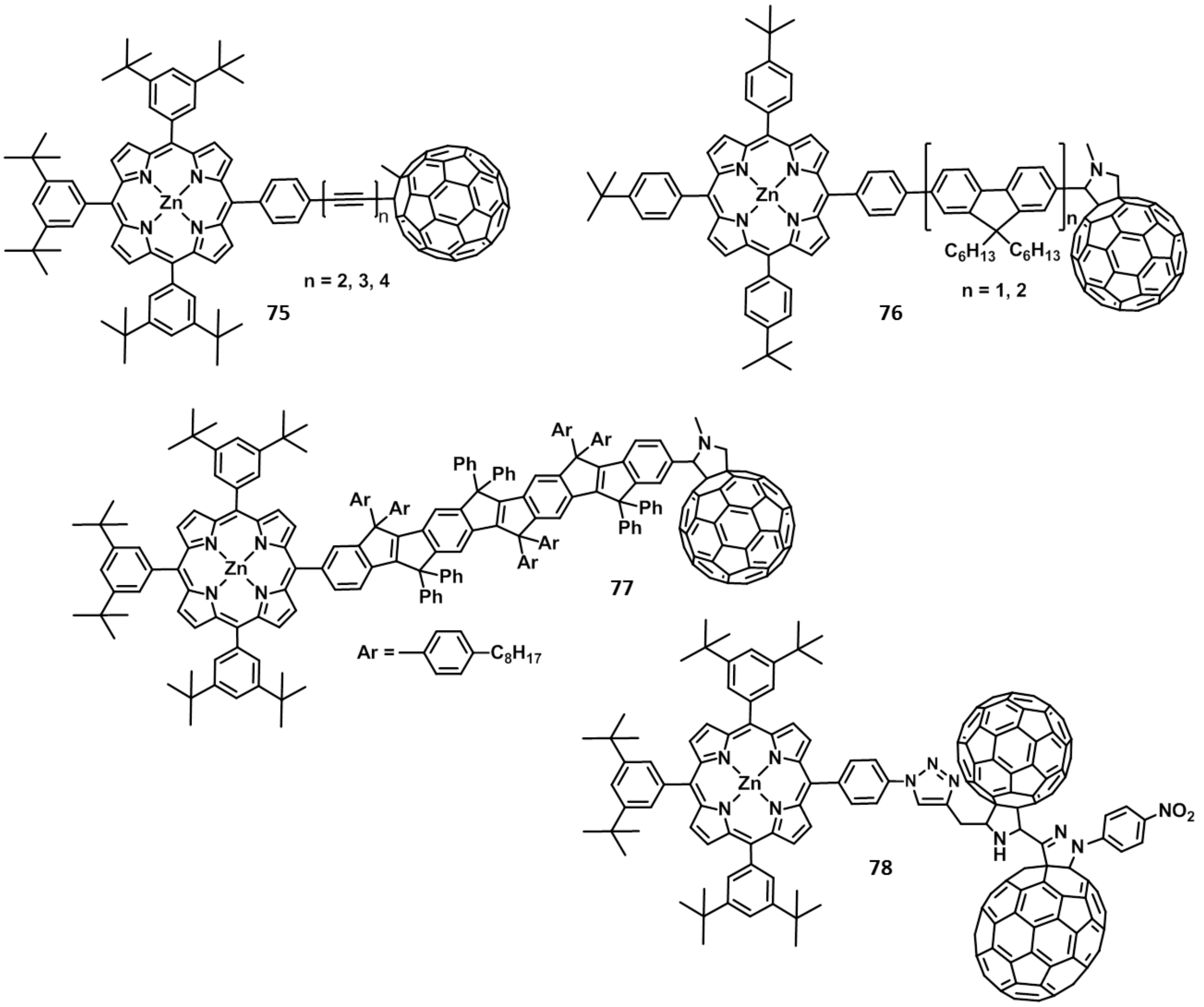

Figure 23. Zn(Porphyrin) complexes covalently attached to the fullerene cage via variable length linkers (**75**,**76**),[183,181] a dyad containing a carbon-bridged oligo-p-phenylenevenylene wire bridge (**77**)[184] and a Zn(Porphyrin)-C_{60}-C_{70} triad (**78**).[180] Reprinted with permission from ref 183, Copyright 2005 WILEY-VCH Verlag GmbH & Co. KGaA, Weinheim; and ref 181, Copyright 2010 American Chemical Society; ref 184, Copyright 2014 Nature Publishing Group; ref 180, Copyright 2011 Royal Society of Chemistry.

As in the case of monodentate C_{60}-pyridine ligands coordinated to the axial position of Zn(Porphyrin) systems mentioned above, the longest CS state lifetimes were observed in systems which incorporated additional chromophores or electron donors which allow positive charge (hole) shifts from the Zn(Porphyrin)$^{\cdot+}$ to the electron donor resulting in better spatial separation and the formation of more stable radical ion pairs. Addition of three triphenylamine groups into a Zn(Porphyrin)-C_{60} dyad (Figure 24, **79**) resulted in a lifetime of 2 μs in polar benzonitrile.[186] Triphenylamine moieties act as primary chromophores generating an energy-transfer from the excited state of triphenylamine to the Zn porphyrin moiety, which is followed by electron transfer from the Zn porphyrin to the fullerene cage. Significant stabilisation of the charge-separated state is attributed to the stabilisation of the Zn(Porphyrin) radical-cation due to charge delocalisation over the three triphenylamine groups.[186] Combining Zn(Porphyrin) which contains a BODIPY unit or ferrocene unit with C_{60} via an Os_3 cluster created a unique, fully conjugated donor-acceptor moiety which undergoes ultrafast light-induced processes (Figure 24, **80**).[199,200] Furthermore, these molecules can form SAMs on ITO surfaces which have been used to build a photochemical cell with 29 % efficiency which is the highest ever reported for SAM based devices.[199] The addition of a ferrocene moiety covalently attached to the Zn(Porphyrin) enabled a positive charge shift to be achieved from the Zn(Porphyrin)$^{\cdot+}$ to the ferrocene moiety with the formation of a long distance separated $C_{60}^{\cdot-}$-Zn(Porphyrin)-Ferrocene$^{\cdot+}$ radical ion pair with the lifetime of 7.5-8.5 μs[187,188] (Figure 24, compound **81**) and up to 630 μs due to the formation of a triplet charge-separated state.[192] Interesting, separating the ferrocene donor and C_{60} acceptor by one, two or four Zn(Porphyrin) units (Figure 24, **82**) did not result in a significant increase in the CS state lifetimes.[198] However separation of the Ferrocene-Zn(Porphyrin) moiety and C_{60} by incorporating an additional H_2(Porphyrin) unit into the system (Figure 24, structure **83**) resulted in a significant increase in lifetime up to 0.38 s which is one of the longest observed for arthificial synthetic systems and is comparable to the bacterial photosynthetic reaction centre.[189]

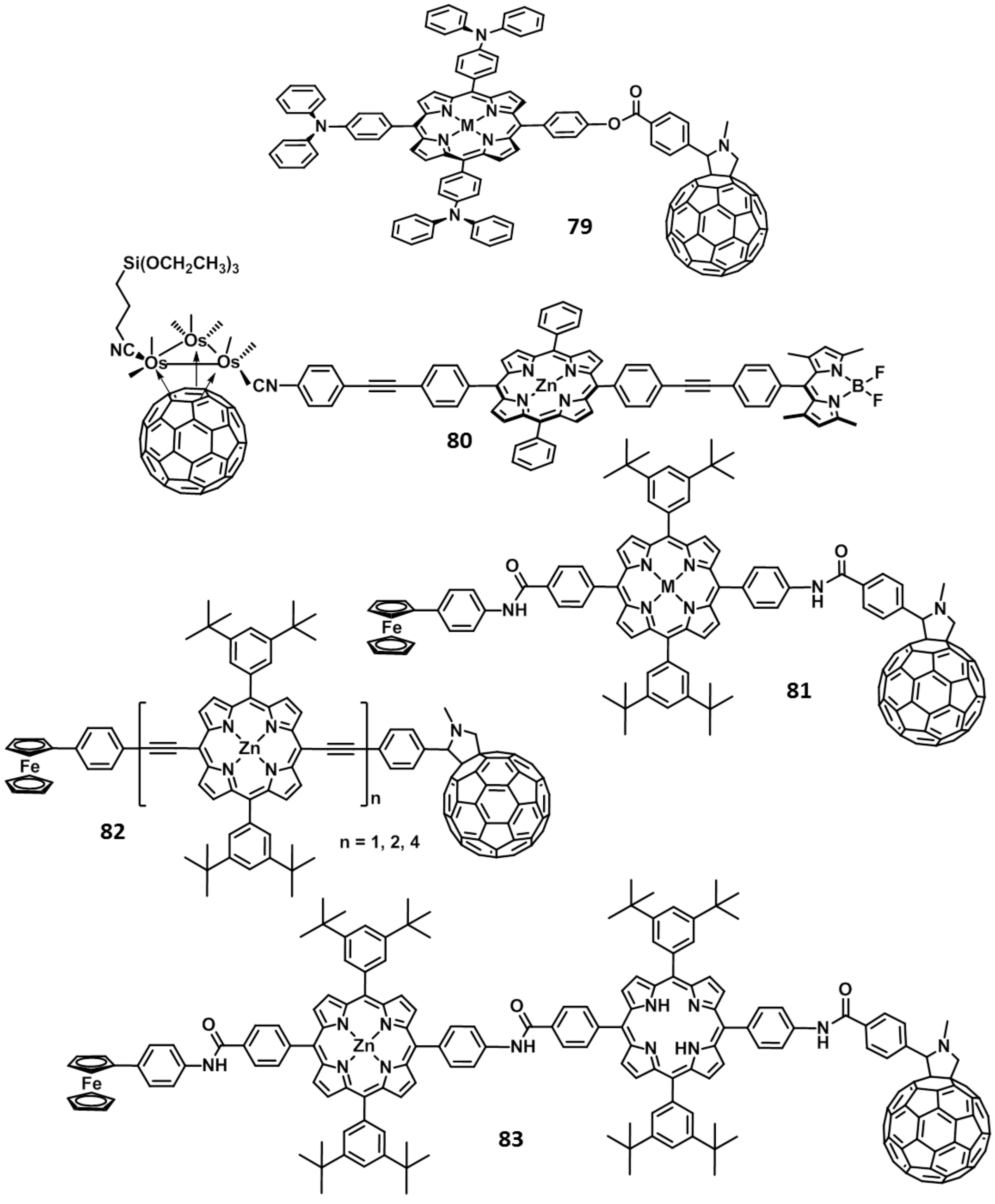

Figure 24. Ferrocene-Zn(Porphyrin)-C$_{60}$ triads (**79**), where M=Zn,[186] (**80**),[199] (**81**), where M=Zn,[188] (**82**),[198] and (**83**).[189] Reprinted with permission from ref 186, Copyright 2007 American Chemical Society; ref 199, Copyright 2010 WILEY-VCH Verlag GmbH & Co. KGaA, Weinheim; ref 188, Copyright 2001 American Chemical Society; ref 198, Copyright 2007 American Chemical Society; and ref 189, Copyright 2001 American Chemical Society.

C_{60} can be incorporated into Al(Porphyrin) complexes via a benzoate spacer in the axial position of an Al^{III} centre (Figure 25, **84**). In similarly fashion to Zn(Porphyrin)C_{60} dyads, spectroscopic studies of Al(Porphyrin)C_{60} complexes suggest that the ground state electronic structures of both fullerene and Al(Porphyrin) units are not perturbed, whereas efficient electron transfer exists upon photoexcitation with the formation of an Al(Porphyrin)$^{\cdot+}$-$C_{60}^{\cdot-}$ radiacal-ion pair with a lifetime of 39 ns. Interestingly, incorporating ferrocene, which is a stronger electron donor, into this system (Figure 25, **85**) resulted in a decrease in the CS state lifetime to 17 ns which was attributed to more efficient charge recombination process via a low-lying triplet state of ferrocene, as discussed earlier in section 2.[205] Incorporating a phenothiazine (PTZ) axially coordinated to the Al centre as a second electron donor (Figure 25, **86**) resulted in a hole shift from the porphyrin radical-cation initially formed upon photoexcitation, and the formation of a PTZ$^{\cdot+}$-Al(Porphyrin)-$C_{60}^{\cdot-}$ radical ion pair with a lifetime of up to 100 ns.[204]

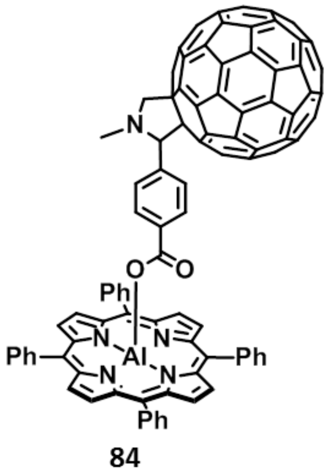

84

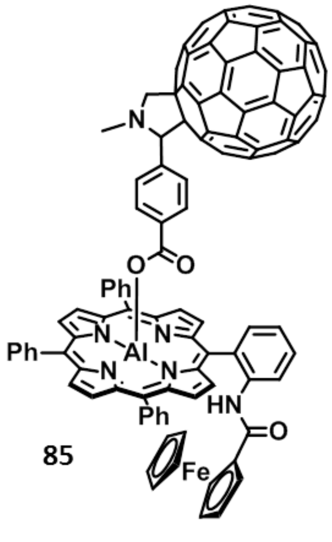

85

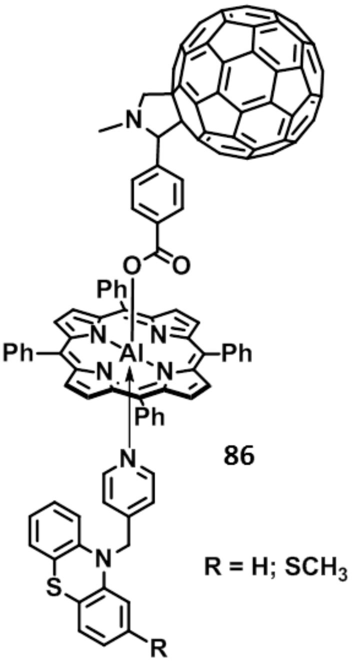

86

Figure 25. C_{60}-Al(Porphyrin) complexes (**84**),[205] (**85**),[205] and (**86**).[204] Reprinted with permission from ref 205, Copyright 2010 American Chemical Society; ref 204, Copyright 2011 American Chemical Society.

Endohedral fullerene cages have also been functionalised with metal porphyrin moieties. A N@C_{60}-Cu(Porphyrin) dyad (Figure 26, **87**) showed strong electronic coupling between the N atom and the Cu centre which was proposed to have significant application in quantum computing.[171] $Ce_2@C_{80}$ (Figure 26, **88**), $La_2@C_{80}$ and $Sc_3N@C_{80}$ (Figure 26, **89**) all exhibit photophysical properties similar to those of C_{60} containing molecules with charge separated state lifetime dependent on the linker length between the fullerene and metal porphyrin units.[201-203] Interestingly, $Ce_2@C_{80}$ (Figure 26, **88**) showed a solvent dependence on the nature of the charge separated state, forming $(Ce_2@C_{80})^{\cdot-}$-Zn(Porphyrin))$^{\cdot+}$ in non-polar solvents and forming a unique p-type fullerene material, $(Ce_2@C_{80})^{\cdot+}$-(Zn(Porphyrin))$^{\cdot-}$, in polar solvents.[203]

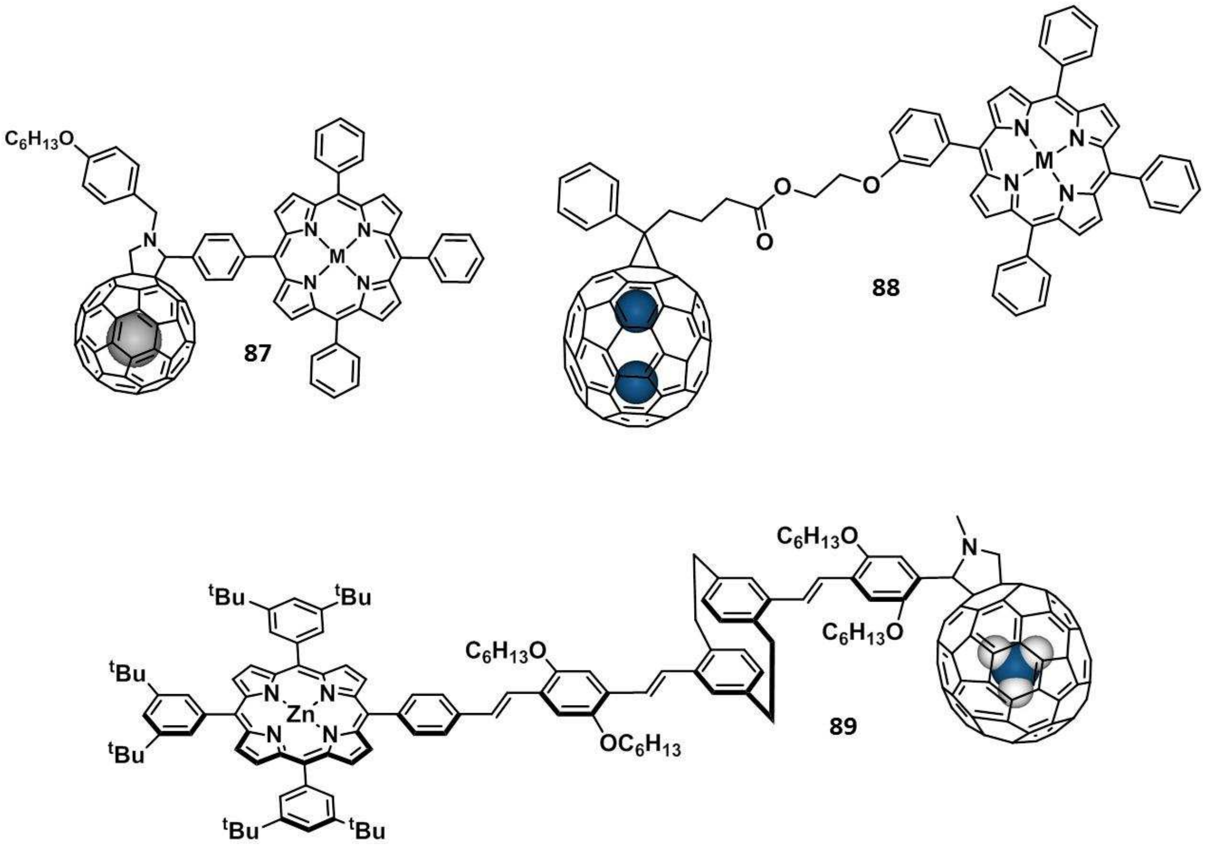

Figure 26. Endohedral fullerene-porphyrin complexes N@C_{60}-MPorphyrin(**87**), where M=Cu,[171]; Ce_2@C_{80}-M(Porphyrin) (**88**) where M=Zn,[203]; and (**89**), Sc_3N@C_{80}-Zn(Porphyrin).[202] Reprinted with permission from ref 171, Copyright 2012 American Chemical Society; ref 203, Copyright 2010 American Chemical Society; ref 202, Copyright 2011 Royal Society of Chemistry.

Fullerene containg tetradentate N-donor ligand complexes have been shown to exhibit a range of other useful properties. For example, a C_{60}-Zn(Phthalocyanine) dyad containing a flexible spacer (Figure 27, **90**) displays liquid crystalline properties self-organizing in columnar stacks within a rectangular arrangement.[215] A C_{60}-Cu(Pthalocyanine) dyad (Figure 27, **91**) forms nanoparticles in solution with enhanced optical limiting properties compared to the solution sample which creates the possibility of using nanoparticles of organic materials as propmising optical limiting materials.[211] Catalytic and photocatalytic properties of fullerene-metalloporphyrin complexes have also been explored. Thus, a C_{60}-Zn(Porphyrin) dyad (Figure 27, **92**) was incorporated into a multicomponent system effective for photoinduced H_2 evolution.[190] Furthermore, Co and Fe complexes of a fullerene-tribenzotetraazachlorin dyad (Figure 27, **93**) showed high efficiency in electrocatalytic oxygen reduction at relatively low onset potentials.[218]

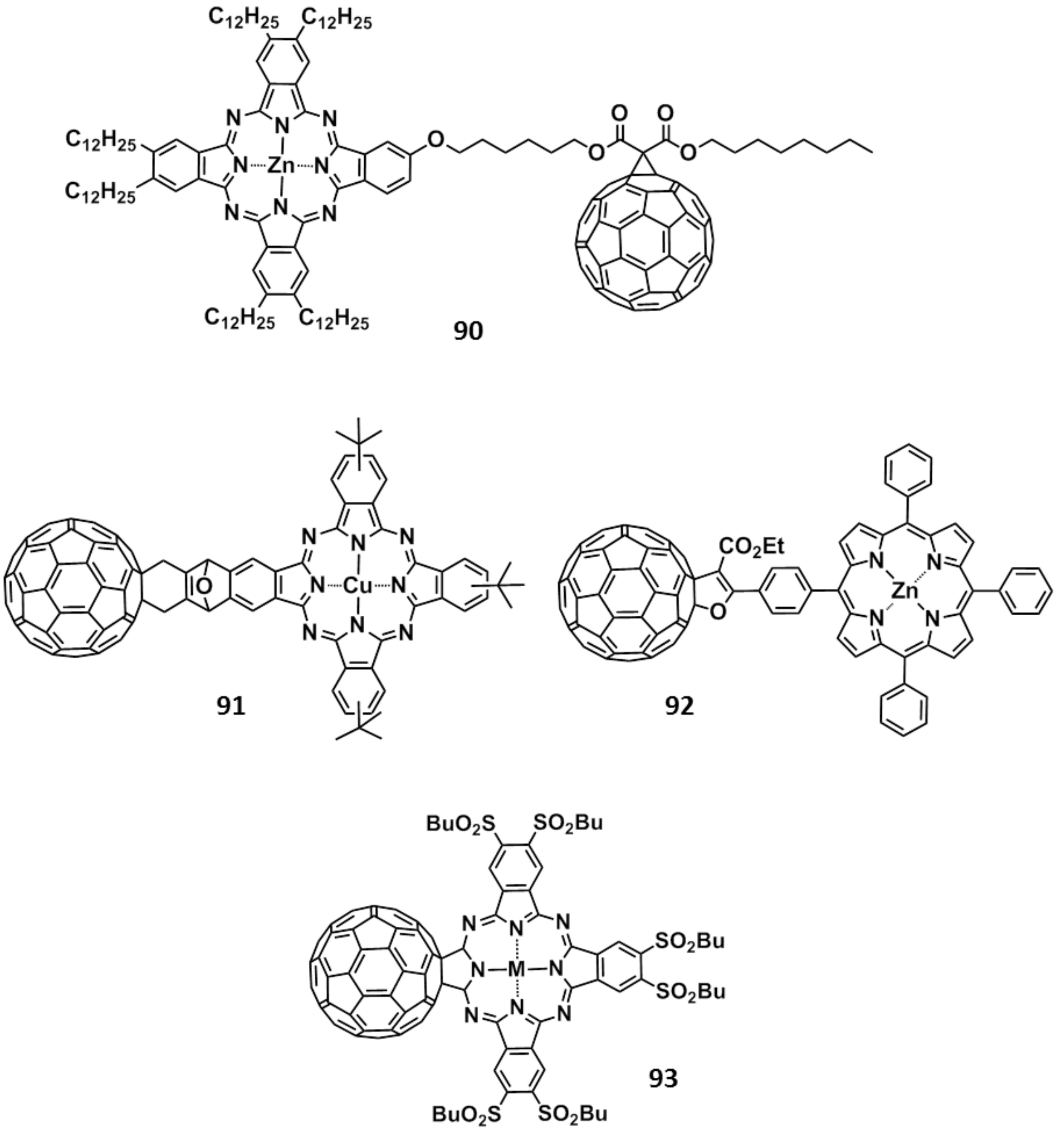

Figure 27. Examples of a C_{60}-Zn(Phthalocyanine) (**90**),[215] and C_{60}-Cu(Phthalocyanine) dyads (**91**),[211] and the catalytically active C_{60}-Zn(Porphyrin) complex (**92**),[190] and C_{60}-tribenzotetraazachlorin dyad (**93**), where M=Co or Fe.[218] Reprinted with permission from ref 215, Copyright 2011 Royal Society of Chemistry; ref 211, Copyright 2005 Elsevier; ref 190, Copyright 2011 American Chemical Society; ref 218, Copyright 2009 Elsevier.

3.1.2. Other ligand groups.

Other metal binding units have been covalently attached to the fullerene cage and are summarised in Table 5.

Table 5. Non-N-donor metal binding units covalently attached to the fullerene cage.

Fullerene cage	Metal	Metal binding unit	C_{60}:M ratio	Properties	Ref
C_{60}	$V^{IV}O$, Cr^{III}, Mn^{III}, Fe^{III}, Co^{II}, Ni^{II}, Cu^{II}, Zn^{II}, Pd^{II}	Salen (N_2O_2-donor)	1:1	Redox activity; absorption on nanotubes; catalyst for styrene epoxidation	219
C_{60}	Cu^{II}	Salen (N_2O_2-donor)	1:1	Homogeneous and heterogeneous catalyst for styrene epoxidation	220
C_{60}	Re^{I}, Ir^{III}, Pt^{II}	2-oxyphenyl isoxazoline (N,O-donor)	1:1	Catalytically active	221
C_{60}	Mn^{I}, Re^{I}	1,2-benzoquinone (O,O-donor)	1:1	Paramagnetic complex	222
C_{60}	Os^{0}	Diphenylphospino fullerene (P,η^2-donor)	1:6	-	223
C_{60}	W^{0}, Os^{0}, Ru^{0}	Diphenylphospino fullerene (P,η^2-donor)	1:1, 1:3	Redox activity	224
C_{60}	Re^{I}	Diphenylphospino fullerene (P,η^2-donor)	1:1, 1:2	Redox activity	225
C_{60}	Fe	Azadithiolate (S,S-donor)	1:2; 1:4	[Fe]Hydrogenase active site mimic	226
C_{60}	Fe	Azadithiolate (S,S-donor)	1:2	[Fe]Hydrogenase active site mimic	227
C_{60}	Pt^{II}	Acetylide	2:1	Photoinduced charge separation with 400 ps lifetime; organic photovoltaic device fabricated	228
C_{60}	Pt^{I}	Acetylide	1:1	Luminescence; photoinduced energy transfer	229

The N_2O_2-donor salen group attached to C_{60} has been reported to form complexes with a range of first and second row transition metals including $V^{IV}O$, Cr^{III}, Mn^{III}, Fe^{III}, Co^{II}, Ni^{II}, Cu^{II}, Zn^{II} and Pd^{II} with either square-planar or square-pyramidal metal centres (Figure 28, **94**).[219] These complexes were found to possess rich, metal dependant electrochemistry. Furthermore, the Cu-salen-C_{60} complex was found to promote double bond epoxidation reactions and was incorporated into heterogeneous carbon nanostructure supported catalysts with excellent activity and recyclability.[220] The 2-oxyphenyl isoxazoline N,O-donor binding ligand (Figure 28, **95**) was found to bind heavier second and third row transition metals such as Re^{I}, Ir^{I}, Pt^{II} forming metal fullerene compounds that are also potentially catalytically active.[221] A quinone type O,O-donor fullerene ligand is reported to bind Mn and Re with the formation of paramagnetic compounds (Figure 28, **96**).[222]

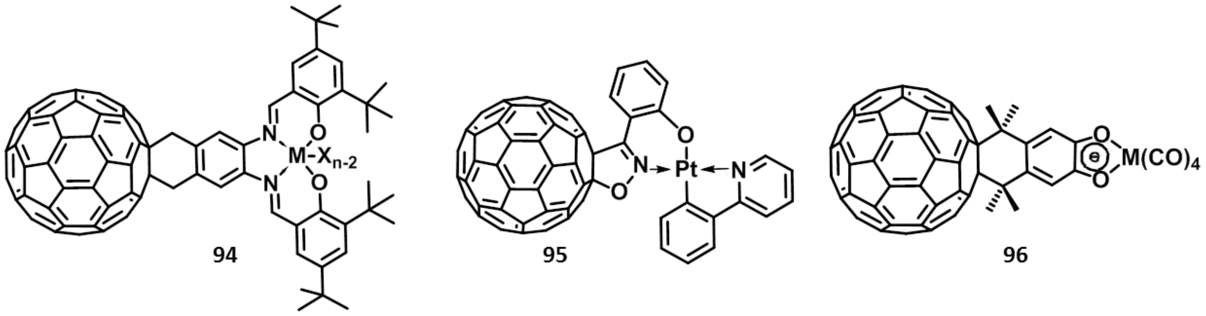

Figure 28. Metal salen N_2O_2 complexes (**94**), where M= VO, Cr^{III}, Mn^{III}, Fe^{III}, Co^{II}, Ni^{II}, Cu^{II}, Zn^{II}, and Pd^{II}; and X=Cl)[219], a N,O-donor Pt receptor (**95**),[221], and a quinone-type complex (**96**), where M=Mn and Re[222] covalently attached to the fullerene cage. Reprinted with permission from ref 219, Copyright 2013 WILEY-VCH Verlag GmbH & Co. KGaA, Weinheim; and ref 221, Copyright 2011 American Chemical Society; ref 222, Copyright 2001 Springer.

P-donor diphenyl phosphine was successfully attached to fullerene to form a new class of compounds with the formula $C_{60}(H)PPh_2$ that can coordinate heavy second and third row transition metals in what is formally a η^3 mode involving the electron pair of the phosphorus atom and the π-π system of one or more of the C-C bonds of the fullerene cage (Figure 29, **97**).[223-225] These complexes have been reported to catalyse a variety of reactions in which the activity and selectivity of the reaction can be controlled by the steric and electronic effects of the substituents at the phosphorous atom. $C_{60}(H)PPh_2$ has also been used to act as redox-active unit which when attached to a model [FeFe]hydrogenase core can mimic the activity of the hydrogenase enzyme (Figure 29, **98**).[226,227] These complexes exhibit extensive electron communication in the doubly reduced state between the reduced fullerene cage and the Fe_2 centres. Acetylide was successfully used as a ligand to attach a Pt centre to the fullerene cage in combination with either a secondary electron accepting terpyridine[229] or an electron donating thiophene group.[228] This resulted in the formation of photoactive systems exhibiting energy transfer and electron transfer with a 400 ps lifetime upon photoexcitation. The thiophene containing triad (Figure 29, **99**) was also utilised as an active material in an organic photovoltaic (OPV) device with comparatively good efficiency.

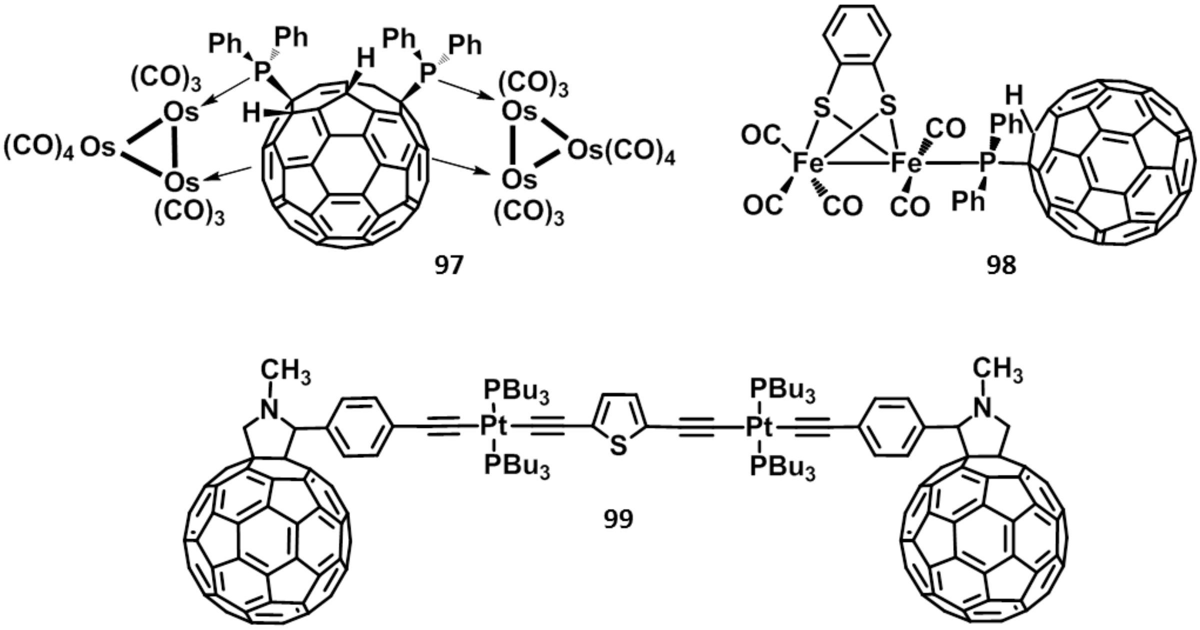

Figure 29. Other metal binding units attached to the fullerene cage including P-donor (**97**),[223] S,S-donor (**98**)[227] and acetylide (**99**)[228] ligands. Reprinted with permission from ref 223, Copyright 2011 American Chemical Society; ref 227, Copyright 2012 American Chemical Society; and ref 228, Copyright 2007 Royal Society of Chemistry.

3.2. Fullerene-Metal complexes based on non-covalent interactions.

Creating systems in which metal containing moieties and fullerene cages are held together using non-covalent interactions is an attractive strategy as it provides the opportunity to create systems which can be influenced by applied stimuli such as pH, solvent polarity, temperature etc. Also synthetically non-facile, multi-step routes to form asymmetric metal centres can be avoided. A variety of approaches have been used to form such systems, including fullerene and metal centres functionalised with complementary hydrogen bonding motifs, ammonia and crown ether coordination sites and the targeted preparation of mechanically interlocked systems such as catenanes and rotaxanes. These approaches and the resulting fullerene-metal supramolecular assemblies are summarised in Table 6.

Table 6. Non-covalent transition metal-fullerene complexes.

Fullerene cage	Metal	Metal binding unit	C_{60}:M ratio	Type of non-covalent interaction	Binding constant (K_a, M^{-1})	Lifetime of charge-separated state	Ref
C_{60}	Fe^{II}	Ferrocene	1:1	Quadruple hydrogen bonding	-	Inefficient CT; Triplet-triplet energy transfer k=$9.2x10^5$ s^{-1}	230
C_{60}	Zn^{II}	Porphyrin	1:1	Quadruple hydrogen bonding	-	4 μs	231
C_{60}	Zn^{II}	Porphyrin	1:2	Three-point hydrogen bonding	$6.2x10^3$ in CH_3CN/ODCB	200 ns	232
C_{60}	Zn^{II}	Porphyrin	1:1	Watson-Crick hydrogen bonding	$5.1x10^4$ in CH_2Cl_2	2.02 μs	233
C_{60}	Zn^{II}	Phthalocyanine	1:1	Watson-Crick hydrogen bonding	$2.6x10^6$ in toluene/CH_2Cl_2	3 ns	234
C_{60}	Zn^{II}	Porphyrin	1:1	Hamilton type hydrogen bonding	$4.4x10^3$ in ODCB	20 μs	235
C_{60}	Zn^{II}, Sn^{IV}	Porphyrin	1:1	Hamilton type hydrogen bonding	$2.8x10^3$-$7.5x10^4$ in CH_2Cl_2	CT in ZnP, ET in SnP	236
C_{60}	Zn^{II}	Porphyrin	1:1	Hamilton type hydrogen bonding	$1.5x10^2$-$4.6x10^4$ in CH_2Cl_2	Not observed in the longest spacer	237
C_{60}	Zn^{II}	Porphyrin	2:1	Hamilton receptor hydrogen bonding	$2.0x10^3$ in ODCB	3 ns	238
C_{60}	Zn^{II}	Porphyrin	1:1	Amidinium-carboxylate hydrogen bonding	$2.1x10^7$ in toluene; $3.3x10^5$ in THF	CT; 10 μs	239
C_{60}	Zn^{II}	Porphyrin	1:2	Quanidinium-carboxylate bonding	$2.3x10^6$ in ODCM	1.3-2.1 ns	240
C_{60}	Fe^{II}	Ferrocene	1:1; 1:2	Ammonia-crown ether coordination	$5x10^3$-$1x10^4$ in benzonitrile	130-240 ns	241
C_{60}	Co^{II}, Ni^{II}, Cu^{II}, Zn^{II}	Porphyrin	1:1	Ammonia-crown ether coordination	$3.16x10^5$-$7.9x10^6$ in CH_2Cl_2	-	242
C_{60}	Zn^{II}	Porphyrin	1:1	Ammonia-crown ether coordination	$1x10^4$ in benzonitrile	-	243
C_{60}	Zn^{II}	Porphyrin	1:1	Ammonia-crown	$1.9x10^3$ in	100 μs	244

				ether coordination	benzonitrile		
C_{60}	Zn^{II}	Porphyrin, Phthalocyanine	1:1	Ammonia-crown ether coordination	$4.8x10^{3}$ in benzonitrile	80 ns; 160-290 ns	245
C_{60}	Zn^{II}	Phthalocyanine	1:1; 1:2	Ammonia-crown ether coordination	$1.4-1.9x10^{4}$ in CH_2Cl_2	1.3-1.5 μs	246
C_{60}	Zn^{II}	Porphyrin	1:1	Ammonia-crown ether coordination; rotaxane	n/a	160-180 ns; 400-560 ns	247
C_{60}	Zn^{II}	Porphyrin; 3-Pyridyl	1:2; 2:2	Two-point bonding (ammonia-crown ether coordination and axial coordination)	-	-	248
C_{60}	Zn^{II}	Porphyrin; 3-Pyridyl	1:1	Two-point bonding (ammonia-crown ether coordination and axial coordination)	$1.3x10^{3}-4.5x10^{4}$ in benzonitrile	50-210 ns	249
C_{60}	Zn^{II}	Porphyrin; 3-Pyridyl	1:1	Two-point bonding (ammonia-crown ether coordination and axial coordination)	$4.4x10^{4}$ in benzonitrile	Not specified	250
C_{60}	Zn^{II}	Chlorin; 3-Pyridyl	1:1	Two-point bonding (ammonia-crown ether coordination and axial coordination)	$4.6x10^{3}-4.6x10^{5}$ in ODCB	55-187 ps	251
C_{60}	Zn^{II}	Porphyrin; 3-Pyridyl	2:2	Two-point bonding (ammonia-crown ether coordination and axial coordination)	$2.5x10^{3}$ in benzonitrile	4.8 μs	252
C_{60}	Zn^{II}, Mg^{II}	Porphyrin; 3-Pyridyl	2:1	Two-point bonding (ammonia-crown ether coordination and axial coordination)	$1-6x10^{10}$ M^{-2} in benzonitrile	46-217 ns	253
C_{60}	Fe^{II}; Ru^{II}	Ferrocene; Porphyrin	1:2; 1:3	Rotaxane; axial coordination	n/a	-	254
C_{60}	Fe^{II}	Ferrocene	1:1	Rotaxane	n/a	23-143 ns; temperature dependent	255
C_{60}	Fe^{II}	Ferrocene	1:1	Rotaxane	n/a	10-30 ns	256
C_{60}	Zn^{II}	Porphyrin	1:2	Rotaxane	n/a	180 ns	257
C_{60}	Zn^{II}	Porphyrin	1:2	Rotaxane	n/a	180-645 ns	258
C_{60}	Zn^{II}	Porphyrin	1:1	Rotaxane	n/a	170-500 ns	259
C_{60}	Tb^{III}	Terpyridine	1:1	Rotaxane	-	-	260
C_{60}	Cu^{I}	Phenanthroline	1:1	Rotaxane	n/a	-	261
C_{60}	Cu^{I}; Zn^{II}	Phenanthroline; Porphyrin	1:1:2	Rotaxane; catenane	$2.0x10^{5}$ in CH_2Cl_2	500 ns	262

C_{60}	Cu^{I}; Zn^{II}	Phenanthroline; Porphyrin	1:1:2 1:1:1	Rotaxane; catenane	n/a	0.24-1.1 μs	263
C_{60}	Cu^{I}; Zn^{II}	Phenanthroline; Porphyrin	1:1:2	Rotaxane; catenane	n/a	0.49-1.17 μs	264
C_{60}	Cu^{I}; Zn^{II}	Phenanthroline; Porphyrin	2:1:1	Rotaxane	n/a	32 μs	265
C_{60}	Cu^{I}; Zn^{II}	Phenanthroline; Porphyrin	1:1:1	Catenane	n/a	1.06 μs	266
C_{60}	Cu^{I}; Zn^{II}	Phenanthroline; Porphyrin	1:1:1	Rotaxane; catenane	n/a	Not specified	267
C_{60}	Ru^{II}; Re^{I}	4-Pyridyl; 2-Pyridyl-1-aminomethane	1:2	Fullerene-cyclodextrin host-guest complexation	-	-	268
C_{60}	Pt^{IV}	o-Diselenobenzene	1:1 intermolecular polymer	Fullerene-β-cyclodextrin host-guest complexation	-	-	269

Supramolecular systems have been assembled in solution by combining C_{60} and metal containing precursors derivatised with complementary hydrogen bonding groups. A number of different bonding motifs have been utilised including three- and four-point hydrogen bonding between a C_{60} containing precursor and Zn porphyrin or ferrocene moieties (Figure 30, **101**) which results in the formation of stable, supramolecular dyads with moderate association constants of 10^3 M^{-1}.[230-232] Complementary Hamilton receptor type binding motifs (Figure 30, **100**) produce supramolecular assemblies with a slightly higher association constant of up to 10^4 M^{-1}.[235-238] Whilst a Watson-Crick motif (Figure 30, **102**) shows stronger interactions with association constants of 10^4-10^6 M^{-1}.[233,234] However the strongest interactions were reported for a quanidinium-carboxylate and amidinium-carboxylate bonded dyads which have a formation constants in the order of 10^6-10^7 M^{-1} (Figure 30, **103**).[240,239] All of these systems exhibit properties consistent with the individual C_{60} and metal containing fragments without any evidence of electronic interactions between the fullerene and transition metal in the ground state, however, strong through-space electronic communication is observed in the excited state. Zn-porphyrin containing dyads efficiently form charge separated species upon photoexcitation with lifetimes ranging from several nanoseconds[232,234,238] up to 20 μs.[231,233,235,239] In contrast the analogous Sn-porphyrin containing dyad does not exhibit features indicative of radical ion pair formation due to the higher oxidation potentials of the Sn-porphyrin compared to the Zn analogue.[236] Interestingly, no signs of charge separation were observed for ferrocene containing dyads, instead efficient triplet-triplet energy transfer from the triplet excited state of fullerene to the triplet excited state of ferrocene was observed.[230]

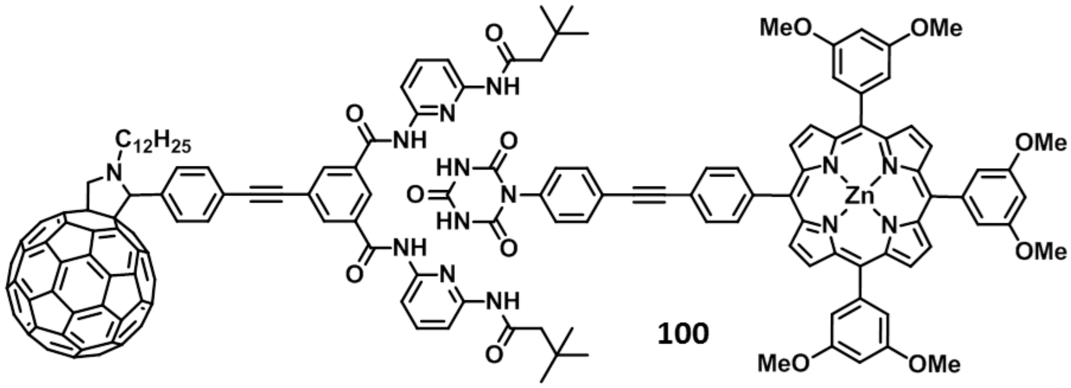

100

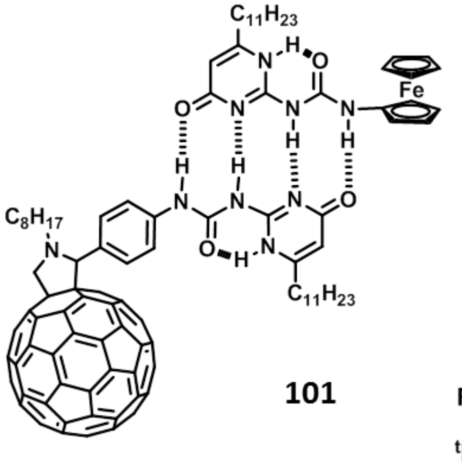

101

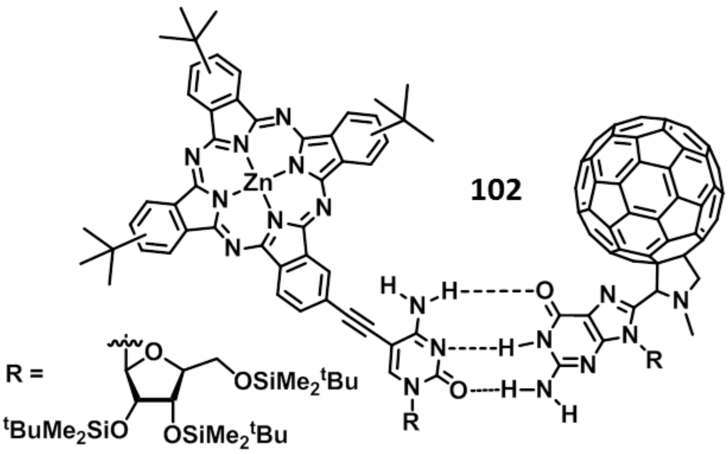

102

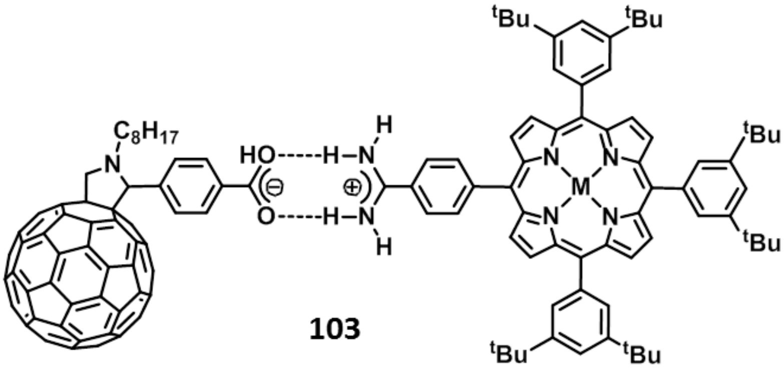

103

Figure 30. C_{60}-metal supramolecular assemblies constructed via Hamilton receptor type hydrogen bonding (**100**),[236] quadruple hydrogen bonding (**101**),[230] Watson-Crick hydrogen bonding (**102**)[234] and amidinium-carboxylate ydrogen bonding (M=Zn) (**103**).[239] Reprinted with permission from ref 230, Copyright 2013 WILEY-VCH Verlag GmbH & Co. KGaA, Weinheim; ref 236, Copyright 2007 American Chemical Society; ref 234, Copyright 2007 Royal Society of Chemistry; and ref 239, Copyright 2006 WILEY-VCH Verlag GmbH & Co. KGaA, Weinheim.

The coordination of ammonia cations by appropriately sized crown ethers has been used to obtained stable supramolecular systems with association constants of 10^3-10^4 M^{-1}.[241-247] A variety of rigid and flexible linkers have been utilised within these systems to control the distance between the metal centre and the fullerene moiety (Figure 31, **104**). In general they possess excellent photophysical properties and are capable of generating relatively long-lived charge-separated states with lifetimes ranging from hundreds of nanoseconds[241,245,247] to several microseconds,[246] up to hundreds of microseconds[244]. The addition of an axially coordinated pyridyl ligand was successfully used to bind the metal in closer proximity to the fullerene cage (Figure 31, **105**, **106**). The systems formed using this two-point binding arrangement displayed slightly higher association constants of the order of 10^4 M^{-1}.[248-253] It was possible to generate charge-separated species upon photoexcitation however the average lifetimes were slightly lower than the non-pyridyl systems in the hundreds of nanoseconds range.[249,253]

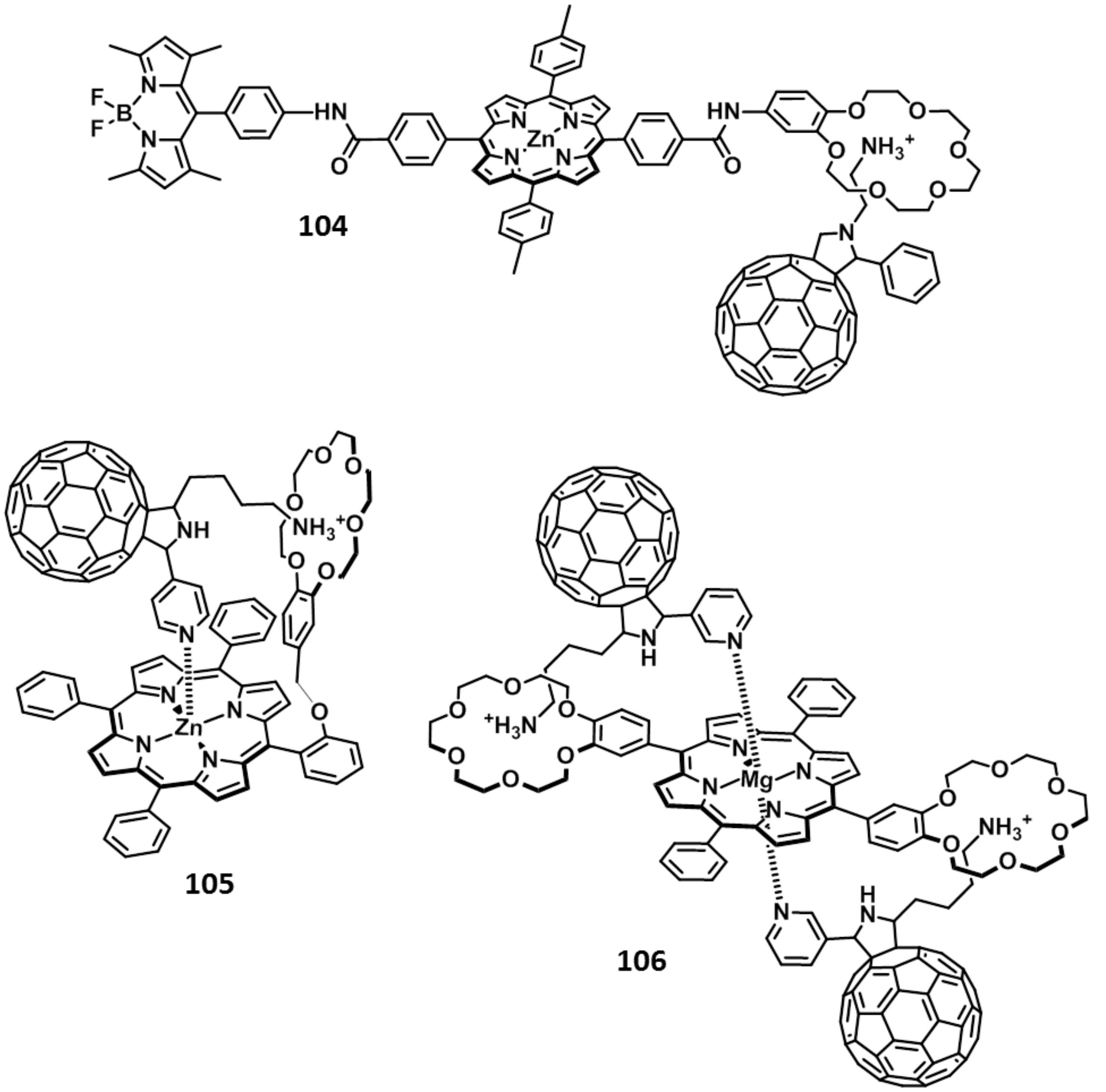

104

105

106

Figure 31. C_{60}-metal supramolecular assemblies formed via ammonia-crown ether coordination (**104**)[244] and by two-point binding of both ammonia-crown ether coordination and pyridine-metal axial coordination (**105**)[249] and (**106**).[253]) Reprinted with permission from ref 244, Copyright 2011 Royal Society of Chemistry; ref 249, Copyright 2005 WILEY-VCH Verlag GmbH & Co. KGaA, Weinheim; and ref 253, Copyright 2006 American Chemical Society.

Mechanically interlocked rotaxane type supramolecular assemblies can be prepared by the in situ generation of a macrocyclic ring attached to the fullerene cage around a metal binding moiety containing thread (Figure 32, **107, 108**) [255-258] or vice versa (Figure 32, **109**).[247,254,259] All of these systems are potential candidates for artificial photosynthesis devices as they can generate relatively long-lived charge separated species with lifetimes in the hundreds of nanoseconds range via a through space electron transfer mechanism.

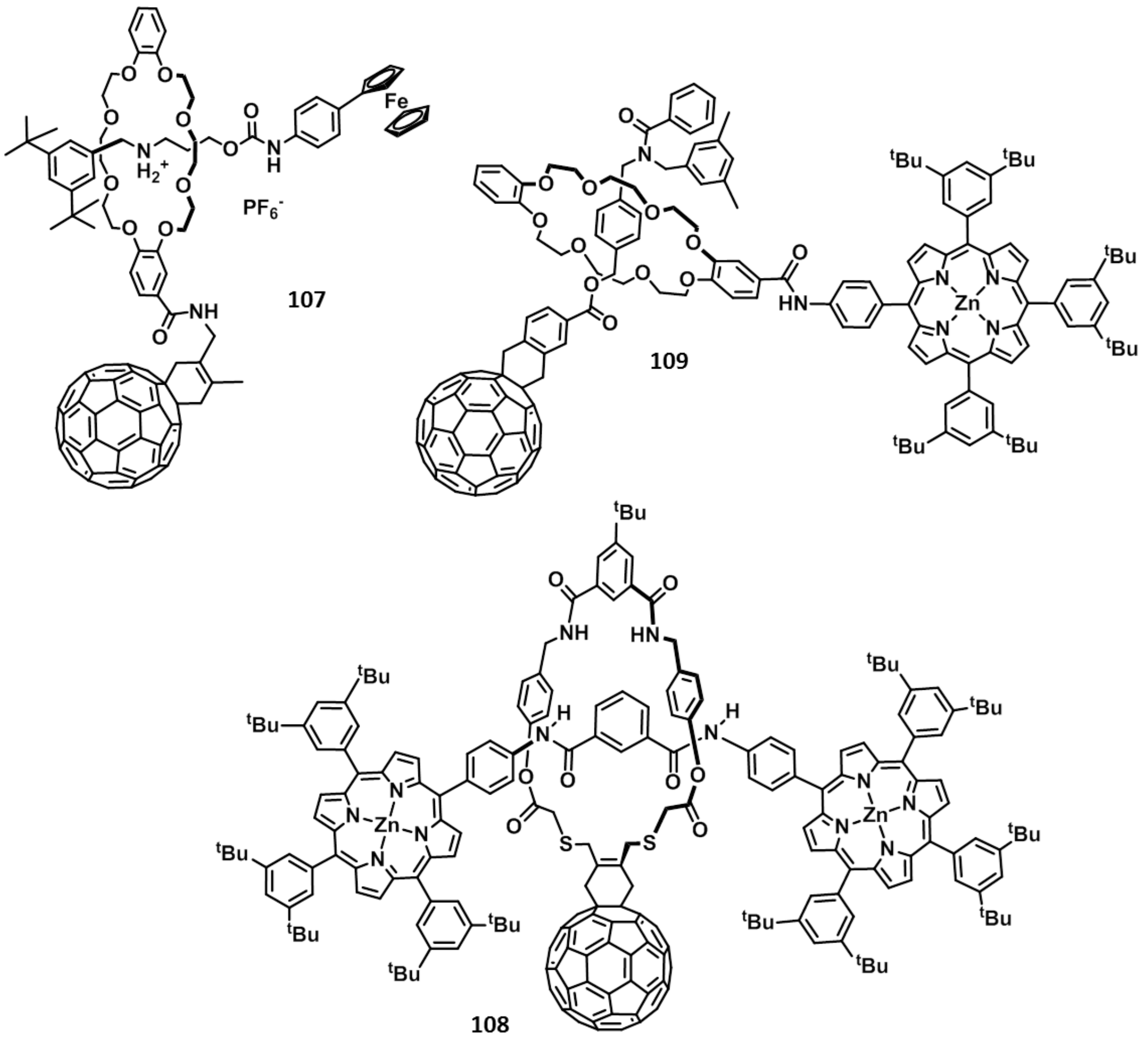

107

109

108

Figure 32. Rotaxanes of fullerenes and transition metal complexes (**107**),[255256] (**108**), [257] and (**109**).[259] Reprinted with permission from ref 255, Copyright 2006 American Chemical Society; ref 257, Copyright 2003 WILEY-VCH Verlag GmbH & Co. KGaA, Weinheim; ref 259, Copyright 2010 American Chemical Society.

The most fascinating example incorporates a rotaxane system interlocked via phenanthroline metal binding sites which are able to coordinate Cu^I ions, one of the first examples of which was reported in 1998,[261] which holds a molecular thread containing two Zn porphyrin end groups (Figure 33, **110**).[262-265] Furthermore, this system can be converted into the analogous catenane by locking the two ends of the thread either by covalent interactions (Figure 33, **111**)[263,266,267] or non-covalent two-point axial coordination of either 4,4’-bipyridine or 1,4-diazabicyclo[2.2.2.]octane (DABCO) to the two Zn(Porphyrin) groups (Figure 33, **112**).[262,263] Formation of the supramolecular DABCO coordinated catenane occurs with a relatively high formation constant ($2.0\text{x}10^5$ M^{-1}) indicating that it is a highly stable system.[262] Transient absorption studies reveal that multistep electron transfer processes occur in both rotaxane and catenane systems resulting in the formation of long-lived charge-separated radical-ion pairs, the lifetime of which varies from 0.24 μs for the rotaxane, (**110**), to 1.03 μs in the non-covalent DABCO-coordinated catenane, (**112**), and 1.1 μs in the covalently locked catenane, (**111**). This reveals that creation of a catenane from a rotaxane topology inhibits the charge recombination process. The Cu-phenanthroline centre plays a crucial role in the charge transfer process as removal of the Cu ion (Figure 33, **113**) not only results in significant structural and topological changes but also in the formation of triplet excited states on the fullerene and Zn-porphyrin moieties instead of the formation of a radical-ion pair.[263]

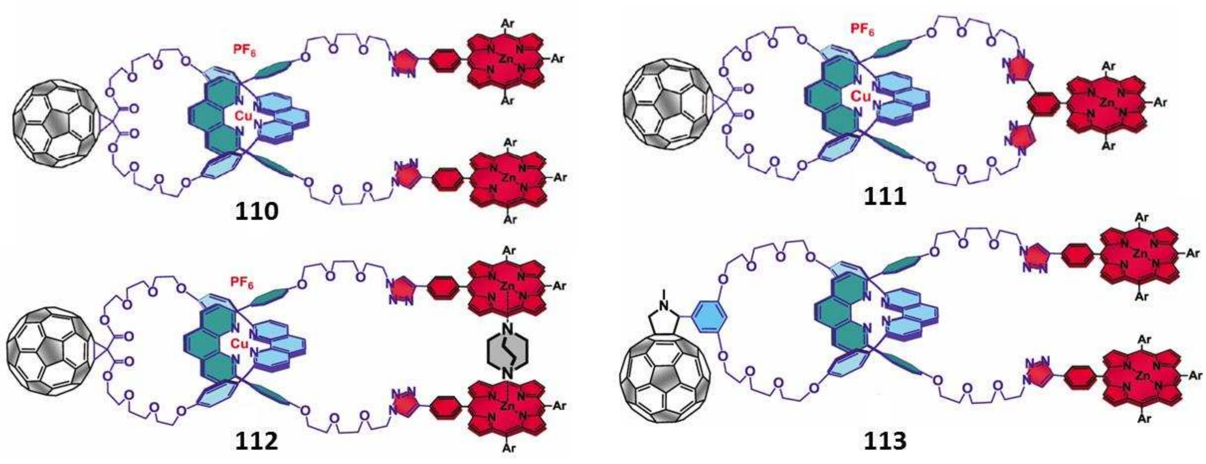

Figure 33. C_{60}-Cu(Phenanthroline)-Zn(Porphyrin) supramolecular assemblies (where Ar = 3,5-di-tert-butylphenyl) capable of forming; a rotaxane type system (**110**), a mechanically interlocked catenane system (**111**), a DABCO-coordinated catenane (**112**), or, upon removal

of the Cu^{I} ions, a demetallated rotaxane (**113**).[263] Reprinted with permission from ref 263, Copyright 2012 American Chemical Society.

In addition, fullerenes are known to form inclusion complexes with β-cyclodextrins which can be utilised to create supramolecular fullerene-metal assemblies. The complexation of C_{60} fullerene with metal binding moiety functionalised cyclodextrins produced 1:2 fullerene-Ru and Re assemblies (Figure 34, **114**)[268] and C_{60}-Pt coordination polymers (Figure 34, **115**)[269] which were found to be soluble in solvents typically considered incapable of solubilising fullerene molecules such as EtOH, DMF and water. These systems also exhibit evidence of electronic interactions between the fullerene cage and the metal containing moiety in the excited state which results in significant quenching of the emission of the metal containing luminophore by the fullerene cage.[268]

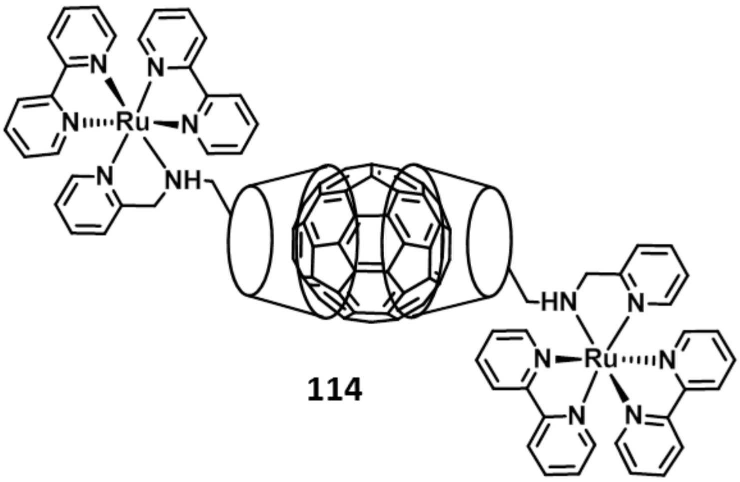

114

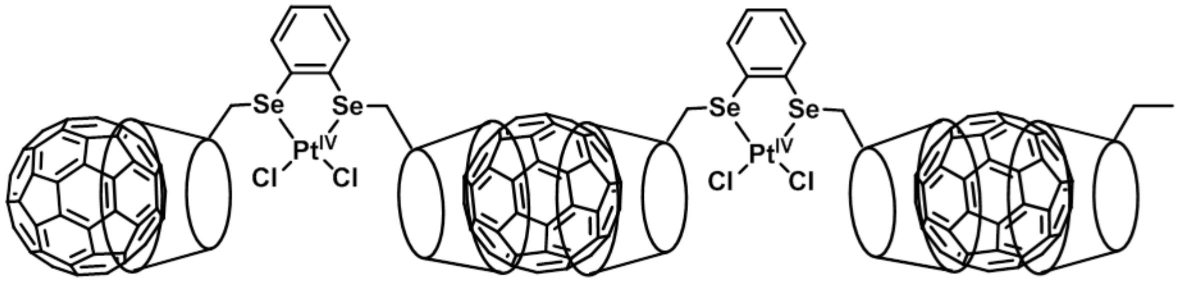

115

Figure 34. Supramolecular systems formed by the host-guest complexation of β-cyclodextrin metal binding moieties and C_{60} fullerene (**114**),[268] and (**115**).[269] Reprinted with permission from ref 268, Copyright 2006 Royal Society of Chemistry; and ref 269, Copyright 2004 WILEY-VCH Verlag GmbH & Co. KGaA, Weinheim.

4. Complexes based on non-directional intermolecular interactions.

An alternative to using fullerene as a ligand, either directly or with a chemically attached binding moiety, is to use pristine neutral fullerenes or negatively charged fullerides and allow them to bind with various metals or metal-containing molecules in solution or in the solid state. In these complexes the fullerene cage and metal-containing moieties are held together by non-covalent intermolecular interactions such as electrostatic forces, van der Waals forces or π-π interactions.

4.1 Ionic fulleride salts.

Being excellent electron acceptors, pristine fullerenes can be easily reduced chemically or electrochemically in the presence of metals to give fulleride ionic compounds with the charge on the fullerene varying from -1 to -6 thus resulting in a number of different fullerene-metal stoichiometries. The most common are fullerides prepared from alkali or alkali earth metals such as Li,[270] Na,[271] K,[272] Cs,[273] Rb,[274] Mg,[275], and Ba,[276], the lanthanide group metals Sm,[277] Eu,[278] and Yb,[279] and mixed metal compounds which have all been studied and reviewed extensively in recent years. Alkali metal doped fullerides display a range of useful properties such as superconductivity,[280,281] ferromagnetism and magnetoresistance, as well as the potential for application in hydrogen storage.[282] Examples of transition metal doped fullerides are less abundant, and are summarised in Table 7.

Table 7. Transition metal doped fulleride compounds.

Fullerene cage	Metal	Formula	Properties	Ref
C_{60}	Ti	$Ti_{3.5}C_{60}$	-	283
C_{60}	V	$(\eta^6\text{-sim-}Me_3H_3C_6)_2V^{\cdot+}C_{60}^{\cdot-}$	Temperature dependence of heat capacity	284
C_{60}	Cr^I	$(\eta^6\text{-}PhCH(CH_3)_2)_2Cr^{\cdot+}C_{60}^{\cdot-}$	Dimerisation on cooling	285
C_{60}	Cr^I	$(\eta^6\text{-ethylbenzene})_2Cr^{\cdot+}C_{60}^{\cdot-}$	Dimerisation on cooling; temperature dependence of heat capacity	286
C_{60}	Cr	$(\eta^6\text{-ethoxybenzene})_2Cr^{\cdot+}C_{60}^{\cdot-}$	Dimerisation on cooling; temperature dependence of heat capacity	287
C_{60}	Cr^I	$(\eta^6\text{-(o-xylene)})_2Mo^{\cdot+}C_{60}^{\cdot-}$	Temperature dependence of heat capacity	288
C_{60}	Cr^I	$(Ph_2)_2Cr^{+\cdot}[1,4\text{-}(CMe_2CN)_2C_{60}]^{\cdot-}$	Paramagnetism	289
C_{60}	Cr^I	$(\eta^6\text{-}Ph_2)_2Cr^{\cdot+}C_{60}^{\cdot-}$	Temperature dependence of heat capacity	290
C_{60}	Cr^I	$(\eta^6\text{-}C_6Me_6)_2Cr^{\cdot+}C_{60}^{\cdot-}$	Paramagnetism	291
C_{60}	Cr^I	$Cr(C_9H_{12})_2^{\ +}\ C_{60}^{\cdot-}$	Dimerisation on cooling	292
C_{60}	Cr^I	$Cr(C_7H_8)_2^{\ +}\ C_{60}^{\cdot-}$	Dimerisation on cooling	293, 294
C_{60}	Cr^I, Mo	$(\eta^6\text{-}Ph_2)_2Cr^{\cdot+}C_{60}^{\cdot-}$ $(\eta^6\text{-}C_{10}H_{12})_2\ Cr^{\cdot+}C_{60}^{\cdot-}$ $(\eta^6\text{-}PhCH_3)_2\ Mo^{\cdot+}C_{60}^{\cdot-}$	Dimerisation on cooling; thermal stability	295
C_{60}	Mn^{II}, Fe^{II}, Co^{II}, Ni^{II}, Eu^{II}, Cd^{II}	$(M^{2+})(DMF)_x(C_{60}^{\cdot-})_2$	Antiferromagnetic interactions; formation of diamagnetic dimers	296
C_{60}	Fe^{II}, Fe^{III}, Co^{II}, Ni^{II}, Cu^{I}, Cu^{II}, Ag^{I}	K_2MC_{60}	Superconductivity with T_c=13.9-16.5 K	297
C_{60}	Mo	$(\eta^6\text{-(m-xylene)})_2Mo^{\cdot+}C_{60}^{\cdot-}$	Dimerisation on cooling; temperature dependence of heat capacity	298
C_{60}	Pd, Pt	$Li_6Pt_{0.11}C_{60}$ $Li_6Pd_{0.07}C_{60}$	Enhanced hydrogen storage capacity	299
C_{60}	Pt	PtC_{60}	Hydrogen storage 1.6 wt % at high working temperatures	300
C_{60}	Pt	PtC_{60}	-	301
C_{60}	Au	AuC_{60}	-	302

Among the transition metals fulleride compounds most common are smaller first row transition metals derivatives, with various examples of Cr compounds [285-295] as well as Ti,[283] V,[284] Mn,[296] Ni,[296,297] Fe[296,297] and Cu.[297] A few examples of larger second row transition metals such as Mo,[295,298] Pd,[299] Ag[297] and Cd[296], Pt[299-301] and Au[302] of the third row have also been reported. These compounds are usually prepared by in situ reduction of the fullerene cage with the corresponding metal precursor, and are mainly one electron reductions which yield 1:1 fullerene-metal stoichiometries. The resulting materials are usually microcrystalline powders, and X-Ray characterisation is not straightforward. These compounds are paramagnetic as both transition metal and reduced fullerene cage components contain unpaired electrons, and have been studied by EPR spectroscopy at various temperatures to show different temperature dependant phase transformations. The majority of compounds containing C_{60} monoanions undergo reversible fullerene dimerization with the formation of diamagnetic fullerene dimers upon cooling to low temperatures. These transformations are endothermic and are characterised by calorimetric studies of temperature-dependant heat capacity to determine the thermodynamic constants of these processes.[284-295]

Inclusion of transition metals into alkali metal compounds with the formation of mixed metal fullerides has also been reported. Thus, Fe^{II}, Fe^{III}, Co^{II}, Ni^{II}, Cu^{I}, Cu^{II} and Ag^{I} have been added into the potassium fulleride containing fullerene trianion with the formation of compounds with the general stoichiometric formula K_2MC_{60}.[297] These compounds display properties typical of alkali metal fullerides exhibiting ferromagnetism and superconductivity with critical temperatures varying from 13.9 to 16.5 K.

Intercalation of transition metals such as Pd and Pt into fulleride compounds was found to improve the hydrogen storage capacity of these compounds. Chemical absorption of hydrogen on the fullerene cage is based on breaking of the H-H bond of dihydrogen which requires high energy and therefore a relatively high working temperature. However the energy of H-H bond dissociation is significantly lowered in the presence of transition metals such as Pd and Pt. Thus, a Pt-C_{60} compound was able to absorb 1.6 wt % of hydrogen, however relatively high work temperatures were still required.[300] Inclusion of small non-stoichiometric quantities of Pt or Pd into Li_6C_{60} fulleride resulted in an increase in the hydrogen absorption capacity absorbing a total of 5.9 wt % of hydrogen.[299]

4.2 Solution associates and cocrystallates of fullerenes with transition metal complexes.

Due to their highly electron-deficient π-surface and spheroidal shape pristine fullerenes can associate in solution or cocrystallise with various transition metal compounds such as porphyrins and phthalocyanines, metallocenes, dialkyldithiocarbamates or phosphates or porous coordination capsules binding via non-covalent van der Waals or π-π stacking interactions.

4.2.1. Fullerenes in porous coordination capsules.

Fullerenes can be efficiently encapsulated into porous coordination capsules exhibiting selective host-guest interactions between the fullerene molecule tightly surrounded by a metal containing coordination cage host. Examples of these structures are summarised in Table 8.

Table 8. Fullerene binding coordination capsules.

Fullerene cage	Metal	Ligand forming the coordination capsule	Properties	Ref
C_{60}	Fe^{II}	Bis(2,2'-bipyridine) perylene bisimide	-	303
C_{60}, C_{70}	Fe^{II}	2-formylpyridine, bis(4-aminophenyl) pyrene	Alteration of cage diastereomer distribution upon fullerene binding	304
C_{60}, C_{70}	Fe^{II}, Cu^{I}	2-formylpyridine, diamino(Ni(II)porphyrin)	Heterobimetallic cage	305
C_{60}, C_{70}	Co, Pd	2,4,6-tris(4-pyridyl)-1,3,5-triazine	Preferential binding of C_{70}	306, 307
C_{60}	Pd	Bispyridyl dianthracene	-	308
C_{60}	Pd	3-Pyridylsubphthalocyanine	-	309
C_{60}	Pd	Bispyridine	-	310
C_{60}	Pd	4-Pyridyl calix[3]arene	-	311
C_{60}, C_{70}, C_{60}PCBM	Pd, Pt	3-Pyridylsubphthalocyanine	Strong host-guest interactions due to energy transfer from the host framework to the fullerene guest	312
C_{60}	Ag	Bispyridyl dianthracene	Light-responsive guest catch and release; preferential binding of C_{60}	313
C_{60}, C_{70}	Hg	Bispyridyl dianthracene	Preferential binding of C_{60}; strong host-guest interactions due to energy transfer from the host framework to the fullerene guest	314

Coordination capsules are constructed of a number of ligands connected with metal ion hinges to form a cage. To be able to selectively bind fullerenes the ligands in the cage usually bear large aromatic panels such as anthracene, subphthalocyanine, pyrene, perylene bisimiine, metalloporphyrin or a number of benzene rings. The ligand size is designed so that the volume of the cage pore is sufficient to accommodate a fullerene molecule (Figure 35, **116-119**).

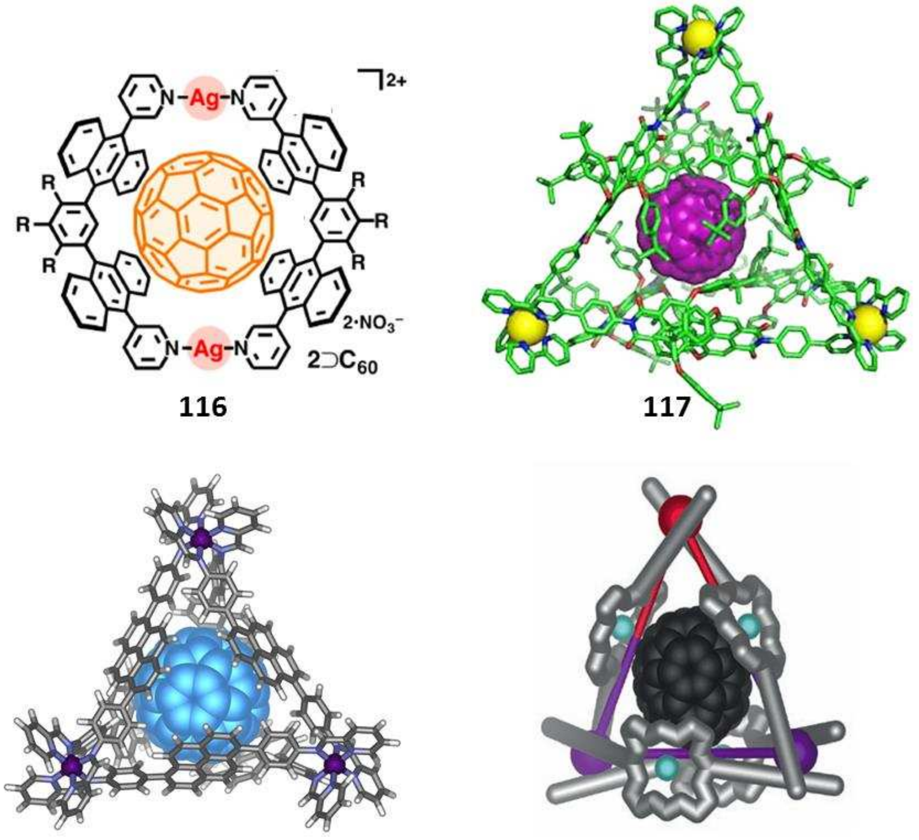

116 **117**

118 **119**

Figure 35. C_{60} fullerene encapsulated in a coordination capsule constructed of two anthracene bearing bispyridine ligands and two Ag^{I} ions, where R = $-OC_2H_4OCH_3$ (**116**),[313] three perylene bisimide bearing (bis)-2,2'-bipyridine ligands and three Fe^{II} ions (**117**),[303] pyrene-edged $Fe^{II}_4L_6$ cage (**118**)[304] and a Ni(II)Porphyrin-edged heterobimetallic $Cu^{I}Fe^{II}_2L_4$ coordination capsule (**119**).[305] Reprinted with permission from ref 313, Copyright 2013 American Chemical Society; ref 303, Copyright 2014 American Chemical Society; ref 304, Copyright 2013 American Chemical Society; ref 305, Copyright 2015 WILEY-VCH Verlag GmbH & Co. KGaA, Weinheim.

Depending on the pore volume the cages can recognise and preferentially bind fullerenes of different sizes. It was shown that the cage formed by two pyridyl bearing dianthracene ligands linked by Hg ions (Figure 36, **120**) can bind both C_{60} and C_{70} fullerenes in their respective solutions but preferentially binds C_{60} out of the fullerene mixture.[314] In contrast, a Pd linked coordination network bearing 2,4,6-tris(4-pyridyl)-1,3,5-triazine ligands (Figure 36, **121**) preferentially extracts C_{70} from the fullerene mixture.[306] Binding between the fullerene and coordination cage is relatively strong, with binding constants ranging from $1.2x10^4$ to $6.2x10^4$ M^{-1} determined by UV/vis titrations, NMR titrations or fluorescence quenching experiments.[312] The resulting host-guest structures are robust and stable, therefore release mechanisms are quite important. The common strategy is chemical decomposition of the coordination capsule by treatment with strong acid.[306] Milder non-invasive methods have also been reported, for example, a light-responsive capsule was designed which releases the fullerene under photoirradiation as a result of decomposition of the cage and precipitation of Ag^0 (Figure 35, **116**).[313]

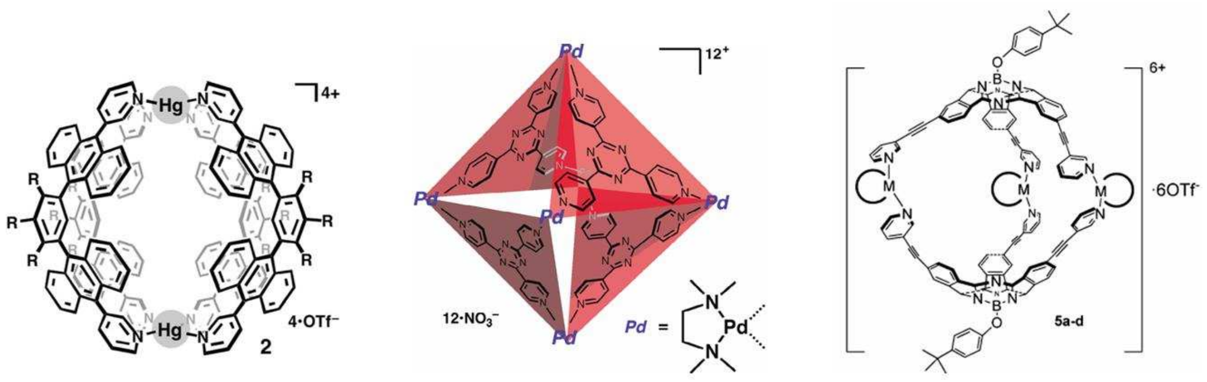

120 **121** **122**

Figure 36. Examples of coordination cages capable of fullerene encapsulation (**120**, R = $OC_2H_4OCH_3$**)**,[314] (**121**),[306] and (**122**), where M=Pd.[312]. Reprinted with permission from ref 314, Copyright 2014 WILEY-VCH Verlag GmbH & Co. KGaA, Weinheim; ref 306,

Copyright 2010 Macmillan Publishers Ltd; ref 312, Copyright 2013 American Chemical Society.

The binding between fullerene and the coordination cage is relatively strong, and excited state intramolecular interactions can often be observed with transient absorption and fluorescence spectroscopy utilised to investigate the photoinduced electronic properties in these systems. Thus, fluorescence spectroscopy of the Hg linked cage bearing anthracene moieties (Figure 36, **120**) shows blue emission upon photoexcitation with an absolute quantum yield of $\Phi = 16$ %, however the corresponding host-guest complexes of the capsule with C_{60} and C_{70} are both non-emissive owing to strong host-guest interactions and efficient energy transfer from the host framework to the fullerene guest.[314] In contrast, only weak quenching of the fluorescence of the subphthalocyanine moiety by encapsulated C_{60} fullerene was observed in the Pd linked coordination capsule (Figure 36, **122**).[312] Transient absorption spectroscopy of the same system upon photoexcitation of the SubPc moiety reveals transduction of the singlet excited-state energy to the fullerene guest which is then subject to an intersystem crossing before the energy is transferred back to form the triplet excited state of the SubPc in the capsule.[312]

4.2.2. Solution associates of fullerenes with porphyrin and phthalocyanine derivatives.

The nature of the carbon cage means that fullerenes are spontaneously attracted to metalloporphyrins and phthalocyanines due to both the formation of π-π stacking interactions and interactions between the electron density located at the [6.6] bond of the fullerene cage and the positively charged centre of the porphyrin macrocycle.[315] This results in strong association between various fullerene cages and metalloporphyrins in solution (Table 9).

Table 9. Compounds formed by association between fullerenes and porphyrin and phthalocyanine derivates in solution.

Fullerene cage	Metal	Complex	Binding constant (K_a, M^{-1})	Properties/comments	Ref
C_{60}	Mn^{II}, Fe^{II}, Co^{II}, Cu^{II}, Zn^{II}, Pd^{II}	Porphyrin	$0.5\text{-}5.2x10^3$	-	316
C_{60}	Ni^{II}	Porphyrin	$2.0x10^5$	Anisotropic high electron mobility; triplet state upon photoexcitation; self-assembled porphyrin nanotube with C_{60} peapods	317
C_{60}	Ni^{II}, Zn^{II}	Porphyrin	$5.0x10^7$	Formation of a 1:2 complex	318
C_{60}	Zn^{II}	Porphyrin	-	-	319
C_{60}	Zn^{II}	Porphyrin dimer	$6.7x10^5$	-	320
C_{60}	Zn^{II}, Co^{II}, Rh^{III}, Ni^{II}, Cu^{II}, Ag^{I}	Porphyrin dimer	$5.1\text{-}7.4x10^5$	-	321
C_{70}			$6.3\text{-}8.0x10^5$		
C_{60}, C_{70}, C_{76}, C_{96}, C_{102}-C_{110}	Zn^{II}	Porphyrin dimer	$1.1x10^5\text{-}1.3x10^7$	-	322
C_{60}	Zn^{II}	Porphyrin	$2x10^6$	-	323
C_{70}			$2x10^8$		
C_{86}, $La@C_{82}$			too strong to measure		
C_{60}	Zn^{II}	Porphyrin	$1.4x10^3$	Photoinduced charge separation with a lifetime of 350-550 ps	324
$Sc_3N@C_{80}$			$1.7x10^5$	Photoinduced charge separation with a lifetime of 780 ps	
$Lu_3N@C_{80}$			$1.8x10^5$	-	
$Li^+@C_{60}$	Zn^{II}	Porphyrin	$3x10^5$	Photoinduced charge separation with a lifetime of 300 μs	325
C_{60}	Zn^{II}	Porphyrin	$2.5x10^3$	-	326
$Li^+@C_{60}$	Zn^{II}	Chlorin	$7.7x10^4$	Photoinduced charge separation with a lifetime of 170 μs	327
C_{60}	Zn^{II}; Fe^{II}	Porphyrin, Ferrocene	$1.1x10^4$	Absorption and emission, photoinduced energy transfer	328
C_{70}			$7.1x10^4$		
C_{60}	Zn^{II}	Phthalocyanine	$1.3x10^4$	Fluorescence; charge transfer	329
C_{70}			$2.8x10^4$		
C_{60}	Zn^{II}	Phthalocyanine	$1.8x10^4$	Low selectivity; fluorescence quenching; photoinduced energy transfer	330
C_{70}			$1.9x10^4$		
C_{60}	Co^{II}, Cu^{II}	Corrole	$1.0\text{-}1.1x10^3$	Host-guest interactions in solution and in solid state	331
C_{70}			$3.9\text{-}4.3x10^3$		

A variety of different metalloporphyrins with “jaw-like” or “tweezer-like” structures (Figure 37, **123-125**) or cyclic porphyrin dimers (Figure 37, **126**)[320-322] and cyclic or acyclic porphyrin trimers (Figure 37, **127-128**) form stable host-guest inclusion complexes with fullerene in solution. Formation of this type of systems is monitored predominantly by absorption or emission spectroscopic techniques in which the shift of the Soret band (438 nm) of the fullerene cage to a longer wavelength (442 nm) upon association[318] and quenching of fluorescence of the metalloporphyrin receptor upon addition of the fullerene cage are indicative of complex formation.[323] Additionally, this solution association process can be followed by ^{1}H NMR spectroscopy by monitoring the shift of the metalloporphyrin protons upon inclusion of the fullerene cage.[326] These systems possess large binding constants varying from 10^3 to 10^8 M^{-1}[316,317-322] and typically show stronger binding of C_{70} than C_{60} [323,321] with the largest values obtained for the higher C_{76}, C_{86}, C_{96} and C_{102}-C_{110} fullerenes[322] and endohedral fullerene cages such as La@C_{82} and Sc_3N@C_{80} [323,324] and can be utilised for preparative separation of fullerene mixtures. In contrast phthalocyanines show surprising low selectivity for the binding of different fullerene cages with association constants only slightly higher for C_{70} then for C_{60}.[329,330]

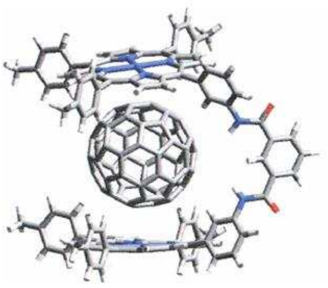

123

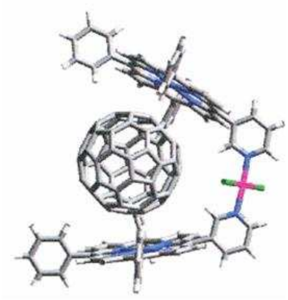

124

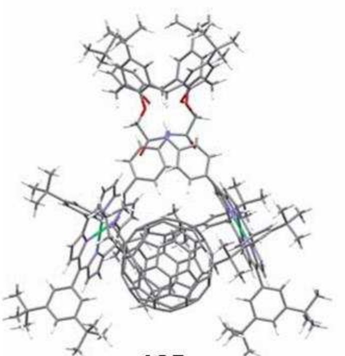

125

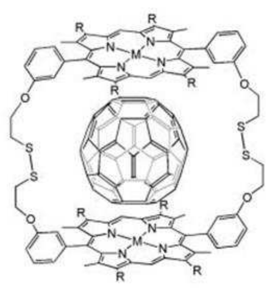

126

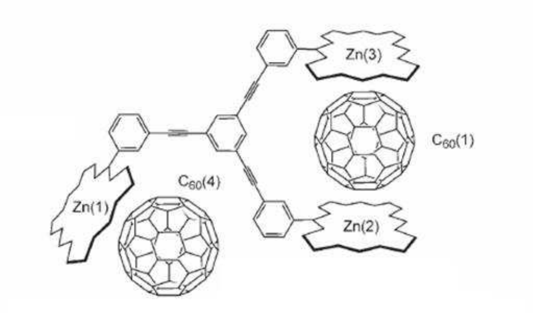

127

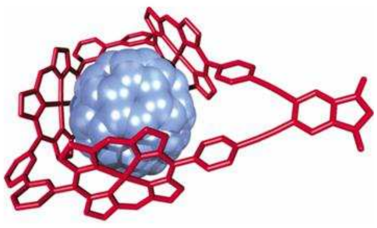

128

Figure 37. Formation of host-guest complexes in solution between C_{60} fullerene and “jaw-like” (**123**,**124**)[316] and “tweezer-like” (**125**)[324] porphyrin dimers, a cyclic

porphyrin dimer (R= -C_6H_{13}) (**126**)[319] and acyclic (**127**)[326] and cyclic (**128**)[323] porphyrin trimers. Reprinted with permission from ref 316, Copyright 2002 American Chemical Society; ref 324, Copyright 2011 Royal Society of Chemistry; ref 319, Copyright 2005 Royal Society of Chemistry; ref 326, Copyright 2008 WILEY-VCH Verlag GmbH & Co. KGaA, Weinheim; ref 323, Copyright 2010 American Chemical Society.

The inclusion of an additional supramolecular recognition motif can lead to a cooperative stabilization of the fullerene complex. This was illustrated through the introduction of an additional ammonium-crown ether interaction to the fullerene-metalloporphyrin associate which dramatically stabilized the resulting complex (Figure 38, **129**). The combination of fullerene-porphyrin and ammonium-crown ether interactions leads to a strong chelate effect as evidenced by a high effective molarity of 3.16 M. Cyclic voltammetry of these supramolecular complexes shows changes in the electrochemical signatures of the metalloporphyrins suggesting fullerene-porphyrin donor-acceptor interactions in the ground state. Further computational studies predict short M-C_{60} distances and strong π-π interactions governed by both electrostatic and dispersion forces.[242]

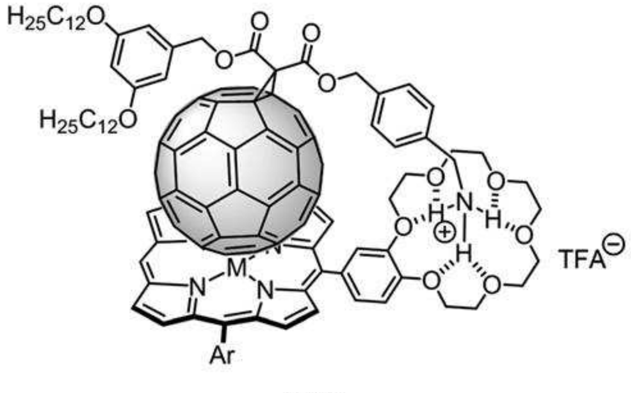

129

Figure 38. Supramolecular C_{60}-M(Porphyrin) complex stabilised by cooperative ammonium-crown-ether and fullerene-porphyrin interactions (**129**, where M = Co^{II}, Ni^{II}, Cu^{II} and Zn^{II}, Ar = 3,5-di-tert-butylphenyl).[242] Reprinted with permission from ref 242, Copyright 2015 WILEY-VCH Verlag GmbH & Co. KGaA, Weinheim.

The properties of these host-guest complexes are determined by the electron-accepting nature of the fullerene cage and electron donating nature of the metalloporphyrins. Due to strong intramolecular electronic coupling these systems exhibit intramolecular energy and charge transfer which results in the formation of charge-separated $C_{60}^{\cdot-}$M(Porphyrin)$^{\cdot+}$ radical ion pairs with lifetimes of 350-780 ps.[324] The longest lifetimes of up to 300 μs are reported for the $Li^+@C_{60}$-Zn(Porphyrin) system due to the strong electron accepting character of the cationic fullerene cage (Figure 39, **130**).[325,327] In addition, cyclic and acyclic porphyrin dimers and C_{60} fullerenes can undergo unidirectional supramolecular polymerisation resulting in the formation of supramolecular metalloporphyrin nanotube based fullerene peapods (Figure 39, **131**). These systems possess excellent thermal stability and display high, anisotropic electron mobility.[317,346]

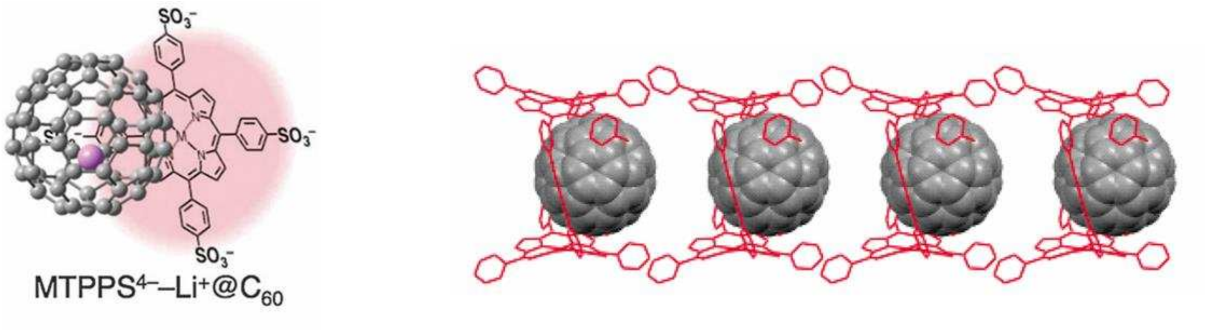

130

131

Figure 39. $Li^+@C_{60}$-ZnP complex (**130**)[325] and formation of C_{60} peapods in a self-assembled porphyrin nanotube (**131**).[317] Reprinted with permission from ref 325, Copyright 2012 Royal Society of Chemistry; ref 317, Copyright 2009 American Chemical Society.

4.2.3. Cocrystallates of fullerenes with transition metal complexes.

As mentioned previously, fullerenes and metalloporphyrin derivatives are spontaneously attracted to each other, not only in solution but also in the solid state forming various cocrystallates (Table 10).

Table 10. Cocrystallates of fullerenes with metalloporphyrins and metallophthalocyanines and their derivateves.

Fullerene cage	Metal	Complex	Properties/comments	Ref
C_{70}	Mn^{II}	Porphyrin	Paramagnetic high-spin Mn complex	332
C_{60}, C_{70}	Mn^{II}, Fe^{II}, Co^{II}, Cu^{II}, Zn^{II}	Porphyrin	Paramagnetic complexes, EPR changes from high spin to low spin; no charge transfer detected in the ground state	333
C_{60}	Mn^{II}, Fe^{II}, Co^{II}, Zn^{II}	Porphyrin	Molecular and ionic complexes; paramagnetism, antiferromagnetic spin coupling; formation of Co-C_{60} bond	334
C_{60}, C_{70}	Mn^{II}, Fe^{II}, Co^{II}, Zn^{II}	Porphyrin	Paramagnetic complexes; antiferromagnetoc interactions of spins	335
C_{60}	Mn^{II}, Zn^{II}	Porphyrin	Ionic; Paramagnetic; formation of diamagnetic singly bonded dimers upon cooling; exchange coupling above 320 K	336
C_{60}	Mn^{II}, Zn^{II}	Porphyrin	Ionic; paramagnetic with strong exchange interactions; formation of diamagnetic singly bonded dimers upon cooling	337
C_{60}	Fe^{III}	Porphyrin	-	338
C_{60}	Co^{II}	Porphyrin	Ionic complex; non-bonded paramagnetic vs. σ-bonded diamagnetic C_{60}-Co(Porphyrin) assembly	339
C_{60}	Co^{II}	Porphyrin	Ionic complex; non-bonded paramagnetic vs. σ-bonded diamagnetic C_{60}-Co(Porphyrin) assembly	340
C_{60}	Co^{II}	Porphyrin	Ionic complex; non-bonded paramagnetic vs. σ-bonded diamagnetic C_{60}-Co(Porphyrin) assembly	341
C_{60}	Co^{II}	Porphyrin	Ambipolar transport characteristics with nearly balanced hole/electron mobilities	342
C_{60}	Co^{II}, Cu^{II}	Porphyrin	Conformational changes in the porphyrin macrocycle	343
$GdSc_2N@C_{80}$; $Gd_2ScN@C_{80}$; $TbSc_2N@C_{80}$	Ni^{II}	Porphyrin	Dipole and electrostatic forces ordering of the solid state structure	344
$La@C_{82}$	Ni^{II}	Porphyrin	High electron mobility with large anisotropy	345

C_{60}, C_{70}	Zn^{II}	Porphyrin	Formation of a self-assembled porphyrin nanotube with C_{60} peapods with high aspect ratio and thermal stability	346
C_{60}	Zn^{II}	Porphyrin	Paramagnetic complexes; antiferromeagnetic interactions of spins; neutral and ionic complexes	347
C_{60}	Zn^{II}	Porphyrin	Neutral ground state; charge transfer bands in UV/Vis	348
C_{60}	Zn^{II}	Porphyrin	Luminescence quenching, ground state charge transfer	349
C_{60}	Zn^{II}	Porphyrin	Charge transfer bands in UV/Vis	350
C_{60}	Dy^{III}	Tetrapyrrole	Single molecule magnet	351
C_{60}, C_{70}	Co^{II}, Zn^{II}; Fe^{II}	Porphyrin; Ferrocene	Weak charge transfer bands in UV/Vis	352
C_{60}	In^{III}; Fe^{II}	Porphyrin, Ferrocene	-	353
C_{60}, C_{70}	Co^{II}, Cr^{0}	Porphyrin, bis(benzene) chromium	Ionic complex; semiconductor; magnetism	354
C_{60}	Mg^{II}	Phthalocyanine	Paramagnetic complexes; ionic complexes	355
C_{60}	Mn^{II}, Zn^{II}	Phthalocyanine	Ionic complex (binary salts), paramagnetic	356
C_{70}	Fe^{I}	Phthalocyanine	Paramagnetic low-spin Fe complex; C_{70} forms dimers which are EPR silent	357
C_{60}	Sn^{II}, Ir^{II}	Phthalocyanine; metallocene	Ionic complex; diamagnetic due to formation of a coordination Ir-C60 bond	358

Metalloporphyrins and phthalocyanines can be easily cocrystallised with various fullerene cages to form neutral or ionic solid state complexes, structures of which have been extensively studied by X-ray diffraction methods.[332-337,338-344,347-350] Various approaches to design such supramolecular assemblies of fullerenes and metalloporphyrins or metallophthalocyanines have been recently reviewed by Konarev et al.[359] Additionally, other metal containing moieties such as metallocenes can be added to form multicomponent cocrystallates.[352-354] The crystal packaging of these complexes exhibits short van der Waals contacts between the fullerene cage and metalloporphyrin moieties (Figure 40, structure **132**).[347] The properties of these solid state materials depend strongly on the nature of the metal. Weak metalloporphyrin-fullerene MLCT bands are observed in the absorption spectra of these systems in the 600-900 nm region.[348-352,353] Metals centres such as Mn^{II}, Fe^{II}, Co^{II} and Cu^{II} form paramagnetic porphyrin complexes and combination with fullerene results in paramagnetic solid state fullerene-metalloporphyrin cocrystallates.[332-343,354-357] These have been probed by electron paramagnetic resonance (EPR) spectroscopy. Neutral metalloporphyrin-fullerene complexes generally exhibit metal dependent EPR signals with strong exchange coupling interactions between adjacent spins in the solid state.[336,337]

The conformation of the porphyrin macroring is altered slightly upon cocrystallisation which results in changes in the geometry of the metal centre and hence its properties. This was observed for Mn^{II} porphyrin-fullerene cocrystallates in which EPR spectroscopy detected a change from high spin to low spin for the Mn^{II} complex upon cocrystallisation.[333] Smaller but still notable changes in the EPR signal were also observed in the Cu, Co and Fe complexes due to the flattening of the metalloporphyrin ring.[333,343] Ionic complexes containing anionic C_{60}^{-} or C_{70}^{-} cages, which can be formed either by cocrystallisation of pre-formed fulleride salts with corresponding metal porphyrins[339] or in situ by reduction and subsequent crystallisation of neutral fullerenes,[340] are inherently paramagnetic due to the presence of an unpaired electron located on the fullerene cage. These also exhibit a strong EPR signal with exchange or antiferromagnetic coupling between the fullerene and porphyrin coordinated metal centre based spins when cocrystallised with diamagnetic or paramagnetic transition metal complexes.[334,335] Additionally, the magnetic properties of these materials are temperature dependant and can be tuned by the appropriate choice of temperature. Thus, anionic fullerene fragments which are paramagnetic at room temperature tend to dimerise upon cooling to 120 K forming σ-bonded fullerene dimers which are EPR silent.[336,337,357] Additionally, ionic complexes containing C_{60}^{-} moieties tend to form reversible σ-bonds with the electropositive centres of metalloporphyrins, for example Co-C bond formation was observed in Co-porphyrin–fullerene cocrystallates (Figure 40,

133).[334,339-341] This results in dramatic changes in the magnetic properties of these complexes in the solid state at different temperatures as σ-bonded complexes are diamagnetic and exhibit no electron paramagnetic resonance (EPR) signal. Upon heating to temperatures above 320 K the Co-C bond dissociates forming unbound Co^{II} porphyrins and C_{60}^{-} which are both paramagnetic and exhibit strong EPR signals.

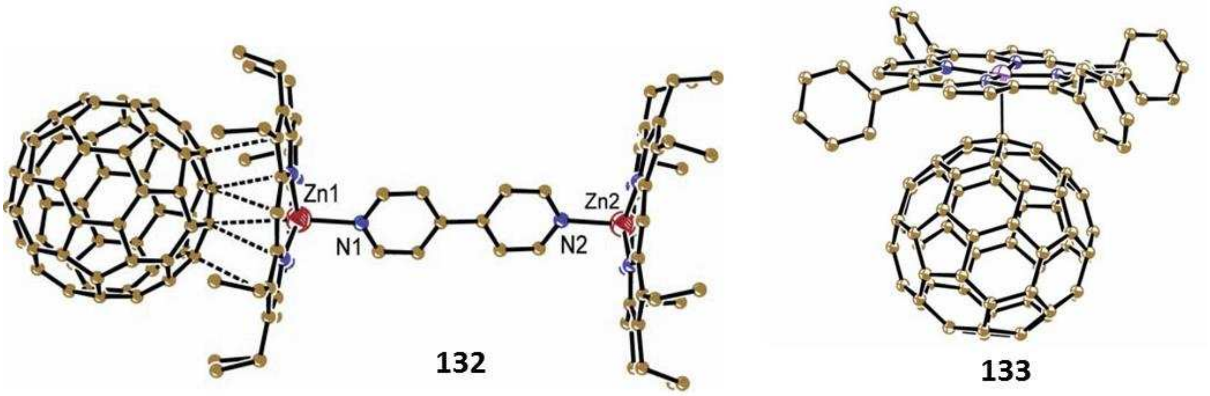

132

133

Figure 40. The neutral complex formed by cocrystallisation of C_{60} and a Zn(Porphyrin) dimer (**132**)[347] and an ionic C_{60}-Co(Porphyrin) cocrystallate (**133**).[341] Reprinted with permission from ref 347, Copyright 2007 Royal Society of Chemistry; and ref 341, Copyright 2009 Royal Society of Chemistry.

Table 11. Cocrystallates of fullerenes with other types of transition metal complexes.

Fullerene cage	Metal	Complex	Properties	Ref
C_{60}, C_{70}	Mn^{II}, Fe^{II}, Cu^{II}, Zn^{II}, Cd^{II}, Hg^{II}	Dithiocarbamate	Paramagnetism; photoconductivity	360
C_{60}	Mn^{II}, Fe^{II}, Zn^{II}, Cd^{II}, Hg^{II}	Dithiocarbamate	Paramagnetic complexes; photoconductivity; charge transfer from complex to C_{60}	361
C_{60}, C_{70}	Mn^{II}, Ni^{II},Cu^{II}, Cu^{I}, Zn^{II}, Ag^{I}, Cd^{II}, Pt^{II}, Hg^{II}	Dialkyldithiocarbamate	Neutral complexes; paramagnetic; strong ferromagnetic coupling; photoconductivity	362
C_{60}	Cu^{II}	Diethyldithiocarbamate	Paramagnetism; photoconductivity	363
C_{60}	Cd^{II}	Diethyldithiocarbamate	Paramagnetic; formation of diamagnetic singly bonded dimers upon	364

			cooling	
C_{60}	Cr^{I}, Ni^{II}, Cu^{II}, Pd^{II}, Pt^{II}	Dithiocarbamate; bis(benzene)chromium	Neutral and ionic complexes; paramagnetic; formation of diamagnetic singly bonded dimers upon cooling	365
C_{60}, C_{70}	$V^{IV}O$, Co^{II},Ni^{II}	Dithiophosphate	IR spectroscopy (superposition of signals of individual parts)	366
C_{60}	Mn^{II}, Fe^{II}, Co^{II}, Ni^{II}, Cu^{II}, Zn^{II}, Pd^{II}	Dialkyldithiophosphate	Non-linear optical properties with strong two-photon absorption cross-section	367
C_{60}	Co^{II}	Bis(diphenylphosphino)ethane	Ionic complex; paramagnetic	368
C_{60}	Ni^{II}	Terpyridine	Coordination network templated with C_{60}	369
C_{60}	Ru^{I}, Ru^{II}	Bipyridine	Paramagnetism; semiconductors	370
C_{60}	Co	Co_8S_{15} cluster	Electrochemistry, magnetism; photoinduced charge separation with 6ps lifetime	371
C_{60}	Cr^{II}, Co^{II}	Metallocene	Ionic complexes; paramagnetic; formation of field-induced short-range antiferromagnetically ordered clusters	372
C_{60}	Cr^{0}	Bis(benzene)chromium	Ionic complex; paramagnetic, strong exchange coupling between ion-radicals	373
C_{60}	Co^{II}	Cobaltocene	Fullerene dianion; singlet vs triplet states	374
C_{60}	Ag^{I}	$AgNO_3$	Formation of crystalline coordination polymers	375

Other main classes of metal containing moieties that have been cocrystallised with fullerenes include dithiocarbamates (Figure 41, structure **134**),[361-366] dithiophosphates,[367] phosphines,[368] metallocenes (Figure 41, structure **135**),[372-374] bipyridines[370] and terpyridines.[369] A wide range of metals have been used and depending on the ligand varies from small first row transition metals such as Mn, Fe, Cu, Zn, Ni and VO to heavy second and third row transition metals such as Ag, Cd, Pt and Hg.[361-367] The structure and properties of these cocrystallate structures are essentially similar to those of the metalloporphyrins showing formation of neutral or ionic complexes with short fullerene-metal contacts in the solid state. The resultant magnetic properties are strongly metal dependant, forming paramagnetic compounds with Cr, Mn, Fe, Co and Cu complexes.[361-366,368,370-374] In addition, dithiocarbamate complexes possess good photoconductivity with conductivity increasing by up to 10^3 times under white light irradiation.[362] The main contribution to the generation of free charges is provided by photoexcitation of the metal dithiocarbamate molecules (as found for the Cu^{II} complexes) or by direct charge transfer from the metal dithiocarbamate to the fullerene cage (as found for Mn^{II}, Zn^{II} or Cd^{II} complexes).[360,361,362]

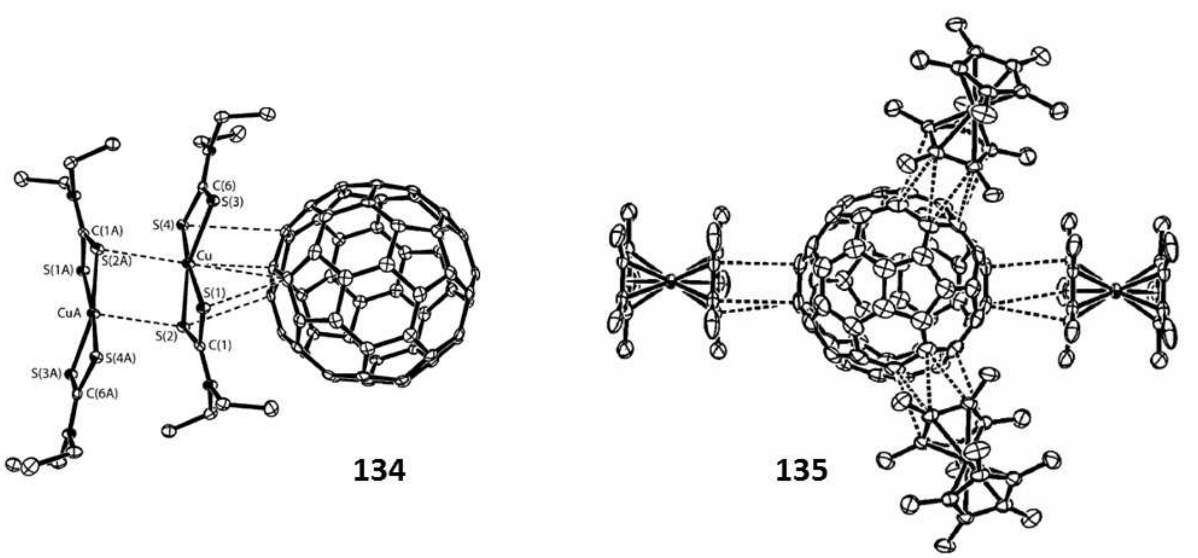

Figure 41. Cocrystallates of C_{60} fullerene and Cu dithiocarbamate (**134**)[363] and C_{60} fullerene and decamethylcobaltocene (**135**).[374] Reprinted with permission from ref 363, Copyright 2005 Royal Society of Chemistry; and ref 374, Copyright 2003 American Chemical Society.

5. Conclusions.

Transition metal containing moieties can be combined with fullerene cages in a number of different ways either endohedrally, encased within the fullerene cage, or exohedrally, attached to the cage exterior.

Organometallic fullerene derivatives in which the transition metal is coordinated directly to the C-C bond of the exterior of the fullerene cage can be easily synthesised from transition metal containing precursors and pristine fullerenes. The range of metals that can be coordinated includes the majority of first, second and third row transition metals. In these systems strong electronic coupling between the fullerene cage and the metal centre is observed in both ground and excited states. However the fullerene-metal distance in these systems and the geometry of the metal centre cannot be adjusted and hence it is difficult to tune the properties of the resulting systems. Depending on the nature of the transition metal centre, this compounds exhibit interesting photophysical properties, and are capable of forming charge separated states upon photoexcitation which are however short-lived (lifetimes in a picaseconds range). This is attributed to strong electronic coupling between the fullerene cage and the metal centre and therefore efficient charge recombination processes. On the contrary complexes containing spatially separated ferrocene moieties with no ground-state electronic coupling exhibit competitive energy transfer processes as well as charge transfer, and decay via ferrocene triplet state formation rather than through radical-ion pairs.

Coordinating transition metals to a metal binding group attached to the fullerene cage via covalent or non-covalent interactions is the most versatile approach and enables the whole of the transition block of metals to be attached to fullerenes. The geometry of the metal centre can be precisely controlled by the choice of the metal binding group and the fullerene-metal distance can be adjusted by changing the size and shape of the linker. These systems do not exhibit any ground state electronic interactions between the fullerene cage and the metal centre, however strong coupling is observed in the excited state which results in the formation of long-lived charge-separated states upon photoexcitation and makes these systems ideal candidates for applications in photovoltaic devices. The photophysical properties of these compounds depend strongly on the nature of the transition metal containing moiety as well as the distance from the fullerene cage and the presence of additional chromophores or electron donors in the molecule. Bidentate and tridentate ruthenium and rhenium complexes attached to the fullerene cage exhibit mainly eneregy transfer processes upon photoexcitation with limited examples of charge separated state formation. On the contrary, tetradentate metalloporphyrin derivatives exhibit formation of charge separated states upon photoexcitation with lifetimes in the picosecond range for complexes with a short fullerene-metalloporphyrin distance and in the nanosecond range for complexes with longer fullerene-metalloporphyrin distances. Incorporation of additional electron donors or chromophores results in long charge separated state lifetimes in the microseconds range.

Combining fullerene cages and transition metal containing molecules using van der Waals or electrostatic forces can be utilised to obtain various weakly bound cocrystallates and inclusion host-guest complexes. The stability of these systems is however limited as they are often found to be air sensitive and in the case of cocrystallates can only exist as solid state materials. These compounds exhibit weak or no ground state electronic interactions with the properties being generally a superposition of the properties of the individual components. Some of these complexes show evidence of weak excited state interactions resulting in fluorescence quenching of the metal containing unit by the fullerene cage but no evidence of charge transfer processes has been observed. This strategy does however lead to magnetic solid state fullerene containing structures which exhibit good photoconductivity and might find application in electronic devices.

To summarise, the most versatile approach to create fullerene-transition metal arrays is attaching a metal binding group to the exterior of the fullerene. It enables the formation of robust, stable and soluble systems in which the fullerene-to-metal distance can be adjusted by the choice of the suitable linker, and the geometry of the metal centre can be precisely controlled by the choice of the metal binding group. However, only a limited number of metal binding groups have been attached to the fullerene cage, these have mainly consist of N-donor ligands such as pyridine, bipyridine, terpyridine or porphyrin derivatives, each of them can specifically bind a small number of transition metals. Currently no universal fullerene based metal receptor exists that can bind a wide range of different transition metals in an identical fashion. The most promising systems to date, porphyrin and phthalocyanine functionalised fullerenes, have showed potential in this area, however, are difficult to synthesise as they require preparation and separation of asymmetric precursors.

The ability to systematically vary the metal centre within fullerene-transition metal arrays whilst retaining the same fullerene based framework will allow the light-absorbing, redox and consequently photoexcited state properties of these systems to be investigated and optimised for use in photovoltaic devices. Additionally the unique properties of the fullerene cage such as the ability to reversibly accept electrons and a high affinity for a variety of carbon nanostructures will allow the formation of well-ordered 2D and 1D arrays of spin active metal-fullerene centres. These novel functional nanoscale materials have potential to find use in a wide range of applications including molecular electronics and quantum computing.

In conclusion, fullerene-transition metal complexes are an interesting class of compounds that have evolved significantly over the past decade. These compounds possess unique properties combining the advantages of both the carbon based nanosized fullerene cage and transition metals, and as such they can find applications in various fields including catalysis, molecular electronics and photovoltaics.

6. Acknowledgemetns.

We acknowledge the European Research Council, Engineering and Physical Sciences Research Council (UK) and the University of Nottingham for financial support.

Biographies.

Maria A. Lebedeva graduated with an MSci degree in Chemistry from Lomonosov Moscow State University in 2010. She then joined the Nottingham Nanocarbon group and completed a PhD under the supervision of Prof. A.N. Khlobystov and Prof. M. Schröder investigating the combination of functionalised fullerenes and transition metal complexes for optoelectronic and catalytic applications and was awarded a PhD degree in 2014.

She is currently a postdoctoral research fellow in Nottingham Nanocarbon group working on utilising functionalised fullerenes, carbon nanotubes and graphitised nanofibres as nanoreactors and developing extraction techniques and separation methods for nanostructured materials formed in quasi-1D nanotube templates.

Thomas W. Chamberlain graduated with a MSci in Chemistry in 2005 before studying a PhD in the synthesis of novel functional fullerene molecules and the subsequent formation of fullerene/carbon nanotube hybrid structures, 2009, both at the University of Nottingham.

He joined the Nottingham Nanocarbon group as a postdoctoral research associate on a project using supramolecular forces, such as van der Waals, to organise molecules in 1D and 2D arrays utilising carbon nanotubes as quasi 1D templates. He currently works on a European Research Council funded projects developing carbon nanotubes as catalytic nanoreactors for the formation of novel molecular and nanostructured products.

Andrei N. Khlobystov is director of Nottingham Nanotechnology & Nanoscience Centre and Professor in Nanomaterials at the University of Nottingham. His research group in the School of Chemistry has over 10 years of experience in preparation, processing and characterisation of carbon nanotubes, fullerenes and other carbon nanostructures. Current research topics in his group include aspects of the non-covalent chemistry of carbon nanotubes, inorganic nanoparticles and functional carbon nanomaterials, with a particular emphasis on the carbon nanocontainers and nanoreactors. He has received a European Young Investigator Award and a Royal Society University Research Fellowship.

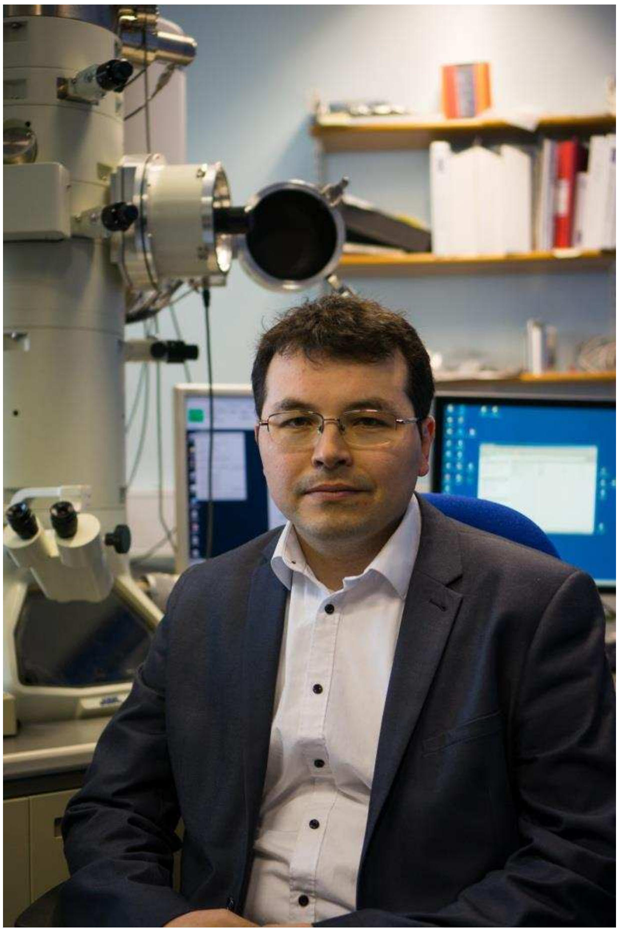

7. References.

(1.) Martin, C. A.; Ding, D.; Sørensen, J. K.; Bjørnholm, T.; van Ruitenbeek, J. M.; van der Zant, H. S. J. Fullerene-Based Anchoring Groups for Molecular Electronics. J. Am. Chem. Soc., **2008**, 130, 13198-13199.

(2.) Benjamin, S. C.; Ardavan, A.; Briggs, G. A. D.; Britz, D. A.; Gunlycke, D.; Jefferson, J.; Jones, M. A. G.; Leigh, D. F.; Lovett, B. W.; Khlobystov, A. N.; Lyon, S. A.; Morton, J. J. L.; Porfyrakis, K.; Sambrook, M. R.; Tyryshkin, A. M. Towards a Fullerene-Based Quantum Computer. J. Phys.: Condens. Matter, **2006**, 18, S867-S883.

(3.) Li, C.-Z.; Yip, H.-L.; Jen, A. K.-Y. Functional Fullerenes for Organic Photovoltaics. J. Mater. Chem., **2012**, 22, 4161-4177.

(4.) Chuard T.; Deschenaux, R. Design, Mesomorphic Properties, and Supramolecular Organization of [60]fullerene-containing Thermotropic Liquid Crystals. J. Mater. Chem., **2002**, 12, 1944-1951.

(5.) Innocenzi, P.; Brusatin, G.; Guglielmi, M.; Signorini, R.; Meneghetti, M.; Bozio, R.; Maggini, M.; Scorrano, G.; Prato, M. Optical Limiting Devices Based on C_{60} Derivatives in Sol-Gel Hybrid Organic-Inorganic Materials. J. Sol-Gel Sci. Technol. **2000**, 19, 263-266.

(6.) Montellano, A.; Da Ross, T.; Bianco, A.; Prato, M. Fullerene C_{60} as a Multifunctional System for Drug and Gene Delivery. Nanoscale, **2011**, 3, 4035-4041.

(7.) Chen, Z.; Ma, L.; Liu, Y.; Chen, C. Applications of Functionalised Fullerenes in Tumor Theranostics. Theranostics, **2012**, 2, 238-250.

(8.) Mroz, P.; Tegos, G.P.; Gali, H.; Wharton, T.; Sarna, T.; Hamblin, M.R. Photodynamic Therapy with Fullerenes. Photochem. Photobiol. Sci., **2007**, 6, 1139-1149.

(9.) Orlova, M. A.; Trofimova, T. P.; Orlov, A. P.; Shatalov, O. A. Perspectives of Fullerene Derivatives in PDT and Radiotherapy of Cancer. British J. Med.&Med. Res., **2013**, 3, 1731-1756.

(10.) Prato, M. [60]Fullerene Chemistry for Materials Science Applications. J. Mater. Chem., **1997**, 7, 1097-1109.

(11.) Echegoyen, L.; Echegoyen, L. E. Electrochemistry of Fullerenes and Their Derivatives. Acc. Chem. Res., **1998**, 31, 593-601.

(12.) Ajie, H.; Alvarez, M. M.; Anz, S. J.; Beck, R. D.; Diederich, F.; Fostiropoulos, K.; Huffman, D. R.; Krätschmer, W.; Rubin, Y.; Schriver, K. E.; Senshanarma, D.; Whetten, R.

L. Characterization of the Soluble All-Carbon Molecules C_{60} and C_{70}. J. Phys. Chem., **1990**, 94, 8630-8633.

(13.) Guldi, D. M.; Prato, M. Excited-State Properties of C_{60} Fullerene Derivatives. Acc. Chem. Res., **2000**, 33, 695-703.

(14.) Balch, A. L.; Olmstead, M. M. Reaction of Transition Metal Complexes with Fullerenes (C_{60}, C_{70},etc.) and Related Materials. Chem. Rev., **1998**, 98, 2123-2165.

(15.) (a) Troshin, P. A.; Koeppe, R.; Peregudov, A. S.; Peregudova, S. M.; Egginger, M.; Lyubovskaya, R. N.; Sariciftci, N. S. Supramolecular Association of Pyrrolidinofullerenes Bearing Chelating Pyridyl Groups and Zinc Phthalocyanine for Organic Solar Cells. Chem. Mater., **2007**, 19, 5363-5372; (b) D'Souza, F.; Ito, O. Supramolecular Donor-Acceptor Hybrids of Porphyrins/Phthalocyanines with Fullerenes/Carbon Nanotubes: Electron Transfer, Sensing, Switching, and Catalytic Applications. Chem. Commun., **2009**, 4913-4928; (c) Armaroli, N. Feom Metal Complexes to Fullerene Arrays: Exploring the Exciting World of Supramolecular Photochemistry Fifteen Years after its Birth. Photochem. Photobiol. Sci, **2003**, 73-87; (d) Schuster, D. I.; Li, K.; Guldi, D. M. Porphyrin-Fullerene Photosynthetic Model Systems with Rotaxane and Catenane Architectures. C.R. Chimie, **2006**, 9, 892-908; (e) Accorsi, G.; Armaroli, N. Taking Advantage of the Electronic Excited States of [60]-Fullerenes. J. Phys. Chem. C, **2010**, 114, 1385-1403.

(16.) (a) Chamberlain, T. W.; Pfeiffer, R.; Peterlik, H.; Kuzmany, H.; Zerbetto, F.; Melle-Franco, M.; Staddon, L.; Champness, N. R.; Briggs, G. A. D.; Khlobystov, A. N. Taking Advantage of the Electronic Excited States of [60]-Fullerenes. Small, **2008**, 4, 2262-2270; (b) Chamberlain, T. W.; Camenisch, A.; Champness, N. R.; Briggs, G. A. D.; Benjamin, S. C.; Ardavan, A.; Khlobystov, A. N. Toward Controlled Spacing in One-Dimensional Molecular Chains: Alkyl-Chain-Functionalized Fullerenes in Carbon Nanotubes. J. Am. Chem. Soc, **2007**, 129, 8609-8614; (c) Gimenez-Lopez, M. del C.; Chuvilin, A.; Kaiser, U.; Khlobystov, A. N.; Functionalised Endohedral Fullerenes in Single-walled Carbon Nanotubes. Chem. Commun., **2011**, 47, 2116-2118; (d) Chamberlain, T. W.; Champness, N. R.; Schröder, M.; Khlobystov, A. N. A Piggyback Ride for Transition Metals: Encapsulation of Exohedral Metallofullerenes in Carbon Nanotubes. Chem. Eur. J., **2011**, 17, 668-674; (e) Chamberlain, T.W.; Lebedeva, M.A.; Abuajwa, W.; Suyetin, M.; Lewis, W.; Bichoutskaia, E.; Schröder, M.; Khlobystov, A.N. Switching Intermolecular Interactions by Confinement in Carbon Nanotubes. Chem. Commun., **2015**, 51, 648-651.

(17.) Bonifazi, D.; Enger, O.; Diedrich, F. Supramolecular [60]fullerene chemistry on surfaces. Chem. Soc. Rev., **2007**, 36, 390-414.

(18.) Dubacheva, G. V.; Liang, C.-K.; Bassani, D. M. Functional Monolayers from Carbon Nanostructures – Fullerenes, Carbon Nanotubes, and Graphene – as Novel Materials for Solar Energy Conversion. Coord. Chem. Rev., **2012**, 256, 2628-2639.

(19.) Popov, A. A.; Yang, S.; Dunsch, L. Endohedral Fullerenes. Chem. Rev., **2013**, 113, 5989-6113.

(20.) Meijer, M. D.; van Klink, G. P. M.; van Koten, G. Metal-Chelating Capacities Attached to Fullerenes. Coord. Chem. Rev., **2002**, 230, 141-163.

(21.) Denisovichz, L. I.; Peregudova, S. M.; Novikov, Y. N. Electrochemical Properties of Transition Metal Complexes with C_{60} and C_{70} Fullerene Ligands. Rus. J. Electrochem., **2010**, 46, 3-20.

(22.) Soto, D.; Salcedo, R. Coordination Modes and Different Hapticities for Fullerene Organometallic Complexes. Molecules, **2012**, 17, 7151-7168.

(23.) Bowles, F. L.; Olmstead, M. M.; Balch, A. L. Preparation and Crystallographic Characterization of $C_{60}\{\eta^1\text{-Ru(CO)}_2(\eta^5\text{-}C_5H_5)\}_2$: A Locally Crowded Organometallic Fullerene Without the Usual η^2-Bonding. J. Am. Chem. Soc., **2014**, 136, 3338-3341.

(24.) Konarev, D. V.; Troyanov, S. I.; Nakano, Y.; Ustimenko, K. A.; Otsuka, A.; Yamochi, H.; Saito, G.; Lyubovskaya, R. N. Magnetic Coupling in the Fullerene Dimer $\{\text{Co}(Ph_3P)(C_6H_5CN)\}_2(\mu_2\text{-}\eta^2\text{:}\eta^2\text{-}C_{60})_2$ with Two Zerovalent Cobalt Atoms as Bridges. Organomet., **2013**, 32, 4038-4041.

(25.) Konarev, D. V.; Troyanov, S. I.; Ustimenko, K.A.; Nakano, Y.; Shestakov, A. F.; Otsuka, A.; Yamochi, H.; Saito, G.; Lyubovskaya, R. N. Formation of $\{\text{Co(dppe)}\}_2\{\mu_2\text{-}\eta^2\text{:}\eta^2\text{-}\eta^2\text{:}\eta^2\text{ -}[(C_{60})_2]\}$ Dimers Bonded by Single C-C Bonds and Bridging η^2-Coordinated Cobalt Atoms. Inorg. Chem., **2015**, 54, 4597-4599.

(26.) Konarev, D. V.; Khasanov, S. S.; Nakano, Y.; Otsuka, A.; Yamochi, H.; Saito, G.; Lyubovskaya, R. N. Linear Coordination Fullerene C_{60} Polymer $[\{\text{Ni}(Me_3P)_2\}(\mu\text{-}\eta^2,\eta^2\text{-}C_{60})]\infty$ Bridged by Zerovalent Nickel Atoms. Inorg. Chem., **2014**, 53, 11960-11965.

(27.) Konarev, D. V.; Khasanov, S. S.; Yudanova, E. I.; Lyubovskaya, R. N. The η^2 Complex of Nickel Bis(diphenylphosphanyl)propane with Fullerene: $\{\text{Ni(dppp)}(\eta^2\text{-}C_{60})\}\cdot$(Solvent) Obtained by Reduction. Eur. J. Inorg. Chem., **2011**, 816-820.

(28.) Konarev, D. V.; Simonov, S. V.; Khasanov, S. S.; Lyubovskaya, R. N. Preparation of η^2-Complexes of Fullerenes by Reduction. Crystal Structure and Optical Properties of $\{Ni(dppp)\cdot(\eta^2\text{-}C_{70})\}\cdot(C_6H_4Cl_2)_{0.5}$. Dalton Trans., **2011**, 40, 9176-9179.

(29.) Zanello, P.; de Biani, F.F.; Cinquantini, A.; Grigiotti, E. Electrochemistry of the Metallo-Bisfullerene $[Mo(\eta^2\text{-}C_{60})_2(CO)_2(dbc\text{-}bipy)]$ (dbc-bipy=4,4’-di(butylcarboxyl)-2,2’bipyridine). C. R. Chimie, **2005**, 8, 1655-1659.

(30.) Jin, X.; Xie, X.; Tang, K. Syntheses and X-ray Crystal Structures of Dumbbell-Shaped Bis-Fullerene Tungsten and Molybdenum Complexes. Chem. Comm., **2002**, 750-751.

(31.) Lee, K.; Song, H.; Kim, B.; Park, J. T.; Park, S.; Choi, M.-G. The First Fullerene-Metal Sandwich Complex: An Unusually Strong Electronic Communication between Two C_{60} Cages. J. Am. Chem. Soc., **2002**, 124, 2872-2873.

(32.) Tsikalova, M. V.; Zheludkov, S. V.; Vorontsov, E. I.; Bashilov, V. V.; Babievskii, K. K.; Sokolov, V. I.; Novikov, Y. N. Optically Active Rhodium and Iridium C_{60} Complexes Containing the Enantiomeric Ligand (+)DIOP: $(\eta^2\text{-}C_{60})MH(CO)[(+)DIOP]$ (M=Rh, Ir). Mendeleev Commun., **2011**, 21, 256-258.

(33.) Starodubtseva, E. V.; Sokolov, V. I.; Bashilov, V. V.; Novikov, Y. N.; Martynova, E. V.; Vinogradova, M.G.; Turova, O. V. Fullerene Complexes with Palladium and Rhodium as Catalysts for Acetylenic Bond Hydrogenation. Mendeleev Commun., **2008**, 18, 209-210.

(34.) Sulman, E.; Matveeva, V.; Semagina, N.; Yanov, I.; Bashilov, V.; Sokolov, V. Catalytic Hydrogenation of Acetylenic Alcohols Using Palladium Complex of Fullerene C_{60}. J. Molec. Cat. A: Chem., **1999**, 146, 257-263.

(35.) Bashilov, V. V.; Magdesieva, T. V.; Kravchuk, D. N.; Petrovskii, P. V.; Ginzburg, A. G.; Butin, K. P.; Sokolov, V. I. A New Heterobimetallic Palladium-[60]Fullerene Complex with Bidentate Bis-1,1’$[P]_2$-Ferrocene Ligand. J. Organomet. Chem., **2000**, 599, 37-41.

(36.) Magdesieva, T. V.; Bashilov, V. V.; Kravchuk, D. N.; Dolgushin, F. M.; Butin, K. P.; Sokolov, V. I. Comparison of Electrochemical Behaviour of Exohedral Palladium Complexes with [60]- and [70]-Fullerenes and Metallocene Ligands. Rus. Chem. Bull. Int. Ed., **2004**, 53, 795-799.

(37.) Song, L.-C.; Su, F.-H.; Hu, Q.-M. Three Novel Bismetallacyclopropa[60]fullerene Complexes Formed via Intermediate Monometallacyclopropa[60]fullerene Diphosphine Ligands. J. Organomet. Chem., **2005**, 690, 1121-1124.

(38.) Yeh, W.-Y. C_{60}-Induced Alkyne-Alkyne Coupling and Alkyne Scission Reactions of a Tungsten Tris(Diphenylacetylene) Complex. Chem. Commun., **2011**, 47, 1506-1508.

(39.) Yeh, W.-Y. Unusual Thermal Reactivity of $[W(\equiv CPh)(NCMe)(\eta^2\text{-}C_{60})(\eta^5\text{-}C_5Ph_5)]$ in Chlorobenzene Involving Activation of All Ligands. Angew. Chem. Int. Ed., **2011**, 50, 12046-12049.

(40.) Chen, C.-H.; Yeh, W.-Y.; Liu, Y.-H.; Lee, G.-H. $[(\mu\text{-}H)_3Re_3(CO)_9(\eta^2,\eta^2,\eta^2\text{–}Sc_2C_2@C_{3v}(8)\text{-}C_{82})]$: Face-Capping Cluster Complex of an Endohedral Fullerene.Angew. Chem. Int. Ed., **2012**, 51, 13046-13049.

(41.) Park, J.T.; Song, H.; Cho, J.-J.; Chung, M.-K.; Lee, J.-H.; Suh, I.-H. Synthesis and Characterization of $\eta^2\text{-}C_{60}$ and $\mu_3\text{-}\eta^2,\eta^2,\eta^2\text{-}C_{60}$ Triosmium Cluster Complexes. Organometallics, **1998**, 17, 227-236.

(42.) Chamberlain, T. W.; Champness, N. R.; Schröder, M.; Khlobystov, A. N. A Piggyback Ride for Transition Metals: Encapsulation of Exohedral Metallofullerenes in Carbon Nanotubes. Chem. Eur. J. **2011**, 17, 668-674.

(43.) Jun, T.; Park, B. K.; Lee, C. Y. Synthesis, characterization, and electrochemical study of $Os_3(CO)_7(1,2\text{-dppm})(\mu_3\text{-}\eta^2{:}\eta^2{:}\eta^2\text{-}C_{60})$ and $Os_3(CO)_7(1,1\text{-dppm})$ $(\mu_3\text{-}\eta^2{:}\eta^2{:}\eta^2\text{-}C_{60})$. J. Organomet. Chem., 2014, 763-764, 20-25.

(44.) Sparta, M.; Jensen, V.R.; Børve, K. Accurate Metal-Ligand Bond Energies in the $\eta^2\text{-}C_2H_4$ and $\eta^2\text{-}C_{60}$ Complexes of $Pt(PH_3)_2$, with Application on their Bis(triphenylphosphine) Analogues. J. Molec. Phys., **2013**, 111, 1599-1611.

(45.) Watanabe, T.; Itoh, M. F.; Komuro, T.; Okada, H.; Sakai, T.; Ono, Y.; Kawachi, K.; Kasama, Y.; Tobita, H. Iridium and Platinum Complexes of $Li^+@C_{60}$. Organometallics, **2014**, 33, 608-611.

(46.) Lee, G.; Cho, Y.-J.; Park, B.K.; Lee, K.; Park, J. T. Two Metal Centers Bridging Two C_{60} Cages as a Wide Passage for Efficient Interfullerene Electronic Interaction. J. Am. Chem. Soc., **2003**, 125, 13920-13921.

(47.) Halim, M.; Kennedy, R. D.; Suzuki, M.; Khan, S. I.; Diaconescu, P.L.; Rubin, Y. Complexes of Gold(I), Silver(I), and Copper(I) with Pentaaryl[60]fullerides. J. Am. Chem. Soc., **2011**, 133, 6841-6851.

(48.) Halim, M.; Kennedy, R.D.; Khan, S.I.; Rubin, Y. Gold(I) Triphenylphosphine Complexes Incorporating Pentaarylfulleride Ligands. Inorg. Chem. **2010**, 49, 3974-3976.

(49.) Lien, S.-T.; Yeh, W.-Y. Complexation and Activation of the Bisfulleroid $C_{64}H_4$ with Triosmium Carbonyl Clusters. J. Organomet. Chem., **2012**, 715, 69-72.

(50.) Matsuo, Y.; Iwashita, A.; Nakamura, E. Group 6 Metal Complexes of the η^5-Pentamethyl[60]Fullerene. Organometallics, **2008**, 27, 4611-4617.

(51.) Itoh, Y.; Kim, B.; Gearba, R. I.; Tremblay, N. J.; Pindak, R.; Matsuo, Y.; Nakamura, E.; Nuckolls, C. Simple Formation of C_{60} and C_{60}-Ferrocene Conjugated Monolayers Anchored onto Silicon Oxide with Five Carboxylic Acids and Their Transistor Applications. Chem. Mater., **2011**, 23, 970-975.

(52.) Chen, T.; Wang, D.; Gan, L.-H.; Matsuo, Y.; Gu, J.-Y.; Yan, H.-J.; Nakamura, E.; Wan, L.-J. Direct Probing of the Structure and Electron Transfer of Fullerene/Ferrocene Hybrid on Au(111) Electrodes by in Situ Electrochemical STM. J. Am. Chem. Soc., **2014**, 136, 3184-3191.

(53.) Matsuo, Y.; Tahara, K.; Nakamura, E. Synthesis and Electrochemistry of Double-Decker Buckyferrocenes. J. Am. Chem. Soc., **2006**, 128, 7154-7155.

(54.) Matsuo, Y.; Muramatsu, A.; Kamikawa, Y.; Kato, T.; Nakamura, E. Synthesis and Structural, Electrochemical, and Stacking Properties of Conical Molecules Possessing Buckyferrocene on the Apex. J. Am. Chem. Soc., **2006**, 128, 9586-9587.

(55.) Li, C.-Z.; Matsuo, Y.; Nakamura, E. Octupole-like Supramolecular Aggregates of Conical Iron Fullerene Complexes into a Three-Dimentional Liquid Crystalline Lattice. J. Am. Chem. Soc., **2010**, 132, 15514-15515.

(56.) Marczak, R.; Wielopolski, M.; Gayathri, S. S.; Guldi, D. M.; Matsuo, Y.; Matsuo, K.; Tahara, K.; Nakamura, E. Uniquely Shaped Double-Decker Buckyferrocenes-Distinct Electron Donor-Acceptor Interactions. J. Am. Chem. Soc., **2008**, 130, 16207-16215.

(57.) Matsuo, Y.; Kuninobu, Y.; Muramatsu, A.; Sawamura M.; Nakamura, E. Synthesis of Metal Fullerene Complexes by the Use of Fullerene Halides. Organometallics, **2008**, 27, 3403-3409.

(58.) Nakae, T.; Matsuo, Y.; Nakamura, E. Synthesis of C_5-Symmetric Functionalized [60]Fullerenes by Copper-Mediated 5-Fold Addition of Reformatsky Reagents. Org. Lett., **2008**, 10, 621-623.

(59.) Matsuo, Y.; Kuninobu, Y.; Ito, S.; Sawamura, M.; Nakamura, E. Friedel-Crafts Functionalization of the Cyclopentadienyl Ligand in Buckymetallocenes. Dalton Trans., **2014**, 43, 7407-7412.

(60.) Guldi, D. M.; Rahman, G. M. A.; Marczak, R.; Matsuo, Y.; Yamanaka, M.; Nakamura, E.Sharing Orbitals: Ultrafast Excited State Deactivations with Different Outcomes in Bucky Ferrocenes and Ruthenocenes. J. Am. Chem. Soc., **2006**, 128, 9420-9427.

(61.) Matsuo, Y.; Ichiki, T.; Nakamura, E. Molecular Photoelectric Switch Using a Mixed SAM of Organic [60]Fullerene and [70]Fullerene Doped with a Single Iron Atom. J. Am. Chem. Soc., **2011**, 133, 9932-9937.

(62.) Matsuo, Y.; Tahara, K.; Fujita, T.; Nakamura, E. Di- and Trinuclear [70]Fullerene Complexes: Syntheses and Metal-Metal Electronic Interactions. Angew. Chem. Int. Ed., **2009**, 48, 6239-6241.

(63.) Maruyama, M.; Guo, J.-D.; Nagase, S.; Nakamura, E.; Matsuo, Y. Isolation of Planar Four-Membered Aromatic Systems by Using Confined Spaces of Cobalt Pantaaryl[60]fullerene Complexes. J. Am. Chem. Soc., **2011**, 133, 6890-6893.

(64.) Matsuo, Y.; Maruyama, M.; Gayathri, S.S.; Uchida, T.; Guldi, D.M.; Kishida, H.; Nakamura, A.; Nakamura, E. π-Conjugated Multidonor/Acceptor Arrays of Fullerene-Cobaltadithiolene-Tetrathiafulvallene: From Synthesis and Structure to Electronic Interactions. J. Am. Chem. Soc., **2009**, 131, 12643-12649.

(65.) Gao, G.; Xu, X.; Kang, H.S. A Theoretical Study on Fullerene-Dizincocene Hybrids. J. Comput. Chem., **2008**, 978-982.

(66.) Matsuo, Y.; Muramatsu, A.; Lu, J.; Nakamura, E. Highly Soluble Penta[(alkyl)dimethylsilylmethyl][60]fullerenes and Their Ruthenium and Palladium Complexes. Chem. Lett., **2010**, 39, 342-343.

(67.) Matsuo, Y.; Uematsu, T.; Nakamura, E. Synthesis and Catalytic Activity of η^1-Allyl and η^3-Allyl, Ethyl, and Hydrido Complexes of Ruthenium-Pentamethyl[60]Fullerene. Eur. J. Inorg. Chem., **2007**, 2729-2733.

(68.) Matsuo, Y.; Nakamura, E. Synthesis of Trialkyl[60]Fullerene $C_{60}(CH_2SiMe_3)_3H$ and its Potassium and Rhodium(I) Complexes. Inorg. Chim. Acta, **2006**, 359, 1979-1982.

(69.) Stewart, M.P.; Butterick III, R.; Sneddon, L.G.; Matsuo, Y.; Geiger, W.E. Voltammetry of half-sandwich manganese group complexes of η^6-$PhC_3B_7H_9$ and η^5-$C_{60}Bn_2PhH_2$, two ligands that are cyclopentadienyl mimicks. Inorg. Chim. Acta, **2010**, 364, 251-254.

(70.) Bashilov, V.V.; Magdesieva, T.V.; Kravchuk, D.N.; Petrovskii, P.V.; Ginzburg, A.G.; Butin, K.P.; Sokolov, V.I. A New Heterobimetallic Palladium–[60]fullerene Complex with Bidentate bis-1,1’-$[P]_2$-ferrocene Ligand. J. Organomet. Chem., **2000**, 599, 37-41.

(71.) Song, L.-C.; Wang, G.-F.; Liu, P.-C.; Hu, Q.-M. Synthetic and Structural Studies on Transition Metal Fullerene Complexes Containing Phosphorus and Arsenic Ligands: Crystal and Molecular Structures of (η^2-C_{60})M(dppf) (dppf=1,1’-Bis(diphenylphosphino)ferrocene;

M = Pt, Pd), (η^2-C_{60})Pt($AsPh_3$)$_2$, (η^2-C_{60})Pt(dpaf) (dpaf = 1,1’-Bis(diphenylarsino)ferrocene), and (η^2-C_{70})Pt(dpaf). Organometallics, **2003**, 22, 4593-4598.

(72.) Guldi, D.M.; Maggini, M.; Scorrano, G.; Prato, M. Intramolecular Electron Transfer in Fullerene/Ferrocene Based Donor-Bridge-Acceptor Dyads. J. Am. Chem. Soc., **1997**, 119, 974-980.

(73.) Figueira-Duarte, T.M.; Rio, Y.; Listorti, A.; Delavaux-Nicot, B.; Holler, M.; Marchioni, F.; Ceroni, P.; Armaroli, N.; Nierengarten, J.-F. Synthesis and Electronic Properties of Fullerene Derivatives Substituted with Oligophenylenevinylen-Ferrocene Conjugates. New J. Chem., **2008**, 32, 54-64.

(74.) Campidelli, S.; Vázquez, E.; Milic, D.; Prato, M.; Barberá, J.; Guldi, D.M.; Marcaccio, M.; Paolucci, D.; Paolucci, F.; Deschenaux, R. Liquid-Crystalline Fullerene-Ferrocene Dyads. J. Mater. Chem., **2004**, 14, 1266-1272.

(75) Nakamura, T.; Kanato, H.; Araki, Y.; Ito, O.; Takimiya, K.; Otsubo, T.; Aso, Y. Effects of Extension or Prevention of ð-Conjugation on Photoinduced Electron Transfer Processes of Ferrocene-Oligothiophene-Fullerene Triads. J. Phys. Chem. A, **2006**, 110, 3471-3479.

(76.) Yeh, W.-Y.; Wu, S.-H. Functionalization of the Tetrairon Cluster $Cp_4Fe_4(CO)_4$ with Fulleropyrrolidine. Dalton Trans., **2013**, 42, 12260-12264.

(77.) Campidelli, S.; Pérez, L.; Rodríguez-López, J.; Barberá, J.; Langa, F.; Deschenaux, R. Dendritic Liquid-Crystalline Fullerene-Ferrocene Dyads. Tetrahedron, **2006**, 62, 2115-2122.

(78.) Chen, C.; Zhu, Y.-Z.; Zhao, H.-Y.; Zheng, J.-Y. Syntheses of N-bridged Ferrocene/Porphyrin-Fullerene Dyads and Influence of Iminofullerene Isomers on the Attached Chromophores. Tetrahedron Lett., **2013**, 54, 1607-1611.

(79.) Miao, X.; Liu, L.; Wang, S.; Lin, H.; Sun, B.; Hu, J.; Li, M. Elctrochemical Synthesis of a Ferrocenecarboxylic acid-C_{60} Composite and its Electrocatalysis to Hydrogen Peroxide. Electrochem. Comm., **2010**, 12, 90-93.

(80.) Kumar, A.; Menon, S. K. Fullerene-Ferrocene Dyad Linked by Rigid Bilinkage: Synthesis, Photophysical Properties and Application as Copper Ion Sensor. J. Phys. Org. Chem., **2009**, 22, 661-669.

(81.) Pinzón, J. R.; Plonska-Brzezinska, M. E.; Cardona, C. M.; Athans, A.J.; Gayathri, S. S.; Guldi, D. M.; Herranz, M. Á.; Martín, N.; Torres, T.; Echegoyen, L. $Sc_3N@C_{80}$-Ferrocene Electron-Donor/Acceptor Conjugates as Promising Materials for Photovoltaic Applications Angew. Chem. Int. Ed., **2008**, 47, 4173-4176.

(82.) Bandi, V.; El-Khouly, M. E.; Ohkubo, K.; Nesterov, V. N.; Zandler, M. E.; Fukuzumi, S.; D'Souza, F. Excitation-Wavelength-Dependent, Ultrafast Photoinduced Electron Transfer in Bisferrocene/BF_2-Chelated-Azadipyrromethene/Fullerene Tetrads. Chem. Eur. J., **2013**, 19, 7221-7230.

(83.) Delgado, J. L.; El-Khouly, M. E.; Araki, Y.; Gómez- Escalonilla, M. J.; de la Cruz, P.; Oswald, F.; Ito, O.; Langa, F. Synthesis and Photophysical Properties of a [60]Fullerene Compound with Dimethylaniline and Ferrocene Connected through a Pyrazolino Group: a Study by Laser Flash Photolysis. Phys. Chem. Chem. Phys., **2006**, 8, 4104-4111.

(84.) Campidelli, S.; Séverac, M.; Scanu, D.; Deschenaux, R.; Vázquez, E.; Milic, D.; Prato, M.; Carano, M.; Marcaccio, M.; Paolucci, F.; Rahmang, G. M. A.; Guldi, D. M. Photophysical, Electrochemical, and Mesomorphic Properties of a Liquid-Crystalline [60]Fullerene-Peralkylated Ferrocene Dyad. J. Mater. Chem., **2008**, 18, 1504-1509.

(85.) Wijesinghe, C. A.; El-Khouly, M. E.; Blakemore, J. D.; Zandler, M. E.; Fukuzumi, S.; D'Souza, F. Charge Stabilization in a Closely Spaced Ferrocene-Boron Dipyrrin-Fullerene Triad. Chem. Commun., **2010**, 46, 3301-3303.

(86.) González-Rodríguez, D.; Carbonell, E.; de Miguel Rojas, G.; Castellanos, C. A.; Guldi, D. M.; Torres, T. Activating Multistep Charge-Transfer Processes in Fullerene-Subphthalocyanine-Ferrocene Molecular Hybrids as a Function of π-π Orbital Overlap J. Am. Chem. Soc., **2010**, 132, 16488-16500.

(87.) Spänig, F.; Kovacs, C.; Hauke, F.; Ohkubo, K.; Fukuzumi, S.; Guldi, D.M.; Hirsch, A. Tuning Charge Transfer Energetics in Reaction Center Mimics via T_h-Functionalization of Fullerenes. J. Am. Chem. Soc., **2009**, 131, 8180-8195.

(88.) Supur, M.; El-Khouly, M. E.; Seok, J.H.; Kay, K.-Y.; Fukuzumi, S. Elongation of Lifetime of the Charge-Separated State of FerroceneNaphthalenediimide[60]Fullerene Triad via Stepwise Electron Transfer. J. Phys. Chem. A, **2011**, 115, 14430-14437.

(89.) Pieta, P.; Obraztsov, I.; Sobczak, J. W.; Chernyayeva, O.; Das, S. K.; D'Souza, F.; Kutner, W. A Versatile Material for a Symmetrical Electric Energy Storage Device: A Composite of the Polymer of the Ferrocene Adduct of C_{60} and Single-Wall Carbon Nanotubes Exhibiting Redox Conductivity at Both Positive and Negative Potentials. J. Phys. Chem. C, **2013**, 117, 1995-2007.

(90.) Liu, J.-Y.; El-Khouly, M. E.; Fukuzumi, S.; Ng, D. K. P. Photoinduced Electron Transfer in a Ferrocene–Distyryl BODIPY Dyad and a Ferrocene–Distyryl BODIPY–C_{60} Triad. Chem Phys Chem, **2012**, 13, 2030-2036.

(91.) Andersson, C.-H.; Nyholm, L.; Grennberg, H. Synthesis and Characterization of a Ferrocene-Linked Bis-Fullerene[60] Dumbbell. Dalton Trans., **2012**, 41, 2374-2381.

(92.) Oviedo, J. J.; El-Khouly, M. E.; de la Cruz, P.; Pérez, L.; Garín, J.; Orduna, J.; Araki, Y.; Langa, F.; Ito, O. Synthesis and Photophysical Properties of Ruthenocene-[60]Fullerene Dyads. New J. Chem., **2006**, 30, 93-101.

(93.) Mancel, D.; Jevric, M.; Davies, E. S.; Schröder, M.; Khlobystov, A. N. Triad and Cyclic Diad Compounds of [60]Fullerene with Metallocenes. Dalton Trans., **2013**, 42, 5056-5067.

(94.) Araki, Y.; Yasumura, Y.; Ito, O. Photoinduced Electron Transfer Competitive with Energy Transfer of the Excited Triplet State of [60]Fullerene to Ferrocene Derivatives Revealed by Combination of Transient Absorption and Thermal Lens Measurements. J. Phys. Chem. B **2005**, 109, 9843-9848.

(95.) Armaroli, N.; Diederich, F.; Echegoyen, L.; Habicher, T.; Flamigni, L.; Marconi, G.; Nierengarten, J.-F. A New Pyridyl-Substituted Methanofullerene Derivative. Photophysics, Electrochemistry and Self-Assembly with Zinc(II) meso-Tetraphenylporphyrin (ZnTPP). New J. Chem., **1999**, 77-83.

(96.) Rio, Y.; Seitz, W.; Gouloumis, A.; Vázquez, P.; Sessler, J. L.; Guldi, D. M.; Torres, T. A Panchromatic Supramolecular Fullerene-Based Donor-Acceptor Assembly Derived from a Peripherally Substituted Bodipy-Zinc Phthalocyanine Dyad. Chem. Eur. J., **2010**, 16, 1929-1940.

(97.) Das, S. K.; Song, B.; Mahler, A.; Nesterov, V. N.; Wilson, A. K.; Ito, O.; D'Souza, F. Electron Transfer Studies of High Potential Zinc Porphyrin-Fullerene Supramolecular Dyads. J. Phys. Chem. C, **2014**, 118, 3994-4006.

(98.) KC, C.B.; Lim, G.N.; Karr, P.A.; D'Souza, F. Supramolecular Tetrad Featuring Covalently Linked Bis(porphyrin)-Phthalocyanine Coordinated to Fullerene: Construction and Photochemical Studies. Chem. Eur. J., **2014**, 20, 7725-7735.

(99.) Rodríguez-Morgade, M. S.; Plonska-Brzezinska, M. E.; Athans, A. J.; Carbonell, E.; de Miguel, G.; Guldi, D. M.; Echegoyen, L.; Torres, T. Synthesis, Characterization, and Photoinduced Electron Transfer Processes of Orthogonal Ruthenium Phthalocyanine-Fullerene Assemblies. J. Am. Chem. Soc., **2009**, 131, 10484-10496.

(100.) Fuchsbauer, A.; Troshina, O. A.; Troshin, P. A.; Koeppe, R.; Lyubovskaya, R. N.; Sariciftci, N. S. Luminescent Tags on Fullerenes: Eu^{3+} Complexes with Pendant Fullerenes. Adv. Funct. Mater., **2008**, 18, 2808-2814.

(101.) Konarev, D. V.; Khasanov, S. S.; Kornev, A. B.; Faraonov, M. A.; Troshin, P. A.; Lyubovskaya, R. N. Molecular and Ionic Complexes of Pyrrolidinofullerene Bearing Chelating 3-Pyridyl Units. Dalton Trans., **2012**, 41, 791-798.

(102.) Santos, L. J.; CarvalhoDa-Silva, D.; Rebouças, J. S.; Alves, M. R. A.; Idemori, Y. M.; Matencio, T.; Freitas, R. P.; Alves, R. B. Synthesis of New Porphyrin/Fullerene Supramolecular Assemblies: a Spectroscopic and Electrochemical Investigation of their Coordination Equlibrium in Solution. Tetrahedron, **2011**, 67, 228-235.

(103.) Fan, J.; Wang, Y.; Blake, A. J.; Wilson, C.; Davies, E. S.; Khlobystov, A. N.; Schröder, M. Controlled Assembly of Silver(I)-Pyridylfullerene Networks. Angew. Chem., **2007**, 119, 8159-8162.

(104.) Peng, P.; Li, F.-F.; Neti, V. S. P. K.; Metta-Magana, A. J.; Echegoyen, L. Design, Synthesis, and X-Ray Crystal Structure of a Fullerene-Linked Metal-Organic Framework. Angew. Chem. Int. Ed., **2014**, 53, 160-163.

(105.) D’Souza, F.; Gadde, S.; Schumacher, A. L.; Zandler, M. E.; Sandanayaka, A. S. D.; Araki, Y.; Ito, O. Supramolecular Triads of Free-Base Porphyrin, Fullerene, and Ferric Porphyrins via the “Covalent-Coordinate” Binding Approach: Formation, Sequential Electron Transfer, and Charge Stabilization. J. Phys. Chem. C, **2007**, 111, 11123-11130.

(106.) Xiang, Y.; Wei, X.-W.; Zhang, X.-M.; Wang, H.-L.; Wei, X.-L.; Hu, J.-P.; Yin, G.; Xu, Z. Synthesis of New Pyridinofullerene Ligands Capable of Forming Complexes with Zinc Tetraphenyl Porphyrin. Inorg. Chem. Comm., **2006**, 9, 452-455.

(107.) KC, C. B.; Ohkubo, K.; Karr, P. A.; Fukuzumi, S.; D’Souza, F. A ‘Two-Point’ Bound Zinc Porphyrin-Zinc Phthalocyanine-Fullerene Supramolecular Triad for Sequential Energy and Electron Transfer. Chem. Commun., **2013**, 49, 7614-7616.

(108.) Terazono, Y.; Kodis, G.; Liddell, P.A.; Garg, V.; Gervaldo, M.; Moore, T.A.; Moore, A.L.; Gust, D. Photoinduced Electron Transfer in a Hexaphenylbenzene-based Self-assembled Porphyrin-fullerene Triad. Photochem. and Photobiol., **2007**, 83, 464-469.

(109.) Xie, Y.; Hill, J. P.; Schumacher, A. L.; Sandanayaka, A. S. D.; Araki, Y.; Karr, P. A.; Labuta, J.; D’Souza, F.; Ito, O.; Anson, C. E.; Powell, A. K.; Ariga, K. Twisted, Two-Faced Porphyrins as Hosts for Bispyridyl Fullerenes: Construction and Photophysical Properties. J. Phys. Chem. C, **2008**, 112, 10559-10572.

(110.) Tat, F. T.; Zhou, Z.; MacMahon, S.; Song, F.; Rheingold, A. L.; Echegoyen, L.; Schuster, D. I.; Wilson, S. R. A New Fullerene Complexation Ligand: N-Pyridylfulleropyrrolidine. J. Org. Chem., **2004**, 69, 4602-4606.

(111.) Trabolsi, A.; Urbani, M.; Delgado, J. L.; Ajamaa, F.; Elhabiri, M.; Solladié, N.; Nierengarten, J.-F.; Albrecht-Gary, A.-M. Large Photoactive Supramolecular Ensembles Prepared from C_{60}-Pyridine Substrates and Multi-Zn(II)-Porphyrin Receptors. New J. Chem., **2008**, 32, 159-165.

(112.) Grimm, B.; Schornbaum, J.; Jasch, H.; Trukhina, O.; Wessendorf, F.; Hirsch, A.; Torres, T.; Guldi, D. M. Step-by-step Self-Assembled Hybrids that Feature Control over Energy and Charge Transfer. PNAS, **2012**, 109, 15565-15571.

(113.) D'Souza, F.; Amin, A. N.; El-Khouly, M. E.; Subbaiyan, N. K.; Zandler, M. E.; Fukuzumi, S. Control over Photoinduced Energy and Electron Transfer in Supramolecular Polyads of Covalently Linked azaBODIPY-Bisporphyrin 'Molecular Clip' Hosting Fullerene. J. Am. Chem.Soc., **2012**, 134, 654-664.

(114.) Nair, V. S.; Pareek, Y.; Karunakaran, V.; Ravikanth, M.; Ajayaghosh, A. Cyclotriphosphazene Appended Porphyrins and Fulleropyrrolidine Complexes as Supramolecular Multiple Photosynthetic Reaction Centers: Steady and Excited States Photophysical Investigation. Phys. Chem. Chem. Phys., **2014**, 16, 10149-10156.

(115.) Stangel, C.; Schubert, C.; Kuhri, S.; Rotas, G.; Margraf, J. T.; Regulska, E.; Clark, T.; Torres. T.; Tagmatarchis, N.; Goutsolelos, A. G.; Guldi, D. M. Tuning the Reorganization Energy of Electron Transfer in Supramolecular Ensembles – Metalloporphyrin, Oligophenylenevinylenes, and Fullerene – and the Impact on Electron Transfer Kinetics. Nanoscale, **2015**, 7, 2597-2608.

(116.) Kuramochi, Y.; Satake, A.; Itou, M.; Ogawa, K.; Araki, Y.; Ito, O.; Kobuke, Y. Light-Harvesting Supramolecular Porphyrin Macrocycle Accommodating a Fullerene-Tripodal Ligand. Chem. Eur. J., **2008**, 14, 2827-2841.

(117.) Uyar, Z.; Satake, A.; Kobuke, Y.; Hirota, S. Stable Supramolecular Complex of Porphyrin Macroring with Pyridyl and Fullerenyl Ligands. Tetrahedron Letters, **2008**, 49, 5484-5487.

(118.) Kuramochi, Y.; Satake, A.; Sandanayaka, A. S. D.; Araki, Y.; Ito, O.; Kobuke, Y. Fullerene- and Pyromellitdiimide-Appended Tripodal Ligands Embedded in Light-Harvesting Porphyrin Macrorings. Inorg. Chem., **2011**, 50, 10249-10258.

(119.) Tsuchiya, T.; Rudolf, M.; Wolfrum, S.; Radhakrishnan, S. G.; Aoyama, R.; Yokosawa, Y.; Oshima, A.; Akasaka, T.; Nagase, S.; Guldi, D. M. Coordinative Interactions between Porphyrins and C_{60}, La@C_{82} and La_2@C_{80}. Chem. Eur. J., **2013**, 19, 558-565.

(120.) Pereira, A. M. V. M.; Hausmann, A.; Tomé, J. P. C.; Trukhina, O.; Urbani, M.; Neves, M. G. P. M. S.; Cavaleiro, J. A. S.; Guldi, D. M.; Torres, T. Porphyrin-Phthalocyanine/Pyridylfullerene Supramolecular Assemblies. Chem. Eur. J., **2012**, 18, 3210-3219.

(121.) Ince, M.; Hausmann, A.; Martínez-Díaz, M.V.; Guldi, D.M.; Torres, T. Non-Covalent versus Covalent Donor-Acceptor Systems Based on Near-Infrared Absorbing Azulenocyanines and C_{60} Fullerene Derivatives. Chem. Commun., **2012**, 48, 4058-4060.

(122.) Wu, Z.-Y.; Huang, R.-B.; Xie, S.-Y; Zheng, L.-S. Ruthenium-Bipyridine Complexes bearing Fullerene or Carbon Nanotubes: Synthesis and Impact of Different Carbon-Based Ligands on the Resulting Products. Dalton Trans.,**2011**, 40, 8353-8360.

(123.) Schumacher, A. L.; Sandanayaka, A. S. D.; Hill, J. P.; Ariga, K.; Karr, P. A.; Araki, Y.; Ito, O.; D’Souza, F. Supramolecular Triad and Pentad Composed of Zinc-Porphyrin(s), Oxoporphyrinogen, and Fullerene(s): Design and Electron-Transfer Studies. Chem. Eur. J., **2007**, 13, 4628-4635.

(124.) El-Khouly, M. E.; Wijesinghe, C. A.; Nesterov, V. N.; Zandler, M. E.; Fukuzumi, S.; D’Souza, F. Ultrafast Photoinduced Energy and Electron Transfer in Multi-Modular Donor-Acceptor Conjugates. Chem. Eur. J., **2012**, 18, 13844-13853.

(125.) El-Khouly, M. E.; Ju, D. K.; Kay, K.-Y.; D’Souza, F.; Fukuzumi, S. Supramolecular Tetrad of Subphthalocyanine-Triphenylamine-Zinc Porphyrin Coordinated to Fullerene as an “Antenna-Reactor-Center” Mimic: Formation of a Long-Lived Charge-Separated State in Nonpolar Solvent. Chem. Eur. J., **2010**, 16, 6193-6202.

(126.) Marczak, R.; Sgobba, V.; Kutner, W.; Gadde, S.; D’Souza, F.; Guldi, D. M. Landmuir-Blodgett Films of a Cationic Zinc Porphyrin-Imidazole-Functionalized Fullerene Dyad: Formation and Photoelectrochemical Studies. Langmuir, **2007,** 23, 1917-1923.

(127.) D’Souza, F.; Smith, P. M.; Rogers, L.; Zandler, M. E.; Islam, D.-M. S.; Araki, Y.; Ito, O. Formation, Spectral, Electrochemical, and Photochemical Behavior of Zinc N-Confused Porphyrin Coordinated to Imidazole Functionalized Fullerene Dyads. Inorg. Chem., **2006**, 45, 5057-5065.

(128.) Yoosaf, K.; Iehl, J.; Nierengarten, I.; Hmadeh, M.; Albrecht-Gary, A.-M.; Nierengarten, J.-F.; Armaroli, N. A Supramolecular Photosynthetic Model Made of a Multiporphyrinic Array Constructed around a C_{60} Core and a C_{60}-Imidazole Derivative. Chem. Eur. J., **2014**, 20, 223-231.

(129.) D’Souza, F.; Smith, P. M.; Zandler, M. E.; McCarty, A. L.; Itou, M.; Araki, Y.; Ito, O. Energy Transfer Followed by Electron Transfer in a Supramolecular Triad Composed of Boron Dipyrrin, Zinc Porphyrin, and Fullerene: a Nodel for the Photosynthetic Antenna-Reaction Center Complex. J. Am. Chem. Soc., **2004**, 126, 7898-7907.

(130.) Maligaspe, E.; Kumpulainen, T.; Subbaiyan, N. K.; Zandler, M. E.; Lemmetyinen, H.; Tkachenko, N.V.; D’Souza, F. Electronic Energy Harvesting Multi BODIPY-Zinc Porphyrin Dyads Accommodating Fullerene as Photosynthetic Composite of Antenna-Reaction Center. Phys. Chem. Chem. Phys., **2010**, 12, 7434-7444.

(131.) El-Khouly, M. E.; Rogers, L. M.; Zandler, M. E.; Suresh, G.; Fujitsuka, M.; Ito, O.; D'Souza, F. Studies on Intra-Supramolecular and Intermolecular Electron-Transfer Processes between Zinc Napththalocyanine and Imidazole-Appended Fullerene. ChemPhysChem, **2003**, 4, 474-481.

(132.) Bikram, C. K. C.; Subbaiyan, N. K.; D’Souza, F. Supramolecular Donor-Acceptor Assembly Derived from Tetracarbazole-Zinc Phthalocyanine Coordinated to Fullerene: Design, Synthesis, Photochemical, and Photoelectrochemical Studies. J. Phys. Chem. C, **2012**, 116, 11964-11972.

(133.) Gao, Y.; Wu, X.; Zeng, X. C. Designs of Fullerene-Based Frameworks for Hydrogen Storage. J. Mater. Chem. A, **2014**, 2, 5910-5914.

(134.) El-Khlouly, M.E.; Ito, O.; Smith, P.M.; D’Souza, F. Intermolecular and Supramolecular Photoinduced Electron Transfer Processes of Fullerene–Porphyrin/Phthalocyanine Systems. J. Photochem. Photobiol. C: Photochem. Rev., **2004**, 5, 79-104.

(135.) Brunet, E.; Alonso, M.; Quintana, M. C.; Juanesa, O.; Rodríguez-Ubis, J.-C. Facile Synthesis of New Fullerene-Ru(bpy)$_3$ Dyads Bearing Phosphonate Groups for Hybrid Organic-Inorganic Materials. Tetrahedron Lett., **2007**, 48, 3739-3743.

(136.) Maggini, M.; Guldi, D. M.; Mondini, S.; Scorrano, G.; Paolucci, F.; Ceroni, P.; Roffia, S. Photoinduced Electron Transfer in a Tris(2,2’-Bipyridine)-C$_{60}$-Ruthenium(II) Dyad: Evidence of Charge Recombination to a Fullerene Excited State. Chem. Eur. J., **1998**, 4, 1992-2000.

(137.) Zhou, Z.; Sarova, G.H.; Zhang, S.; Ou, Z.; Tat, F. T.; Kadish, K. M.; Echegoyen, L.; Guldi, D. M.; Schuster, D. I.; Wilson, S. R. Fullerene Polypyridine Ligands: Synthesis, Ruthenium Complexes, and Electrochemical and Photophysical Properties. Chem. Eur. J., **2006**, 12, 4241-4248.

(138.) Modin, J.; Johansson, H.; Grennberg, H. New Pyrazolino- and Pyrrolidino[60]fullerenes with Transition-Metal Chelating Pyridine Substituents: Synthesis and Complexation to Ru(II). Org. Lett., **2005**, 7, 3977-3979.

(139.) Karlsson, S.; Modin, J.; Becker, H.-C.; Hammarström, L.; Grennberg, H. How Close Can You Get? Studies of Ultrafast Light-Induced Processes in Ruthenium-[60] Fullerene Dyads with Short Pyrazolino and Pyrrolidino Links. Inorg. Chem., **2008**, 47, 7286-7294.

(140.) Chaignon, F.; Torroba, J.; Blart, E.; Borgström, M.; Hammarström, L.; Odobel, F. Distance-Independent Photoinduced Energy Transfer over 1.1 to 2.3 nm in Ruthenium Trisbipyridine-Fullerene Assemblies. New J . Chem., **2005**, 29, 1272-1284.

(141.) Allen, B. D.; Benniston, A. C.; Harriman, A.; Mallon, L. J.; Pariani, C. Competing Through-Space and Through-Bond, Intramolecular Triplet-Energy Transfer in a Supposedly Rigid Ruthenium(II) Tris(2,2’-Bipyridine)-Fullerene Molecular Dyad. Phys. Chem. Chem. Phys., **2006**, 8, 4112-4118.

(142.) Cardinali, F.; Gallani, J.-L.; Schergna, S.; Maggini, M.; Nierengarten, J.-F. An Amphiphilic C_{60} Derivative with a Tris(2,2’-Bipyridine)Ruthenium(II) Polar Head Group: Synthesis and Incorporation in Langmuir Films. Tetrahedron Lett., **2005**, 46, 2969-2972.

(143.) Cardinali, F.; Nierengarten, J.-F. Synthesis of a New C60-Substituted Tris(2,2’-Bipyridine)Ruthenium(II) Complex. Tetrahedron Lett., **2003**, 44, 2673-2676.

(144.) Guldi, D. M.; Maggini, M.; Menna, E.; Scorrano, G.; Ceroni, P.; Marcaccio, M.; Paolucci, F.; Roffia, S. A Photosensitizer Dinuclear Ruthenium Complex: Intramolecular Energy Transfer to a Covalently Linked Fullerene Acceptor. Chem. Eur. J., **2001**, 7, 1597-1605.

(145.) Walsh, E.A.; Deye, J.R.; Baas, W.; Sullivan, K.; Lancaster, A.; Walters, K. A. Synthesis and Spectroscopic Studies of Transition-Metal Fullerene Supramolecular Systems. J. Photochem. and Photobiol. A: Chem., **2013**, 260, 24-36.

(146.) Armaroli, N.; Accorsi, G.; Felder, D.; Nierengarten, J.-F. Photophysical Properties of the Re^{I} and Ru^{II} Complexes of a New C_{60}-Substituted Bipyridine Ligand. Chem. Eur. J., **2002**, 8, 2314-2323.

(147.) Possamai, G.; Menna, E.; Maggini, M.; Carano, M.; Marcaccio, M.; Paolucci, F.; Guldi, D. M.; Swartz, A. Phenium(I) and Ruthenium(II) Complexes with a Crown-Linked Methanofullerene Ligand: Synthesis, Electrochemistry and Photophysical Characterization. Photochem. Photobiol. Sci., **2006**, 5, 1154-1164.

(148.) Lee, H. D.; Oh, S. K.; Choi, C. S.; Kay, K.-Y. A Novel Amphiphilic Re^{I} Complex with Bis(Fullerene)-Substituted Bipyridine Ligands: Synthesis, Electrochemistry, and Langmuir Film. Eur. J. Inorg. Chem., **2007**, 503-508.

(149.) Deye, J. R.; Shiveley, A. N.; Goins, S. M.; Rizzo, L.; Oehrle, S. A.; Walters, K. A. Synthesis of a New Ligand for Transition Metal-Fullerene Supramolecular Systems. Inorg. Chem., **2008**, 47, 23-25.

(150.) Fan, J.; Chamberlain, T. W.; Wang, Y.; Yang, S.; Blake, A. J.; Schröder, M.; Khlobystov, A. N. Encapsulation of Transition Metal Atoms into Carbon Nanotubes: a Supramolecular Approach. Chem. Commun., **2011**, 47, 5696-5698.

(151.) Lee, S.-H.; Chan, C. T.-L.; Wong, K. M.-C.; Lam, W. H.; Kwok, W.-M.; Yam, V. W.-W. Design and Synthesis of Bipyridine Platinum(II) Bisalkynyl Fullerene Donor-Chromophore-Acceptor Triads with Ultrafast Charge Separation. J. Am. Chem. Soc., **2014**, 136, 10041-10052.

(152.) Lee, S.-H.; Chan, C. T.-L.; Wong, K. M.-C.; Lam, W. H.; Kwok, W.-M.; Yam, V. W.-W. Synthesis and Photoinduced Electron Transfer in Platinum(II) bis(N-(4-ethynylphenyl)carbazole)-bipyridine Fullerene Complexes. Dalton Trans., **2014**, 43, 17624–17634.

(153.) Rio, Y.; Enderlin, G.; Bourgogne, C.; Nierengarten, J.-F. Ground and Excited State Electronic Interactions in a Bis(phenanthroline) Copper(I) Complex Sandwiched between Two Fullerene Subunits. Inorg. Chem., **2003**, 42, 8783-8793.

(154.) Cardinali, F.; Mamlouk, H.; Rio, Y.; Armaroli, N.; Nierengarten, J.-F. Fullerohelicates: a New Class of Fullerene-Containing Supermolecules. Chem. Commun., **2004**, 1582-1583.

(155.) Listorti, A.; Accorsi, G.; Rio, Y.; Armaroli, N.; Moudam, O.; Gégout, A.; Delavaux-Nicot, B.; Holler, M.; Nierengarten, J.-F. Heteroleptic Copper(I) Complex Coupled with Methano[60]fullerene : Synthesis, electrochemistry, and Photophysics. Inorg. Chem., **2008**, 47, 6254-6261.

(156.) Rio, Y.; Sánchez-García, D.; Seitz, W.; Torres, T.; Sessler, J. L.; Guldi, D. M. A Bisfullerene-Bis(dipyrrinato)zinc Complex : Electronic Coupling and Charge Separation in an Easy-to-Assemble Synthetic System. Chem. Eur. J., **2009**, 15, 3956-3959.

(157.) Valore, A.; Balordi, M.; Colombo, A.; Dragonetti, C.; Righetto, S.; Roberto, D.; Ugo, R.; Benincori, T.; Rampinini, G.; Sannicolò, F.; Demartin, F. Novel Ruthenium(II)

Complexes with Substituted 1,10-Phenanthroline or 4,5-Diazafluorene Linked to a Fullerene as Highly Active Second Order NLO Chromophores. Dalton Trans., **2010**, 39, 10314-10318.

(158.) Dragonetti, C.; Valore, A. ; Colombo, A. ; Righetto, S. ; Rampinini, G. ; Colombo, F. ; Rocchigiani, L.; Macchioni, A. An Investigation on the Second-Order NLO Properties of Novel Cationic Cyclometallated Ir(III) Complexes of the Type [Ir(2-phenylpyridine)$_2$(9-R-4,5-diazafluorene)]$^+$ (R=H, fulleridene) and the Related Neutral Complex with the New 9-Fulleriden-4-Monoazafluorene Ligand. Inorg. Chim. Acta, **2012**, 382, 72-78.

(159.) Nastasi, F.; Puntoriero, F.; Natali, M.; Mba, M.; Maggini, M.; Mussini, P.; Panigati, M.; Campanga, S. Photoinduced Intercomponent Excited-state Decays in a Molecular Dyad Made of a Dinuclear Rhenium(I) Chromophore and a Fullerene Electron Acceptor Unit. Photochem. Photobiol. Sci., **2015**, 14, 909–918.

(160.) Conley, N. R.; Lagowski, J. J. Expanding the Coordination Chemistry of Buckminsterfullerene : Synthesis and Characterisation of (N,N’-dimethylethylenediamine-[60]-fullerene)copper(II) Bromide. Inorg. Chem. Comm., **2004**, 7, 932-934.

(161.) Fu, K.; Henbest, K.; Zhang, Y. J.; Valentin, S.; Sun, Y.-P. Synthesis and Optical Properties of Metal-Centered Dimeric Fullerene Macromolecules. J. Photochem. and Photobiol. A: Chem., **2002**, 150, 143-152.

(162.) Armspach, D.; Constable, E.C.; Diederich, F.; Housecroft, C.E.; Nierengarten, J.-F. Bucky-Ligands: Fullerene-Substituted Oligopyridines for Metallosupramolecular Chemistry. Chem. Comm., **1996**, 2009-2010.

(163.) Armspach, D.; Constable, E.; Diederich, F.; Housecrpft, C.E.; Nierengarten, J.-F. Bucky Ligands: Synthesis, Ruthenium(II) Complexes, and Electrochemical Properties. Chem. Eur. J. **1998**, 4, 723-733.

(164.) El-ghayoury, A.; Schenning, A. P. H. J.; van Hal, P. A.; Weidl, C. H.; van Dongen, J. L. J.; Janssen, R. A. J.; Schubert, U. S.; Meijer, E. W. Metallo-supramolecular Oligo(p-phenylene Vinylene)/[60]fullerene Architectures: Towards Functional Materials. Thin Solid Films, **2002**, 403–404, 97-101.

(165.) Du, C.; Li, Y.; Wang, S.; Shi, Z.; Xiao, S.; Zhu, D. Synthesis and Characterization of [60]Fullerene-Substituted Oligopyridines Ruthenium Complexes. Synth. Met., **2001**, 124, 287-289.

(166.) Gao, Y.; Song, Y.; Li, Y.; Wang, Y.; Liu, H.; Zhu, D. Large Optical Limiting of [60]Fullerene-Substituted Terpyridine Palladium Nanoparticles. Appl. Phys. B, **2003**, 76, 761-763.

(167.) Ichiki, T.; Matsuo, Y.; Nakamura, E. Photostability of a Dyad of Magnesium Porphyrin and Fullerene and its Applications to Photocurrent Conversion. Chem. Commun., **2013**, 49, 279-281.

(168.) Zou, T.; Zhen, M.; Chen, D.; Li, R.; Guan, M.; Shu, C.; Han, H.; Wang, C. The Positive Influence of Fullerene Derivatives Bonded to Manganese(III) Porphyrins on Water Proton Relaxation. Dalton Trans., **2015**, 44, 9114–9119.

(169.) Krokos, E.; Spänig, F.; Ruppert, M.; Hirsch, A.; Guldi, D. M. Dendritic Metalloporphyrin–Fullerene Conjugates: Changing the Microenvironment around Redox-Active Centers and its Impact on Charge-Transfer Reactions. Chem. Eur. J., **2012**, 18, 10427-10435.

(170.) Sutton, L. R.; Scheloske, M.; Pirner, K.S.; Hirsch, A.; Guldi, D. M.; Gisselbrecht, J.-P. Unexpected Change in Charge Transfer Behavior in a Cobalt(II) Porphyrin-Fullerene Conjugate That Stabilizes Radical Ion Pair States J. Am. Chem. Soc., **2004**, 126, 10370-10381.

(171.) Liu, G.; Khlobystov, A. N.; Charalambidis, G.; Coutsolelos, A. G.; Briggs, G. A. D.; Porfyrakis, K. N@C_{60}–Porphyrin: A Dyad of Two Radical Centers. J. Am. Chem. Soc., **2012**, 134, 1938-1941.

(172.) Bonifazi, D.; Diedrich, F. Strong Intramolecular Chromophore Interactions in Novel Bis([60]Fullerene)-Oligoporphyrin Nanoarrays. Chem. Comm., **2002**, 2178-2179.

(173.) Bonifazi, D.; Scholl, M.; Song, F.; Echegoyen, L.; Accorsi, G.; Armaroli, N.; Diederich, F. Exceptional Redox and Photophysical Properties of a Triply Fused Diporphyrin–C_{60} Conjugate: Novel Scaffolds for Multicharge Storage in Molecular Scale Electronics. Angew. Chem. Int. Ed., **2003**, 42, 4966-4970.

(174.) Armaroli, N.; Accorsi, G.; Song, F.; Palkar, A.; Echegoyen, L.; Bonifazi, D.; Diederich, F. Photophysical and Electrochemical Properties of meso,meso-Linked Oligoporphyrin Rods with Appended Fullerene Terminals. ChemPhysChem, **2005**, 6, 732-743.

(175.) Bonifazi, D.; Accorsic, G.; Armaroli, N.; Song, F.; Palkar, A.; Echegoyen, L.; Scholl, M.; Seiler, P.; Jaun, B.; Diederich, F. Oligoporphyrin Arrays Conjugated to [60]Fullerene:

Preparation, NMR Analysis, and Photophysical and Electrochemical Properties. Helv. Chim. Acta, **2005**, 88, 1839-1884.

(176.) Charvet, R.; Jiang, D.-L.; Aida, T. Self-Assembly of a π-electronic Amphiphile Consisting of a Zinc Porphyrin–Fullerene Dyad: Formation of Micro-Vesicles with a High Stability. Chem. Comm., **2004**, 2664-2665.

(177.) Ciammaichella, A.; Dral, P. O.; Clark, T.; Tagliatesta, P.; Sekita M.; Guldi, D. M. A π-Stacked Porphyrin–Fullerene Electron Donor–Acceptor Conjugate That Features a Surprising Frozen Geometry. Chem. Eur. J., **2012**, 18, 14008-14016.

(178.) Tkachenko, N. V.; Lemmetyinen, H.; Sonoda, J.; Ohkubo, K.; Sato, T.; Imahori, H.; Fukuzumi, S. Ultrafast Photodynamics of Exciplex Formation and Photoinduced Electron Transfer in Porphyrin-Fullerene Dyads Linked at Close Proximity. J. Phys. Chem. A, **2003**, 107, 8834-8844.

(179.) Al-Subi, A. H.; Niemi, M.; Tkachenko, N. V.; Lemmetyinen, H. Effect of Anion Ligation on Electron Transfer of Double-Linked Zinc PorphyrinFullerene Dyad. J. Phys. Chem. A, **2011**, 115, 3263-3271.

(180.) Villegas, C.; Delgado, J. L.; Bouit, P.-A.; Grimm, B.; Seitz, W.; Martíın, N.; Guldi, D. M. Powering reductive charge shift reactions—linking fullerenes of different electron acceptor strength to secure an energy gradient. Chem. Sci., **2011**, 2, 1677-1681.

(181.) Wielopolski, M.; de Miguel Rojas, G.; van der Pol, C.; Brinkhaus, L.; Katsukis, G.; Bryce, M. R.; Clark, T.; Guldi, D. M. Control over Charge Transfer through Molecular Wires by Temperature and Chemical Structure Modifications. ACS Nano, **2010**, 4, 6449-6462.

(182.) de Miguel, G.; Wielopolski, M.; Schuster, D. I.; Fazio, M. A.; Lee, O. P.; Haley, C. K.; Ortiz, A. L.; Echegoyen, L.; Clark, T.; Guldi, D. M. Triazole Bridges as Versatile Linkers in Electron Donor_Acceptor Conjugates. J. Am. Chem. Soc., **2011**, 133, 13036-13054.

(183.) Vail, S. A.; Krawczuk, P. J.; Guldi, D. M.; Palkar, A.; Echegoyen, L.; Tomé, J. P. C.; Fazio, M. A.; Schuster, D. I. Energy and Electron Transfer in Polyacetylene-Linked Zinc-Porphyrin-[60]Fullerene Molecular Wires. Chem. Eur. J., **2005**, 11, 3375-3388.

(184.) Sukegawa, J.; Schubert, C.; Zhu, X,; Tsuji, H.; Guldi, D. M.; Nakamura, E. Electron Transfer through Rigid Organic Molecular Wires Enhanced by Electronic and Electron–vibration Coupling. Nat. Chem., **2014**, 6, 899-905.

(185.) Ho, K.-H. L.; Hijazi, I.; Rivier, L.; Gautier, C.; Jousselme, B.; de Miguel, G.; Romero-Nieto, C.; Guldi, D. M.; Heinrich, B.; Donnio, B.; Campidelli, S. Host–Guest

Complexation of [60]Fullerenes and Porphyrins Enabled by “Click Chemistry”. Chem. Eur. J., **2013**, 19, 11374-11381.

(186.) D’Souza, F.; Gadde, S.; Islam, D.-M. S.; Wijesinghe, C. A.; Schumacher, A. L.; Zandler, M. E.; Araki, Y.; Ito, O. Multi-Triphenylamine-Substituted Porphyrin-Fullerene Conjugates as Charge Stabilizing “Antenna-Reaction Center” Mimics. J. Phys. Chem. A, **2007**, 111, 8552-8560.

(187.) Wijesinghe, C. A.; El-Khouly, M. E.; Zandler, M. E.; Fukuzumi, S.; D’Souza, F. A Charge-Stabilizing, Multimodular, Ferrocene-Bis(triphenylamine)-Zinc-porphyrin-Fullerene Polyad. Chem. Eur. J., **2013**, 19, 9629-9638.

(188.) Imahori, H.; Tamaki, K.; Guldi, D. M.; Luo, C.; Fujitsuka, M.; Ito, O.; Sakata, Y.; Fukuzumi, S. Modulating Charge Separation and Charge Recombination Dynamics in Porphyrin-Fullerene Linked Dyads and Triads: Marcus-Normal versus Inverted Region J. Am. Chem. Soc., **2001**, 123, 2607-2617.

(189.) Imahori, H.; Guldi, D. M.; Tamaki, K.; Yoshida, Y.; Luo, C.; Sakata, Y.; Fukuzumi, S. Charge Separation in a Novel Artificial Photosynthetic Reaction Center Lives 380 ms. J. Am. Chem. Soc., **2001**, 123, 6617-6628.

(190.) Song, L.-C.; Liu, X.-F.; Xie, Z.-J.; Luo, F.-X.; Song, H.-B. Synthesis and Structural Characterization of Some New Porphyrin-Fullerene Dyads and Their Application in Photoinduced H_2 Evolution. Inorg. Chem., **2011**, 50, 11162-11172.

(191.) Imahori, H.; Yamada, H.; Guldi, D. M.; Endo, Y.; Shimomura, A.; Kundu, S.; Yamada, K.; Okada, T.; Sakata, Y.; Fukuzumi, S. Comparison of Reorganization Energies for Intra- and Intermolecular Electron Transfer. Angew. Chem. Int. Ed., **2002**, 41, 2344-2347.

(192.) Lee, S.-H.; Larsen, A.G.; Ohkubo, K.; Cai, Z.-L.; Reimers, J.R.; Fukuzumi, S.; Crossley, M. J. Long-Lived Long-Distance Photochemically induced Spin-Polarized Charge Separation in β,β’-Pyrrolic Fused Ferrocene-Porphyrin-Fullerene Systems. Chem. Sci., **2012**, 3, 257-269.

(193.) Wang, C.-L.; Zhang, W.-B.; Hsu, C.-H.; Sun, H.-J.; Van Horn, R. M.; Tu, Y.; Anokhin, D. V.; Ivanov, D. A.; Cheng, S. Z. D. A Supramolecular Structure with an Alternating Arrangement of Donors and Acceptors Constructed by a Trans-Di-C_{60}-Substituted Zn Porphyrin Derivative in the Solid State. Soft Matter, **2011**, 7, 6135-6143.

(194.) Kahnt, A.; Kärnbratt, J.; Esdaile, L. J.; Hutin, M.; Sawada, K.; Anderson, H. L.; Albinsson, B. Temperature Dependence of Charge Separation and Recombination in

Porphyrin Oligomer-Fullerene Donor-Acceptor Systems. J. Am. Chem. Soc., **2011**, 133, 9863-9871.

(195.) Charvet, R.; Yamamoto, Y.; Sasaki, T.; Kim, J.; Kato, K.; Takata, M.; Saeki, A.; Seki, S.; Aida, T. Segregated and Alternately Stacked Donor/Acceptor Nanodomains in Tubular Morphology Tailored with Zinc Porphyrin−C_{60} Amphiphilic Dyads: Clear Geometrical Effects on Photoconduction. J. Am. Chem.Soc., **2012**, 134, 2524-2527.

(196.) Schuster, D. I.; Li, K.; Guldi, D. M.; Palkar, A.; Echegoyen, L.; Stanisky, C.; Cross, R. J.; Niemi, M.; Tkachenko, N. V.; Lemmetyinen, H. Azobenzene-Linked Porphyrin-Fullerene Dyads. J. Am. Chem. Soc., **2007**, 129, 15973-15982.

(197.) Galili, T.; Regev, A.; Levanon, H.; Schuster, D. I.; Guldi, D. M. Spin Dynamics of a "Parachute" Shaped Fullerene-Porphyrin Dyad. J. Phys. Chem. A, **2004**, 108, 10632-10639.

(198.) Winters, M. U.; Dahlstedt, E.; Blades, H. E.; Wilson, C. J.; Frampton, M. J.; Anderson, H. L.; Albinsson, B. Probing the Efficiency of Electron Transfer through Porphyrin-Based Molecular Wires. J. Am. Chem. Soc., **2007**, 129, 4291-4297.

(199.) Yeon Lee, C.; Jang, J. K.; Kim, C. H.; Jung, J.; Park, B. K.; Park, J.; Choi, W.; Han, Y.-K.; Joo, T.; Park, J. T. Remarkably Efficient Photocurrent Generation Based on a [60]Fullerene-Triosmium Cluster/Zn-Porphyrin/Boron-Dipyrrin Triad SAM. Chem. Eur. J., **2010**, 16, 5586-5599.

(200.) Lee, M. H.; Kim, J. W.; Lee, C. Y. [60]Fullerene-porphyrin-ferrocene Triad Self-assembled Monolayers (SAMs) for Photovoltaic Applications. J. Organomet. Chem., **2014**, 761, 20-27.

(201.) Feng, L.; Radhakrishnan, S. G.; Mizorogi, N.; Slanina, Z.; Nikawa, H.; Tsuchiya, T.; Akasaka, T.; Nagase, S.; Martín, N.; Guldi, D. M. Synthesis and Charge-Transfer Chemistry of $La_2@I_h$-C_{80}/$Sc_3N@I_h$-C_{80}_Zinc Porphyrin Conjugates: Impact of Endohedral Cluster. J. Am. Chem. Soc., **2011**, 133, 7608-7618.

(202.) Wolfrum, S.; Pinzón, J. R.; Molina-Ontoria, A.; Gouloumis, A.; Martín, N.; Echegoyen, L.; Guldi, D. M. Utilization of $Sc_3N@C_{80}$ in Long-Range Charge Transfer Reactions. Chem. Commun., **2011**, 47, 2270-2272.

(203.) Guldi, D. M.; Feng, L.; Radhakrishnan, S. G.; Nikawa, H.; Yamada, M.; Mizorogi, N.; Tsuchiya, T.; Akasaka, T.; Nagase, S.; Herranz, M. Á.; Martín, N. A Molecular $Ce_2@I_h$-C_{80} Switch - Unprecedented Oxidative Pathway in Photoinduced Charge Transfer Reactivity J. Am. Chem. Soc., **2010**, 132, 9078-9086.

(204.) Poddutoori, P. K.; Sandanayaka, A. S. D.; Zarrabi, N.; Hasobe, T.; Ito, O.; van der Est, A. Sequential Charge Separation in Two Axially Linked Phenothiazine-Aluminum(III) Porphyrin-Fullerene Triads. J. Phys. Chem. A, **2011**, 115, 709-717.

(205.) Poddutoori, P. K.; Sandanayaka, A. S. D.; Hasobe, T.; Ito, O.; van der Est, A. Photoinduced Charge Separation in a Ferrocene-Aluminum(III) Porphyrin-Fullerene Supramolecular Triad. J. Phys. Chem. B, **2010**, 114, 14348-14357.

(206.) Obondi, C. O.; Lim, G. N.; D’Souza, F. Triplet−Triplet Excitation Transfer in Palladium Porphyrin−Fullerene and Platinum Porphyrin−Fullerene Dyads. J. Phys. Chem. C, **2015**, 119, 176−185.

(207.) Kim, H. J.; Park, K.-M.; Ahn, T. K.; Kim, S. K.; Kim, K. S.; Kim, D.; Kim, H.-J. Novel Fullerene–Porphyrin–Fullerene Triad Linked by Metal Axial Coordination: Synthesis, X-ray Crystal Structure, and Spectroscopic Characterizations of trans-Bis([60]Fullerenoacetato)Tin(IV) Porphyrin. Chem. Commun., **2004**, 2594-2595.

(208.) Xu, H.; Zheng, J. Face-to-Face Alignment of Porphyrin/Fullerene Nanowires Linked by Axial Metal Coordination. Macromol. Chem. Phys., **2010**, 211, 2125-2131.

(209.) Enes, R. F.; Cid, J.-J.; Hausmann, A.; Trukhina, O.; Gouloumis, A.; Vázquez, P.; Cavaleiro, J. A. S.; Tomé, A. C.; Guldi, D. M.; Torres, T. Synthesis and Photophysical Properties of Fullerene–Phthalocyanine–Porphyrin Triads and Pentads Chem. Eur. J., **2012**, 18, 1727-1736.

(210.) Ballesteros, B.; de la Torre, G.; Torres,T. ; Hug, G. L.; Rahman, G. M. A.; Guldi, D. M. Synthesis and Photophysical Characterization of a Titanium(IV) Phthalocyanine-C_{60} Supramolecular Dyad. Tetrahedron, **2006**, 62, 2097-2101.

(211.) Tian, Z.; Heb, C.; Liu, C.; Yang, W.; Yao, J.; Nie, Y.; Gongc, Q.; Liu, Y. Optical Limiting Property of Nanoparticles from a Copper Phthalocyanine-Fullerene Dyad. Materials Chem. and Phys., **2005**, 94, 444-448.

(212.) Isosomppi, M.; Tkachenko, N. V.; Efimov, A.; Vahasalo, H.; Jukola, J.; Vainiotalo, P.; Lemmetyinen, H. Photoinduced Electron Transfer of Double-Bridged Phthalocyanine-Fullerene Dyads. Chem. Phys. Lett., **2006**, 430, 36-40.

(213.) Al-Subi, A. H.; Efimov, A.; Niemi, M.; Tkachenko, N. V.; Lemmetyinen, H. Effect of Anion Coordination on Electron Transfer in Double-Linked Zinc Phthalocyanine-Fullerene Dyad. Chem. Phys. Lett., **2013**, 572, 96-100.

(214.) Cid, J.-J.; Kahnt, A.; Vázquez, P.; Guldi, D. M.; Torres, T. Charge Separation in a Covalently-Linked Phthalocyanine-Oligo(p-phenylenevinylene)-C_{60} System. Influence of the Solvent Polarity. J. Inorg. Biochem., **2012**, 108, 216-224.

(215.) Ince, M.; Martínez-Díaz, M. V.; Barberá, J.; Torres, T. Liquid Crystalline Phthalocyanine-Fullerene Dyads. J. Mater. Chem., **2011**, 21, 1531-1536.

(216.) Bottari, G.; Kahnt, A.; Guldi, D. M.; Torres, T. Protonation-Induced Changes in the Photophysical Properties of a Phthalocyanine and a Covalently-Linked, Phthalocyanine-C_{60} Fullerene Dyad. J. Solid State Science and Tech., **2013**, 2, M3145-M3150.

(217.) Ballesteros, B.; de la Torre, G.; Shearer, A.; Hausmann, A.; Herranz, M. Á.; Guldi, D. M.; Torres, T. Lanthanide(III) Bis(Phthalocyaninato)-[60]Fullerene Dyads: Synthesis, Characterization, and Photophysical Properties. Chem. Eur. J., **2010**, 16, 114-125.

(218.) Ozoemena, K. I.; Mamuru, S. A.; Fukuda, T.; Kobayashi, N.; Nyokong, T. Metal (Co, Fe) Tribenzotetraazachlorin-Fullerene Conjugates: Impact of Direct π-Bonding on the Redox Behaviour and Oxygen Reduction Reaction. Electrochem. Commun., **2009**, 11, 1221-1225.

(219.) Lebedeva, M. A.; Chamberlain, T. W.; Davies, E. S.; Mancel, D.; Thomas, B. E.; Suyetin, M.; Bichoutskaia, E.; Schröder, M.; Khlobystov, A. N. Transition Metal Complexes of a Salen–Fullerene Diad: Redox and Catalytically Active Nanostructures for Delivery of Metals in Nanotubes. Chem. Eur. J., **2013**, 19, 11999-12008.

(220.) Lebedeva, M.A.; Chamberlain, T.W.; Schröder, M.; Khlobystov, A.N. New Pathway for Heterogenization of Molecular Catalysts by Noncovalent Interactions with Carbon Nanoreactors. Chem. Mater., **2014**, 26, 6461-6466.

(221.) Ramírez-Monroy, A.; Swager, T. M. Metal Chelates Based on Isoxazoline[60]fullerenes. Organomet., **2011**, 30, 2464-2467.

(222.) Kalina, O. G.; Bashilov, V. V.; Khodak, A. A.; Tumanskii, B. L. Paramagnetic Metal Chelates of an o-Quinone Derivative of Fullerene with Mn and Re Carbonyls. Russ. Chem. Bull. Int. Ed., **2001**, 50, 566-567.

(223.) Wu, Y.-Y.; Yeh, W.-Y. Synthesis of the Diphosphino_Fullerene 1,2,4,15-$(PPh_2)_2(H)_2C_{60}$ and Its Complexation with Triosmium Carbonyl Clusters. Organomet., **2011**, 30, 4792-4795.

(224.) Chen, C.-H.; Chen, C.-S.; Dai, H.-F.; Yeh, W.-Y. Synthesis of the phosphino–fullerene $PPh_2(o\text{-}C_6H_4)(CH_2NMeCH)C_{60}$ and its function as an η1-P or η3-P,C2 ligand Dalton Trans., **2012**, 41, 3030-3037.

(225.) Chen, C.-H.; Yeh, W.-Y. Re–Re Bond Breaking of $(\mu\text{-H})_3Re_3(CO)_{11}(NCMe)$ upon Reaction with $PPh_2(o\text{-}C_6H_4)(CH_2NMeCH)C_{60}$ to Generates Monorhenium and Dirhenium Phosphino–fullerene Complexes. Dalton Trans., **2013**, 42, 2488-2494.

(226.) Song, L.-C.; Xie, Z.-J.; Liu, X.-F.; Ming, J.-B.; Ge, J.-H.; Zhang, X.-G.; Yan, T.-Y.; Gao, P. Synthetic and Structural Studies on New Diiron Azadithiolate (ADT)-type Model Compounds for Active Site of [FeFe]hydrogenases. Dalton Trans., **2011**, 40, 837-846.

(227.) Liu, Y.-C.; Yen, T.-H.; Tseng, Y.-J.; Hu, C.-H.; Lee, G.-H.; Chiang, M.-H. Electron Delocalization from the Fullerene Attachment to the Diiron Core within the Active-Site Mimics of [FeFe]Hydrogenase Inorg. Chem., **2012**, 51, 5997-5999.

(228.) Guo, F.; Ogawa, K.; Kim, Y.-G.; Danilov, E.O.; Castellano, F.N.; Reynolds, J.R.; Schanze, K.S. A Fulleropyrrolidine End-capped Platinum-Acetylide Triad: the Mechanism of Photoinduced Charge Transfer in Organometallic Photovoltaic Cells. Phys. Chem. Chem. Phys., **2007**, 9, 2724-2734.

(229.) Ventura, B.; Barbieri, A.; Zanelli, A.; Barigelletti, F.; Seneclauze, J.B.; Diring, S.; Ziessel, R. Excited-State Dynamics in a Dyad Comprising Terpyridine-Platinum(II) Ethynylene Linked to Pyrrolidino-[60]Fullerene. Inorg. Chem., **2009**, 48, 6409-6416.

(230.) Feng, K.; Yu, M.-L.; Wang, S.-M.; Wang, G.-X.; Tung, C.-H.; Wu, L.-Z. Photoinduced Triplet–Triplet Energy Transfer in a 2-Ureido-4(1H)-Pyrimidinone-Bridged, Quadruply Hydrogen-Bonded Ferrocene–Fullerene Assembly. ChemPhysChem, **2013**, 14, 198-203.

(231.) Yu, M.-L.; Wang, S.-M.; Feng, K.; Khoury, T.; Crossley, M.J.; Fan, Y.; Zhang, J.-P.; Tung, C.-H.; Wu, L.-Z. Photoinduced Electron Transfer and Charge-Recombination in 2-Ureido-4[1H]-Pyrimidinone Quadruple Hydrogen-Bonded Porphyrin-Fullerene Assemblies. J. Phys. Chem. C, **2011**, 115, 23634-23641.

(232.) Gadde, S.; Islam, D.-M. S.; Wijesinghe, C. A.; Subbaiyan, N. K.; Zandler, M. E.; Araki, Y.; Ito, O.; D'Souza, F. Light-Induced Electron Transfer of a Supramolecular Bis(Zinc Porphyrin)-Fullerene Triad Constructed via a Diacetylamidopyridine/Uracil Hydrogen-Bonding Motif. J. Phys. Chem. C, **2007**, 111, 12500-12503.

(233.) Sessler, J. L.; Jayawickramarajah, J.; Gouloumis, A.; Torres, T.; Guldi, D. M.; Maldonado, S.; Stevenson, K. J. Synthesis and Photophysics of a Porphyrin–fullerene Dyad Assembled through Watson–Crick Hydrogen Bonding. Chem. Commun., **2005**, 1892-1894.

(234.) Torres, T.; Gouloumis, A.; Sanchez-Garcia, D.; Jayawickramarajah, J.; Seitz, W.; Guldi, D. M.; Sessler, J. L. Photophysical Characterization of a Cytidine-guanosine Tethered Phthalocyanine-fullerene Dyad. Chem. Commun., **2007**, 292-294.

(235.) D’Souza, F.; Venukadasula, G. M.; Yamanaka, K.-I.; Subbaiyan, N. K.; Zandler, M. E.; Ito, O. Through-bond Photoinduced Electron Transfer in a Porphyrin-fullerene Conjugate Held by a Hamilton Type Hydrogen Bonding Motif**.** Org. Biomol. Chem., **2009**, 7, 1076-1080.

(236.) Wessendorf, F.; Gnichwitz, J.-F.; Sarova, G. H.; Hager, K.; Hartnagel, U.; Guldi, D. M.; Hirsch, A. Implementation of a Hamiliton-Receptor-Based Hydrogen-Bonding Motif toward a New Electron Donor-Acceptor Prototype: Electron versus Energy Transfer. J. Am. Chem. Soc., **2007**, 129, 16057-16071.

(237.) Wessendorf, F.; Grimm, B.; Guldi, D. M.; Hirsch, A. Pairing Fullerenes and Porphyrins: Supramolecular Wires That Exhibit Charge Transfer Activity. J. Am. Chem. Soc., **2010**, 132, 10786-10795.

(238.) Maurer, K.; Grimm, B.; Wessendorf, F.; Hartnagel, K.; Guldi, D.M.; Hirsch, A. Self-Assembling Depsipeptide Dendrimers and Dendritic Fullerenes with New cis- and trans-Symmetric Hamilton Receptor Functionalized Zn–Porphyrins: Synthesis, Photophysical Properties and Cooperativity Phenomena. Eur. J. Org. Chem., **2010**, 5010-5029.

(239.) Sánchez, L.; Sierra, M.; Martín, N.; Myles, A. J.; Dale, T. J.; Rebek Jr., J.; Seitz, W.; Guldi, D. M. Exceptionally Strong Electronic Communication through Hydrogen Bonds in Porphyrin–C_{60} Pairs Angew. Chem. Int. Ed., **2006**, 45, 4637-4641.

(240.) Calderon, R. M. K.; Valero, J.; Grimm, B.; Mendoza, J.; Guldi, D. M. Enhancing Molecular Recognition in Electron Donor−Acceptor Hybrids via Cooperativity. J. Am. Chem. Soc., **2014**, 136, 11436−11443.

(241.) Araki, Y.; Chitta, R.; Sandanayaka, A. S. D.; Langenwalter, K.; Gadde, S.; Zandler, M. E.; Ito O.; D’Souza, F. Self-Assembled Supramolecular Ferrocene-Fullerene Dyads and Triad: Formation and Photoinduced Electron Transfer. J. Phys. Chem. C, **2008**, 112, 2222-2229.

(242.) Moreira, L.; Calbo, J.; Illescas, B.M.; Aragó, J.; Nierengarten, I.; Delavaux-Nicot, B.; Ortí, E.; Martín, N.; Nierengarten, J.-F. Metal-Atom Impact on the Self-Assembly of Cup-and-Ball Metalloporphyrin–Fullerene Conjugates. Angew. Chem. Int. Ed. **2015**, 54, 1255-1260.

(243.) Sandanayaka, A. S. D.; Araki, Y.; Ito, O.; Chitta, R.; Gadde, S.; D'Souza, F. Electron Transfer Switching in Supramolecular Porphyrin–fullerene Conjugates Held by Alkylammonium Cation-crown Ether Binding. Chem. Commun., **2006**, 4327-4329.

(244.) D'Souza, F.; Wijesinghe, C. A.; El-Khouly, M. E.; Hudson, J.; Niemi, M.; Lemmetyinen, H.; Tkachenko, N. V.; Zandler, M. E.; Fukuzumi, S. Ultrafast Excitation Transfer and Charge Stabilization in a Newly Assembled Photosynthetic Antenna-reaction Center Mimic Composed of Boron Dipyrrin, Zinc Porphyrin and Fullerene. Phys. Chem. Chem. Phys., **2011**, 13, 18168-18178.

(245.) D'Souza, F.; Maligaspe, E.; Sandanayaka, A. S. D.; Subbaiyan, N. K.; Karr, P. A.; Hasobe, T.; Ito, O. Photochemical Charge Separation in Supramolecular Phthalocyanine-Multifullerene Conjugates Assembled by Crown Ether-Alkyl Ammonium Cation Interactions. J. Phys. Chem. A, **2010**, 114, 10951-10959.

(246.) Guldi, D. M.; Ramey, J.; Martínez-Díaz, M.V.; de la Escosura, A.; Torres, T.; Da Ros, T.; Prato, M. Reversible Zinc Phthalocyanine Fullerene Ensembles. Chem. Commun., **2002**, 2774-2275.

(247.) Sasabe, H.; Sandanayaka, A. S. D.; Kihara, N.; Furusho, Y.; Takata, T.; Araki, Y.; Ito, O. Axle Charge Effects on Photoinduced Electron Transfer Processes in Rotaxanes Containing Porphyrin and [60]fullerene. Phys. Chem. Chem. Phys., **2009**, 11, 10908-10915.

(248.) D'Souza, F.; Chitta, R.; Gadde, S.; Rogers, L.M.; Karr, P.A.; Zandler, M.E.; Sandanayaka, A.S.D.; Araki, Y.; Ito, O. Photosynthetic Reaction Center Mimicry of a "Special Pair" Dimer Linked to Electron Acceptors by a Supramolecular Approach: Self-Assembled Cofacial Zinc Porphyrin Dimer Complexed with Fullerene(s). Chem. Eur. J., **2007**, 13, 916-922.

(249.) D'Souza, F.; Chitta, R.; Gadde, S.; Zandler, M.; McCarty, A. L.; Sandanayaka, A. S. D.; Araki, Y.; Ito, O. Effect of Axial Ligation or p–p-Type Interactions on Photochemical Charge Stabilization in "Two-Point"Bound Supramolecular Porphyrin–Fullerene Conjugates. Chem. Eur. J., **2005**, 11, 4416-4428.

(250.) D'Souza, F.; Chitta, R.; Gadde, S.; Zandler, M. E.; Sandanayaka, A. S. D.; Araki, Y.; Ito, O. Supramolecular Porphyrin–fullerene via 'Two-point' Binding Strategy: Axial-coordination and Cation–crown Ether Complexation. Chem. Commun., **2005**, 1279-1281.

(251.) Stranius, K.; Iashin, V.; Nikkonen, T.; Muuronen, M.; Helaja, J.; Tkachenko, N. Effect of Mutual Position of Electron Donor and Acceptor on Photoinduced Electron Transfer in Supramolecular Chlorophyll−Fullerene Dyads J. Phys. Chem. A., **2014**, 118, 1420-1429.

(252.) D’Souza, F.; Maligaspe, E.; Ohkubo, K.; Zandler, M. E.; Subbaiyan, N. K.; Fukuzumi, S. Photosynthetic Reaction Center Mimicry: Low Reorganization Energy Driven Charge Stabilization in Self-Assembled Cofacial Zinc Phthalocyanine Dimer-Fullerene Conjugate. J. Am. Chem. Soc., **2009**, 131, 8787-8797.

(253.) D’Souza, F.; Chitta, R.; Gadde, S.; McCarty, A. L.; Karr, P. A.; Zandler, M. E.; Sandanayaka, A. S. D.; Araki Y.; Ito, O. Design, Syntheses, and Studies of Supramolecular Porphyrin-Fullerene Conjugates, Using Bis-18-crown-6 Appended Porphyrins and Pyridine or Alkyl Ammonium Functionalized Fullerenes. J. Phys. Chem. B, **2006,** 110, 5905-5913.

(254.) Mateo-Alonso, A.; Prato, M. Synthesis of Fullerene-Stoppered Rotaxanes Bearing Ferrocene Groups on the Macrocycle. Eur. J. Org. Chem., **2010**, 1324-1332.

(255.) Rajkumar, G. A.; Sandanayaka, A. S. D.; Ikeshita, K.-I.; Araki, Y.; Furusho, Y.; Takata, T.; Ito, O. Prolongation of the Lifetime of the Charge-Separated State at Low Temperatures in a Photoinduced Electron-Transfer System of [60]Fullerene and Ferrocene Moieties Tethered by Rotaxane Structures. J. Phys. Chem. B, **2006**, 110, 6516-6525.

(256.) Sandanayaka, A. S. D.; Sasabe, H.; Araki, Y.; Kihara, N.; Furusho, Y.; Takata, T.; Ito, O. Photoinduced Electron Transfer Processes in Rotaxanes Containing [60]Fullerene and Ferrocene: Effect of Axle Charge on Light-Induced Molecular Motion. Aust. J. Chem., **2006**, 59, 186-192.

(257.) Watanabe, N.; Kihara, N.; Furusho, Y.; Takata, T.; Araki, Y.; Ito, O. Photoinduced Intrarotaxane Electron Transfer between Zinc Porphyrin and [60]Fullerene in Benzonitrile. Angew. Chem. Int. Ed., **2003**, 42, 681-683.

(258.) Sandanayaka, A. S. D.; Watanabe, N.; Ikeshita, K.-I.; Araki, Y.; Kihara, N.; Furusho, Y.; Ito, O.; Takata, T. Synthesis and Photoinduced Electron Transfer Processes of Rotaxanes Bearing [60]Fullerene and Zinc Porphyrin: Effects of Interlocked Structure and Length of Axle with Porphyrins. J. Phys. Chem. B, **2005**, 109, 2516-2525.

(259.) Sandanayaka, A. S. D.; Sasabe, H.; Araki, Y.; Kihara, N.; Furusho, Y.; Takata, T.; Ito, O. Axle Length Effect on Photoinduced Electron Transfer in Triad Rotaxane with Porphyrin, [60]Fullerene, and Triphenylamine. J. Phys. Chem. A, **2010**, 114, 5242-5250.

(260.) Ding, Z.-J.; Zhang, Y.-M.; Teng, X.; Liu, Y. Controlled Photophysical Behaviors between Dibenzo-24-crown-8 Bearing Terpyridine Moiety and Fullerene-Containing Ammonium Salt. J. Org. Chem., **2011**, 76, 1910-1913.

(261.) Armaroli, N.; Diederich, F.; Dietrich-Buchecker, C.O.; Flamigni, L.; Marconi, G.; Nierengarten, J.-F.; Sauvage, J.-P. A Copper(i)-Complexed Rotaxane with Two Fullerene Stoppers: Synthesis, Electrochemistry, and Photoinduced Processes. Chem. Eur. J., **1998**, 4, 406-416.

(262.) Schuster, D.I.; Li, K.; Guldi, D. M.; Ramey, J. Novel Porphyrin-Fullerene Assemblies: from Rotaxanes to Catenanes. Org. Lett., **2004**, 6, 1919-1922.

(263.) Megiatto Jr., J. D.; Schuster, D. I.; de Miguel, G.; Wolfrum, S.; Guldi, D. M. Topological and Conformational Effects on Electron Transfer Dynamics in Porphyrin-[60]Fullerene Interlocked Systems. Chem. Mater., **2012**, 24, 2472-2485.

(264.) Li, K.; Schuster, D. I.; Guldi, D. M.; Herranz, M. Á.; Echegoyen, L. Convergent Synthesis and Photophysics of [60]Fullerene/Porphyrin-Based Rotaxanes. J. Am. Chem. Soc., **2004**, 126, 3388-3389.

(265.) Li, K.; Bracher, P. J.; Guldi, D. M.; Herranz, M. Á.; Echegoyen, L.; Schuster, D. I. [60]Fullerene-Stoppered Porphyrinorotaxanes: Pronounced Elongation of Charge-Separated-State Lifetimes. J. Am. Chem. Soc., **2004**, 126, 9156-9157.

(266.) Megiatto Jr., J. D.; Schuster, D. I.; Abwandner, S.; de Miguel, G.; Guldi, D. M. [2]Catenanes Decorated with Porphyrin and [60]Fullerene Groups: Design, Convergent Synthesis, and Photoinduced Processes. J. Am. Chem. Soc., **2010**, 132, 3847-3861.

(267.) Jakob, M.; Berg, A.; Levanon, H.; Schuster, D. I.; Megiatto Jr., J. D. Photoinduced Processes in Some Mechanically Interlocked Supramolecules as Studied by Time-Resolved Electron Paramagnetic Resonance. J. Phys. Chem. C, **2011**, 115, 24555-24563.

(268.) McNally, A.; Forster, R. J.; Russell, N. R.; Keyes, T. E. Fullerene bridged Metallocyclodextrin Donor–acceptor Complexes: Optical Spectroscopy and Photophysics. Dalton Trans., **2006**, 1729-1737.

(269.) Liu, Y.; Wang, H.; Liang, P.; Zhang, H.-Y. Water-Soluble Supramolecular Fullerene Assembly Mediated by Metallobridged b-Cyclodextrins. Angew. Chem. Int. Ed., **2004**, 43, 2690-2694.

(270.) Yoshida, A.; Okuyama, T.; Terada, T.; Naito, S. Reversible Hydrogen Storage/Release Phenomena on Lithium Fulleride (Li_nC_{60}) and their Mechanistic Investigation by Solid-state NMR Spectroscopy. J. Mater. Chem., **2011**, 21, 9480-9482.

(271.) Knupfer, M.; Fink, J. Mott-Hubbard-like Behavior of the Energy Gap of A_4C_{60} (A = Na, K, Rb, Cs) and $Na_{10}C_{60}$. Phys. Rev. Lett., **1997**, 79, 2714-2717.

(272.) Stephens, P. W.; Mihaly, L.; Lee, P. L.; Wetten, R. L.; Huang, S.-M.; Kaner, R.; Deiderich, F.; Holczer, K. Structure of Single-phase superconducting K_3C_{60}. Nature, **1991**, 351, 632-633.

(273.) Klupp, G.; Matus, P.; Kamarás, K.; Ganin, A. Y.; McLennan, A.; Rosseinsky, M. J.; Takabayashi, Y.; McDonald, M. T.; Prassides, K. Dynamic Jahn–Teller Effect in the Parent Insulating State of the Molecular Superconductor Cs_3C_{60} Nature Comm., **2012,** 3, 912-914.

(274.) Wiley, J. B.; Huang, S.-M.; Kaner, R. B.; Diederich, F.; Whetten, R. L.; Holczer, K. Structure of Rb:C_{60} compounds. Phys. Rev. B, **1992**, 45, 543-546.

(275.) Heguri, S.; Kobayashi, M. Magnetic Susceptibility of Magnesium Fulleride Mg_4C_{60}. Chem. Phys. Lett., **2010**, 490, 34-37.

(276.) Tanaka, M.; Zhang, S.; Onimaru, T.; Takabatake, T.; Inumaru, K.; Yamanaka, S. Electrical Properties of Ba_3C_{60} Collapsed under High-pressure and High-temperature Conditions. Carbon, **2014**, 73, 125-131.

(277.) Arvanitidis, J.; Papagelis, K.; Margadonna, S.; Prassides, K. Lattice Collapse in Mixed-valence Samarium Fulleride $Sm_{2.75}C_{60}$ at High Pressure. Dalton Trans., **2004**, 3144-3146.

(278.) Shiroka, T.; Riccò, M.; Ligabue, O.; Bolzoni, F.; Concas, G.; Spano, G. Investigation of Eu_6C_{60} Magnetic Properties. J. Magn. Magn. Mater., **2004**, 272-276, 544-545.

(279.) Margadonna, S.; Arvanitidis, J.; Papagelis, K.; Prassides, K. Negative Thermal Expansion in the Mixed Valence Ytterbium Fulleride, $Yb_{2.75}C_{60}$. Chem. Mater., **2005**, 17, 4474-4478.

(280.) Durand, P.; Darling, G. R.; Dubitsky, Y.; Zaopo, A.; Rosseinsky, M. The Mott-Hubbard Insulating State and Orbital Degeneracy in the Superconducting $C_{60}{}^{3-}$Fulleride Family. J. Nature Mater., **2003**, 2, 605-610.

(281.) Margadonna, S.; Prassides, K. Recent Advances in Fullerene Superconductivity. J. Solid State Chem., **2002**, 168, 639-652.

(282.) Mauron, P.; Gaboardi, M.; Remhof, A.; Bliersbach, A.; Sheptyakov, D.; Aramini, M.; Vlahopoulou, G.; Giglio, F.; Pontiroli, D.; Riccò, M.; Züttel, A. Hydrogen Sorption in $Li_{12}C_{60}$. J. Phys. Chem. C, **2013**, 117, 22598-22602.

(283.) Norin, L.; Jansson, U. On the Existence of Transition-Metal Fullerides: Deposition and Characterization of Ti_xC_{60}. Chem. Mater., **1998**, 10, 1184-1190.

(284.) Markin, A. V.; Ruchenin, V. A.; Smirnova, N. N.; Markin, G. V.; Ketkov, S. Yu.; Fagin, A. A. Heat Capacity and Standard Thermodynamic Functions of Bis(η^6-mesitylene)vanadium Fulleride $[(\eta^6\text{-sim-Me}_3H_3C_6)_2V]^{\cdot +}[C_{60}]^{\cdot -}$ over the Range from T = (0 to 345) K. J. Chem. Eng. Data, **2011**, 56, 3100-3105.

(285.) Markin, A. V.; Ruchenin, V. A.; Smirnova, N. N.; Abakumov, G. A.; Markin, G. V.; Shevelev, Yu. A.; Kuropatov, V. A.; Lopatin, M. A.; Cherkasov, V. K.; Domrachev, G. A. Thermodynamic Properties of Bis-(η^6-cumene)chromium Fulleride $[(\eta^6\text{-PhCH}(CH_3)_2)_2Cr]^{\cdot +}[C_{60}]^{\cdot -}$ over the Range from T→(0 to 310) K. J. Chem. Thermodynamics, **2011**, 43, 1495-1499.

(286.) Markin, A. V.; Ruchenin, V. A.; Smirnova, N. N.; Abakumov, G. A.; Markin, G. V.; Shevelev, Yu. A.; Kuropatov, V. A.; Lopatin, M. A.; Cherkasov, V. K.; Domrachev, G. A. Thermodynamic Characteristics of Bis(η^6-ethylbenzene)chromium Fulleride. Rus. J. Phys. Chem. A, **2011**, 85, 1423-1429.

(287.) Ruchenin, V. A.; Markin, A. V.; Smirnova, N. N.; Markin, G. V.; Shevelev, Yu. A.; Kuropatov, V. A.; Lopatin, M. A.; Domrachev, G. A. The Thermodynamic Properties of bis(η^6-Ethoxybenzene)chromium Fulleride from T→ 0 to 340 K. Rus. J. Phys. Chem. A, **2010**, 84, 928-933.

(288.) Markin, A. V.; Ruchenin, V. A.; Smirnova, N. N.; Markin, G. V.; Shevelev, Yu. A.; Kuropatov, V. A.; Domrachev, G. A. The Thermodynamic Properties of Bis(η^6-o-Xylene)chromium(I) Fulleride over the Temperature Range from T→ 0 to 340 K. Rus. J. Phys. Chem. A, **2009**, 83, 1289-1294.

(289.) Markin, G. V.; Shevelev, Yu. A.; Domrachev, G. A.; Kukin, G. K.; Baranov, E. V.; Lopatin, M.A.; Kuropatov, V. A.; Kirillov, A. I.; Shavyrin, A. S.; Kurskii, Yu. A. Synthesis and Properties of Bis(biphenyl)chromium(I) 1,4-Di(2-cyanoisopropyl)-1,4-dihydrofulleride and 1-(2-Cyanoisopropyl)-1,2_Dihydrofullerene. Rus. Chem. Bull. Int. Ed., **2008**, 57, 1970-1974.

(290.) Smirnova, N. N.; Markin, A. V.; Bykova, T. A.; Boronina, I. E.; Domrachev., G. A.; Shevelev, Yu. A.; Markin, G. V. Thermodynamics of Bis-(η^6-diphenyl)chromium (I) Fulleride $[(\eta^6\text{-Ph}_2)_2Cr]^{+}[C_{60}]^{\cdot -}$ in the Range from T→ (0 to 360) K. J. Chem. Thermodynamics, **2006**, 38, 810-816.

(291.) Domrachev, G. A.; Shevelev, Yu. A.; Cherkasov, V. K.; Fukin, G. K.; Markin, G. V.; Kirillov, A. I. Fullerene Complexes with Bis(η^6-hexamethylbenzene)chromium, Hexamethylbenzene, and Hexaethylbenzene. Rus. Chem. Bull. Int. Ed., **2006**, 55, 225-229.

(292.) Hönnerscheid, A.; van Wüllen, L.; Dinnebier, R.; Jansen, M.; Rahmer, J.; Mehring, M. Evidence for C_{60} dimerisation in the fulleride $[Cr(C_9H_{12})_2]^+C_{60}^-$. Phys. Chem. Chem. Phys., **2004**, 6, 2454-2460.

(293.) Hönnerscheid, A.; Dinnebier, R.; Jansen, M. Reversible Dimerization of C_{60} Molecules in the Crystal Structure of the Bis(arene)chromium Fulleride $[Cr(C_7H_8)]_2C_{60}$. Acta Cryst., **2002**, B58, 482-488.

(294.) Hönnerscheid, A.; van Wüllen, L.; Jansen, M.; Rahmer, J.; Mehring, M. Dimer-formation in the Bis(arene)chromium Fulleride $Cr(C_7H_8)_2$ C_{60}. J. Chem. Phys., **2001**, 115, 7161-7165.

(295.) Domrachev, G. A.; Shevelev, Yu. A.; Cherkasov, K. V.; Markin, G. V.; Fukin, G. K.; Khorshev, S. Ya.; Kaverin, B. S.; Karnatchevich, V. L. Formation, Properties, and Thermal Decomposition of Bisarene Chromium(I) and Molybdenum(I) Fullerides. Rus. Chem. Bull. Int. Ed., **2004**, 53, 2056-2059.

(296.) Konarev D. V.; Lyubovskaya, R. N. Magnetic Properties of Fullerene Salts Containing d- and f-Metal Cations (Co^{2+}, Ni^{2+}, Fe^{2+}, Mn^{2+}, Eu^{2+}, Cd^{2+}). Specific Features of the Interaction between $C_{60}^{\bullet-}$ and the Metal Cations. Rus. Chem. Bull. Int. Ed., **2008**, 57, 1944-1954.

(297.) Bulychev, B. M.; Lunin, R. A.; Krechetov, A. V.; Kulbachinskii, V. A.; Kytin, V. G.; Poholok, K. V.; Lips, K.; Rappich, J. Heterometallic fullerides of Fe and Cu groups with the composition K_2MC_{60} (M = Fe^{+2}, Fe^{+3}, Co^{+2}, Ni^{+2}, Cu^{+1}, Cu^{+2}, Ag^{+1}). J. Phys. Chem. Solids, **2004**, 65, 337-342.

(298.) Markin, A. V.; Ruchenin, V. A.; Smirnova, N. N.; Markin, G. V.; Ketkov, S. Yu.; Kuropatov, V. A.; Cherkasov, V. K.; Abakumov, G. A.; Domrachev, G. A. Thermodynamics of the Bis-(η^6-m-xylene)molybdenum Fulleride $[(\eta^6\text{-(m-xylene)})_2Mo]^{\bullet+}[C_{60}]^{\bullet-}$. J. Therm. Anal. Calorim., **2011**, 105, 635-643.

(299.) Aramini, M.; Milanese, C.; Pontiroli, D.; Gaboardi, M.; Girella, A.; Bertoni, G.; Riccò, M. Addition of Transition Metals to Lithium Intercalated Fullerides Enhances Hydrogen Storage Properties. Int. J. Hydrogen Energy, **2014**, 39, 2124-2131.

(300.) Wang, X. L.; Tu, J. P. Characterization and Hydrogen Storage Properties of Pt–C_{60} Compound. Appl. Phys. Lett., **2006**, 89, 064101-1 - 064101-3.

(301.) Gol'dshleger, N. F.; Shul'ga, Yu. M.; Roshchupkina, O. S.; Perov, A. A.; Okotrub, A. V. Reaction of Platinum Fulleride C_{60}Pt with Dihydroanthracene. Rus. J. General Chem., **2001**, 71, 114-118.

(302.) Lyon, J. T.; Andrews, L. Infrared Spectrum of the Au–C_{60} Complex. ChemPhysChem, **2005**, 6, 229-232.

(303.) Mahata, K.; Frischmann, P. D.; Würthner, F. Giant Electroactive M_4L_6 Tetrahedral Host Self-Assembled with Fe(II) Vertices and Perylene Bisimide Dye Edges. J. Am. Chem. Soc., **2013**, 135, 15656-15661.

(304.) Ronson, T. K.; League, A. B.; Gagliardi, L.; Cramer, C, J. Pyrene-Edged $Fe^{II}{}_4L_6$ Cages Adaptively Reconfigure During Guest Binding. J. Am. Chem. Soc., **2014**, 136, 15615−15624.

(305.) Wood, D. M.; Meng, W.; Ronson, T. K.; Stefankiewicz, A. R.; Sanders, J. K. M.; Nitschke, J. R. Guest-Induced Transformation of a Porphyrin-Edged $Fe^{II}{}_4L_6$ Capsule into a $Cu^{I}Fe^{II}{}_2L_4$ Fullerene Receptor. Angew. Chem. Int. Ed. **2015**, 54, 3988–3992.

(306.) Inokuma, Y.; Arai, T.; Fujita, M. Networked Molecular Cages as Crystalline Sponges for Fullerenes and Other Guests. Nature Chem., **2010**, 2, 780-783.

(307.) Matsuzaki, S.; Arai, T.; Ikemoto, K.; Inokuda, Y.; Fujita, M. Networked-Cage Microcrystals for Evaluation of Host−Guest Interactions. J. Am. Chem. Soc., **2014**, 136, 17899−17901.

(308.) Kishi, N.; Li, Z.; Yoza, K.; Akita, M.; Yoshizawa, M. An M_2L_4 Molecular Capsule with an Anthracene Shell: Encapsulation of Large Guests up to 1 nm. J. Am. Chem. Soc., **2011**, 133, 11438-11441.

(309.) Claessens, C.G.; Torres, T. Inclusion of C_{60} fullerene in a M_3L_2 subphthalocyanine cage. Chem. Comm., **2004**, 1298-1299.

(310.) Suzuki, K.; Takao, K.; Sato, S.; Fujita, M. Coronene Nanophase within Coordination Spheres: Increased Solubility of C_{60}. J. Am. Chem. Soc., **2010**, 132, 2544-2545.

(311.) Ikeda, A.; Yoshimura, M.; Udzu, H.; Fukuhara, C.; Shinkai, S. Inclusion of [60]Fullerene in a Homooxacalix[3]arene-Based Dimeric Capsule Cross-Linked by a Pd^{II}-Pyridine Interaction. J. Am. Chem. Soc., **1999**, 121, 4296-4297.

(312.) Sánchez-Molina, I.; Grimm, B.; Calderon, R. M. K.; Claessens, C. G.; Guldi, D. M.; Torres, T. Self-Assembly, Host−Guest Chemistry, and Photophysical Properties of Subphthalocyanine-Based Metallosupramolecular Capsules. J. Am. Chem. Soc., **2013**, 135, 10503-10511.

(313.) Kishi, N.; Akita, M.; Kamiya, M.; Hayashi, S.; Hsu, H.-F.; Yoshizawa, M. Facile Catch and Release of Fullerenes Using a Photoresponsive Molecular Tube. J. Am. Chem. Soc., **2013**, 135, 12976-12979.

(314.) Kishi, N.; Akita, M.; Yoshizawa, M. Selective Host–Guest Interactions of a Transformable Coordination Capsule/Tube with Fullerenes Angew. Chem. Int. Ed., **2014**, 53, 3604-3607.

(315.) Boyd, P. D. W.; Reed, C. A. Fullerene-Porphyrin Constructs. Acc. Chem. Res., **2005**, 38, 235-242.

(316.) Sun, D.; Tham, F. S.; Reed, C. A.; Chaker, L.; Boyd, P. D. W. Supramolecular Fullerene-Porphyrin Chemistry. Fullerene Complexation by Metalated “Jaws Porphyrin” Hosts. J. Am. Chem. Soc., **2002**, 124, 6604-6612.

(317.) Nobukuni, H.; Tani, F.; Shimazaki, Y.; Naruta, Y.; Ohkubo, K.; Nakanishi, T.; Kojima, T.; Fukuzumi, S.; Seki, S. Anisotropic High Electron Mobility and Photodynamics of a Self-Assembled Porphyrin Nanotube Including C_{60} Molecules. J. Phys. Chem. C, **2009**, 113, 19694-19699.

(318.) Song, J.; Aratani, N.; Shinokubo, H.; Osuka, A. A b-to-b 2,5-thienylene-bridged Cyclic Porphyrin Tetramer: its Rational Synthesis and 1 : 2 Binding Mode with C_{60}. Chem. Sci., **2011**, 2, 748-751.

(319.) Kieran, A. L.; Pascu, S. I.; Jarrosson, T.; Sanders, J. K. M. Inclusion of C_{60} into an Adjustable Porphyrin Dimer Generated by Dynamic Disulfide Chemistry. Chem. Commun., **2005**, 1276-1278.

(320.) Tashiro, K.; Aida, T.; Zheng, J.-Y.; Kinbara, K.; Saigo, K.; Sakamoto, S.; Yamaguchi, K. A Cyclic Dimer of Metalloporphyrin Forms a Highly Stable Inclusion Complex with C_{60}. J. Am. Chem. Soc., **1999**, 121, 9477-9478.

(321.) Zheng, J.-Y.; Tashiro, K.; Hirabayashi, Y.; Kinbara, K.; Saigo, K.; Aida, T.; Sakamoto, S.; Yamaguchi, K. Cyclic Dimers of Metalloporphyrins as Tunable Hosts for Fullerenes: A Remarkable Effect of Rhodium(III). Angew. Chem. Int. Ed., **2001**, 40, 1858-1861.

(322.) Shoji, Y.; Tashiro, K.; Aida, T. Selective Extraction of Higher Fullerenes Using Cyclic Dimers of Zinc Porphyrins. J. Am. Chem. Soc., **2004**, 126, 6570-6571.

(323.) Gil-Ramírez, G.; Karlen, S. D.; Shundo, A.; Porfyrakis, K.; Ito, Y.; Briggs, G. A. D.; Morton, J. J. L.; Anderson, H. L. A Cyclic Porphyrin Trimer as a Receptor for Fullerenes. Org. Lett., **2010**, 12, 3544-3547.

(324.) Grimm, B.; Schornbaum, J.; Cardona, C. M.; van Paauwe, J. D.; Boyd, P. D. W.; Guldi, D. M. Enhanced Binding Strengths of Acyclic Porphyrin Hosts with Endohedral Metallofullerenes. Chem. Sci., **2011**, 2, 1530-1537.

(325.) Ohkubo, K.; Kawashimaa, Y.; Fukuzumi, S. Strong Supramolecular Binding of $Li^+@C_{60}$ with Sulfonated meso-Tetraphenylporphyrins and Long-lived Photoinduced Charge Separation. Chem. Commun., **2012**, 48, 4314-4316.

(326.) Tong, L. H.; Wietor, J.-L.; Clegg, W.; Raithby, P. R.; Pascu, S. I.; Sanders, J. K. M. Supramolecular Assemblies of Tripodal Porphyrin Hosts and C_{60}. Chem. Eur. J., **2008**, 14, 3035-3044.

(327.) Kawashima, Y.; Ohkubo, K.; Kentaro, M.; Fukuzumi, S. Electron Transfer in a Supramolecular Complex of Zinc Chlorin Carboxylate Anion with $Li^+@C_{60}$ Affording the Long-Lived Charge-Separated State. J. Phys. Chem. C, **2013**, 117, 21166-21177.

(328.) Lyons, D. M.; Mohanraj, J.; Accorsi, G.; Armaroli, N.; Boyd, P. D. W. A Supramolecular Porphyrin–ferrocene–fullerene Triad. New J. Chem., **2011**, 35, 632-639.

(329.) Ray, A.; Santhosh, K.; Chattopadhyay, S.; Samanta, A.; Bhattacharya, S. Spectroscopic and Theoretical Investigations on Effective and Selective Interaction of Fullerenes C_{60} and C_{70} with a Derivatized Zn-phthalocyanine: Stabilization of Charge-Recombined State by Side-On Approach of C_{70}. J. Phys. Chem. A, **2010**, 114, 5544-5550.

(330.) Ray, A.; Santhosh, K.; Bhattacharya, S. Photophysical and Theoretical Insights on Fullerene/Zincphthalocyanine Supramolecular Interaction in Solution. J. Phys. Chem. B, **2012**, 116, 11979-11998.

(331.) Chen, C.; Zhu, Y.-Z.; Fan, Q.-J.; Song, H.-B.; Zheng, J.-Y. Syntheses of Corrole Derivatives and their Supramolecular Interactions with Fullerenes in Solution and the Solid State. Tetrahedron Lett., **2013**, 54, 4143-4147.

(332.) Konarev, D. V.; Khasanov, S. S.; Lyubovskaya, R. N. Molecular Complex of Fullerene C_{70} with a Trinuclear Coordination Assembly of Manganese(II) Tetraphenylporphyrins with Octaazacryptand. Cryst. Growth & Design, **2010**, 10, 1451-1454.

(333.) Konarev, D. V.; Neretin, I. S.; Slovokhotov, Y. L.; Yudanova, E. I.; Drichko, N. V.; Shul'ga, Y. M.; Tarasov, B. P.; Gumanov, L. L.; Batsanov, A. S.; Howard, J.A.K.; Lyubovskaya, R. N. New Molecular Complexes of Fullerenes C_{60} and C_{70} with Tetraphenylporphyrins [M(tpp)], in which $M=H_2$, Mn, Co, Cu, Zn, and FeCl. Chem. Eur. J., **2001**, 7, 2605-2616.

(334.) Konarev, D. V.; Khasanov, S. S.; Saito, G.; Lyubovskaya, R. N. Design of Molecular and Ionic Complexes of Fullerene C_{60} with Metal(II) Octaethylporphyrins, $M^{II}OEP$ (M = Zn,

---

Co, Fe, and Mn) Containing Coordination M-N(ligand) and M-C(C_{60}^{-}) Bonds. Cryst. Growth & Design, **2009**, 9, 1170-1181.

(335.) Konarev, D. V.; Khasanov, S. S.; Otsuka, A.; Saito, G.; Lyubovskaya, R. N. Formation of Antiferromagnetically Coupled $C_{60}^{\cdot-}$ and Diamagnetic $(C_{70}^{-})_2$ Dimers in Ionic Complexes of Fullerenes with$(MDABCO^{+})_2{\cdot}M^{II}TPP$ (M = Zn, Co, Mn, and Fe) Assemblies. Inorg. Chem., **2007**, 46, 2261-2271.

(336.) Konarev, D. V.; Khasanov, S. S.; Saito, G.; Otsuka, A.; Lyubovskaya, R. N. Ionic and Neutral C_{60} Complexes with Coordination Assemblies of Metal Tetraphenylporphyrins, $M^{II}TPP_2{\cdot}DMP$ (M = Mn, Zn). Coexistence of $(C_{60}^{-})_2$ Dimers Bonded by One and Two Single Bonds in the Same Compound. Inorg. Chem., **2007**, 46, 7601-7609.

(337.) Konarev, D. V.; Khasanov, S. S.; Mukhamadieva, G. R.; Zorina, L. V.; Otsuka, A.; Yamochi, H.; Saito, G.; Lyubovskaya, R. N. Magnetic and Structural Transitions at Dimerization of $C_{60}^{\bullet-}$ in Ionic Fullerene Complexes with Metalloporphyrins: $\{(TMP^{+})_2{\cdot}M^{II}TPP\}{\cdot}(C_{60}^{-})_2{\cdot}(C_6H_4Cl_2)_2{\cdot}(C_6H_5CN)_2$ (M = Zn and Mn). Inorg. Chem., **2010**, 49, 3881-3887.

(338.) Lee, H. M.; Olmstead, M. M.; Gross, G. G.; Balch, A. L. Cocrystallization of Binuclear Iron(III) Porphyrins with C_{60}: Bending of μ-O{Fe^{III}(Octaethylporphyrin)} and the First Structure of the Iron(III) Octaethyloxophlorin Dimer. Cryst. Growth & Design, **2003**, 3, 691-697.

(339.) Konarev, D. V.; Neretin, I. S.; Saito, G.; Slovokhotov, Y. L.; Otsuka, A.; Lyubovskaya, R. N. Multicomponent Ionic Complexes of Cobalt(II) Tetraphenylporphyrin with C_{60} Fullerides - Transition from the σ-Bonded $[(Co^{II}TPP){\cdot}(C_{60}^{-})]$ Anion to Nonbonded Co^{II}TPP and $C_{60}^{\cdot-}$_ Components. Eur. J. Inorg. Chem., **2004**, 1794-1798.

(340.) Konarev, D. V.; Khasanov, S. S.; Otsuka, A.; Saito, G.; Lyubovskaya, R. N. Peculiarities of $C_{60}^{\cdot-}$ Coordination to Cobalt(II) Octaethylporphyrin in Ionic Multicomponent Complexes: Observation of the Reversible Formation of Co-C(C_{60}^{-}) Coordination Bonds. Chem. Eur. J., **2006**, 12, 5225-5230.

(341.) Konarev, D. V.; Khasanov, S. S.; Otsuka, A.; Saito, G.; Lyubovskaya, R. N. Effect of the Co–C(C_{60}^{-}) Bond Formation on Magnetic Properties of the Ionic Complex $\{cryptand[2,2,2]{\cdot}(Na^{+})\}{\cdot}\{Co^{II}TPP{\cdot}(C_{60}^{-})\}{\cdot}(C_6H_4Cl_2)_2$. Dalton Trans., **2009**, 6416-6420.

(342.) Wakahara, T.; D’Angelo, P.; Miyazawa, K.; Nemoto, Y.; Ito, O.; Tanigaki, N.; Bradley, D. D. C.; Anthopoulos, T. D. Fullerene/Cobalt Porphyrin Hybrid Nanosheets with Ambipolar Charge Transporting Characteristics. J. Am. Chem. Soc., **2012**, 134, 7204-7206.

(343.) Bhyrappa, P.; Karunanithi, K. Porphyrin-Fullerene, C_{60}, Cocrystallates: Influence of C_{60} on the Porphyrin Ring Conformation. Inorg. Chem., **2010**, 49, 8389-8400.

(344.) Stevenson, S.; Chancellor, C. J.; Lee, H. M.; Olmstead, M. M.; Balch, A. L. Internal and External Factors in the Structural Organization in Cocrystals of the Mixed-Metal Endohedrals ($GdSc_2N@I_h$-C_{80},$Gd_2ScN@I_h$-C_{80}, and $TbSc_2N@I_h$-C_{80}) and Nickel(II) Octaethylporphyrin. Inorg. Chem., **2008**, 47, 1420-1427.

(345.) Sato, S.; Nikawa, H.; Seki, S.; Wang, L.; Luo, G.; Lu, J.; Haranaka, M.; Tsuchiya, T.; Nagase, S.; Akasaka, T. A Co-Crystal Composed of the Paramagnetic Endohedral Metallofullerene $La@C_{82}$ and a Nickel Porphyrin with High Electron Mobility. Angew. Chem. Int. Ed., **2012**, 51, 1589-1591.

(346.) Yamaguchi, T.; Ishii, N.; Tashiro, K.; Aida, T. Supramolecular Peapods Composed of a Metalloporphyrin Nanotube and Fullerenes. J. Am. Chem. Soc., **2003**, 125, 13934-13935.

(347.) Konarev, D. V.; Khasanov, S. S.; Slovokhotov, Y. L.; Saito, G.; Lyubovskaya, R. N. Neutral and Ionic Complexes of C_{60} with $(ZnOEP)_2{\cdot}BPy$ Coordination Dimers. CrystEngComm, **2008**, 10, 48-53.

(348.) Litvinov, A. L.; Konarev, D. V.; Kovalevsky, A. Y.; Neretin, I. S.; Coppens, P.; Lyubovskaya, R. N. [60]Fullerene Complexes with Supramolecular Zinc Tetraphenylporphyrin Assemblies: Synthesis, Crystal Structures, and Optical Properties. Cryst. Growth & Design, **2005**, 5, 1807-1819.

(349.) Litvinov, A. L.; Konarev, D. V.; Kovalevsky, A. Y.; Coppens, P.; Lyubovskaya, R. N. Synthesis and Crystal Structure of a New Supramolecular Complex: $[(ZnTPP)_2Prz]{\cdot}C_{60}{\cdot}5.34C_7H_8{\cdot}0.66C_6H_5CN$. CrystEngComm, **2003**, 5, 137-139.

(350.) Konarev, D. V.; Litvinov, A. L.; Neretin, I. S.; Drichko, N. V.; Slovokhotov, Y. L.; Lyubovskaya, R. N.; Howard, J. A. K.; Yufit, D. S. Formation of Coordination Porphyrin Pentamers in New Supramolecular Complex of Fullerene: $\{(ZnTPP)_4{\cdot}4\text{-}TPyP\}{\cdot}(C_{60})_2{\cdot}(C_6H_5CN)_{3.5}$. Cryst. Growth & Design, **2004**, 4, 643-646.

(351.) Wang, H.; Qian, K.; Qi, D.; Cao, W.; Wang, K.; Gao, S.; Jiang, J. Co-crystallized Fullerene and a Mixed (Phthalocyaninato)(Porphyrinato) Dysprosium Double-decker SMM. Chem. Sci., **2014**, 5, 3214-3220.

(352.) Konarev, D. V.; Kovalevsky, A. Y.; Li, X.; Neretin, I. S.; Litvinov, A. L.; Drichko, N. V.; Slovokhotov, Y. L.; Coppens, P.; Lyubovskaya, R. N. Synthesis and Structure of Multicomponent Crystals of Fullerenes and Metal Tetraarylporphyrins. Inorg. Chem., **2002**, 41, 3638-3646.

(353.) Dammer, S. J.; Solntsev, P. V.; Sabin, J. R.; Nemykin, V. N. Synthesis, Characterization, and Electron-Transfer Processes in Indium Ferrocenyl-Containing Porphyrins and Their Fullerene Adducts. Inorg. Chem., **2013**, 52, 9496-9510.

(354.) Konarev, D. V.; Khasanov, S. S.; Saito, G.; Lyubovskaya, R. N.; Yoshida, Y.; Otsuka, A. The Interaction of C_{60}, C_{70} , and $C_{60}(CN)_2$ Radical Anions with Cobalt(II) Tetraphenylporphyrin in Solid Multicomponent Complexes. Chem. Eur. J., **2003**, 9, 3837-3848.

(355.) Konarev, D. V.; Zorina, L. V.; Khasanov, S. S.; Lyubovskaya, R. N. Formation of μ^2-Hydroxo-bonded $(MgPc)_2OH^-$ Assemblies and $(C_{60}^-)_2$ Dimers in Ionic Fullerene $\{(MgPc)_2OH^-\}_2\cdot(C_{60}^-)_2\cdot(cation^+)_4$ Complexes. Dalton Trans., **2012**, 41, 9170-9175.

(356.) Konarev, D. V.; Zorina, L. V.; Khasanov, S. S.; Khakimova, E. U.; Lyubovskaya, R. N. Ionic Complexes Simultaneously Containing Fullerene Anions and Coordination Structures of Metal Phthalocyanines with I^- and EtS^- Anions. Rus. Chem. Bull. Int. Ed., **2011**, 60, 1063-1070.

(357.) Konarev, D. V.; Kuzmin, A. V.; Simonov, S. V.; Khasanov, S. S.; Otsuka, A.; Yamochi, H.; Saito, G.; Lyubovskaya, R. N. Ionic Compound Containing Iron Phthalocyanine $(Fe^IPc)^-$ Anions and $(C_{70}^-)_2$ Dimers. Optical and Magnetic Properties of $(Fe^IPc)^-$ in the Solid State. Dalton Trans., **2012**, 41, 13841-13847.

(358.) Konarev, D. V.; Troyanov, S. I.; Kuzmin, A. V.; Nakano, Y.; Khasanov, S. S.; Otsuka, A.; Yamochi, H.; Saito, G.; Lyubovskaya. R. N. Coordination Complexes of Pentamethylcyclopentadienyl Iridium(III) Diiodide with Tin(II) Phthalocyanine and Pentamethylcyclopentadienyl Iridium(II) Halide with Fullerene C_{60}^- Anions. Organometallics, **2015**, 34, 879−889.

(359.) Konarev, D. V.; Khasanov, S. S.; Lyubovskaya, R. N. Fullerene Complexes with Coordination Assemblies of Metalloporphyrins and Metal Phthalocyanines. Coord. Chem. Rev., **2014**, 262, 16-36.

(360.) Konarev, D. V.; Khasanov, S. S.; Lopatin, D. V.; Rodaev, V. V.; Lyubovskaya, R. N. Fullerene Complexes with Divalent Metal Dithiocarbamates: Structures, Magnetic Properties, and Photoconductivity. Rus. Chem. Bull. Int. Ed., **2007**, 56, 2145-2161.

(361.) Konarev, D. V.; Khasanov, S. S.; Kovalevsky, A. Y.; Lopatin, D. V.; Rodaev, V. V.; Saito, G.; Náfrádi, B.; Forró, L.; Lyubovskaya, R. N. Supramolecular Approach to the Synthesis of [60]Fullerene-Metal Dithiocarbamate Complexes, $\{(M^{II}(R_2dtc)_2)_x\cdot L\}\cdot C_{60}$ (M =

Zn, Cd, Hg, Fe, and Mn; x = 1 and 2). The Study of Magnetic Properties and Photoconductivity. Cryst. Growth & Design, **2008**, 8, 1161-1172.

(362.) Konarev, D. V.; Kovalevsky, A. Y.; Khasanov, S. S.; Saito, G.; Lopatin, D. V.; Umrikhin, A. V.; Otsuka, A.; Lyubovskaya, R. N. Synthesis, Crystal Structures, Magnetic Properties and Photoconductivity of C_{60} and C_{70} Complexes with Metal Dialkyldithiocarbamates $M(R_2dtc)_x$, where M = Cu^{II}, Cu^{I}, Ag^{I}, Zn^{II}, Cd^{II}, Hg^{II}, Mn^{II}, Ni^{II}, and Pt^{II}; R = Me, Et, and nPr. Eur. J. Inorg. Chem., **2006**, 1881-1895.

(363.) Konarev, D. V.; Kovalevsky, A. Y.; Lopatin, D. V.; Umrikhin, A. V.; Yudanova, E. I.; Coppens, P.; Lyubovskaya, R. N.; Saito, G. Synthesis, crystal structure and photoconductivity of the first [60]fullerene complex with metal diethyldithiocarbamate: $\{Cu^{II}(dedtc)_2\}_2\cdot C_{60}$. Dalton Trans., **2005**, 1821-1825.

(364.) Konarev, D. V.; Khasanov, S. S.; Otsuka, A.; Yamochi, H.; Saito, G.; Lyubovskaya, R. N. Effect of the Cooling Rate on Dimerization of $C_{60}^{\bullet-}$ in Fullerene Salt $(DMI^+)_2\cdot(C_{60}^{\bullet-})\cdot\{Cd(Et_2NCS_2)_2I^-\}$. Inorg. Chem., **2012**, 51, 3420-3426.

(365.) Konarev, D. V.; Kovalevsky, A. Y.; Otsuka, A.; Saito, G.; Lyubovskaya, R. N. Neutral and Ionic Complexes of C_{60} with Metal Dibenzyldithiocarbamates. Reversible Dimerization of $C_{60}^{\cdot-}$ in Ionic Multicomponent Complex $[Cr^I(C_6H_6)_2^{\cdot+}]\cdot(C_{60}^{\cdot-})\cdot 0.5[Pd(dbdtc)_2]$. Inorg. Chem., **2005**, 44, 9547-9553.

(366.) Konarev, D. V.; Zorina, L. V.; Khasanov, S. S.; Lyubovskaya, R. N. The Formation of 3D Fullerene Packing in Molecular Complexes of C_{60} and C_{70} with Metal Diethyl Dithiophosphates: $[M(dedtp)_2]\cdot[C_{60(70)}]_3$ (M = Ni^{II}, Co^{II}, and $V^{IV}O$). Eur. J. Inorg. Chem., **2013**, 309-314.

(367.) Jian, F.; Wang, J.; Xiao, H.; Zhao, P.; Sun, P.; Huang, L. [60]Fullerene Metal Complexes with Large Effective Two-photon Absorption Cross-section. Dalton Trans., **2010**, 39, 11045-11052.

(368.) Konarev, D. V.; Kuźmin, A. V.; Simonov, S. V.; Khasanov, S. S.; Yudanova, E. I.; Lyubovskaya, R. N. Structure and Properties of Ionic Fullerene Complex $Co^+(dppe)_2\cdot(C_{60}^{\cdot-})\cdot(C_6H_4Cl_2)_2$: Distortion of the Ordered Fullerene Cage of $C_{60}^{\cdot-}$ Radical Anions. Dalton Trans., **2011**, 40, 4453-4458.

(369.) Constable, E. C.; Zhang, G.; Housecroft, C. E.; Zampese, J. A. Bucky-blocks: Templating a Coordination Network with C_{60}. CrystEngComm, **2012**, 14, 1770-1774.

(370.) Hong, J.; Shores, M. P.; Elliott, C. M. Establishment of Structure-Conductivity Relationship for Tris(2,2'-bipyridine) Ruthenium Ionic C_{60} Salts. Inorg. Chem., **2010**, 49, 11378-11385.

(371.) Maruyama, M.; Imoto, K.; König, M.; Guldi, D. M.; Ohkoshi, S.-I.; Nakamura, E.; Matsuo, Y. Selective Synthesis of Co_8S_{15} Cluster in Bowl-Shaped Template of the Pentaaryl[60]fullerene Ligand. J. Am. Chem. Soc., **2013**, 135, 10914-10917.

(372.) Konarev, D. V.; Kovalevsky, A. Y.; Khasanov, S. S.; Saito, G.; Otsuka, A.; Lyubovskaya, R. N. Crystal Structures, EPR Spectra, and Magnetic Properties of a Series of Ionic Multi-Component Complexes $[(TBPDA)_2\cdot(C_{60}^{\cdot-})\cdot(D^+)]$ (D = Cp^*_2Cr, Cp^*_2Co, TDAE). Eur. J. Inorg. Chem., **2005**, 4822-4828.

(373.) Konarev, D. V.; Khasanov, S. S.; Kovalevsky, A. Y.; Saito, G.; Otsuka, A.; Lyubovskaya, R. N. Structural aspects of two-stage dimerization in an ionic C_{60} complex with bis(benzene)chromium: $Cr(C_6H_6)_2\cdot C_{60}\cdot C_6H_4Cl_2$. Dalton Trans., **2006**, 3716-3720.

(374.) Konarev, D. V.; Khasanov, S. S.; Saito, G.; Vorontsov, I. I.; Otsuka, A.; Lyubovskaya, R. N.; Antipin, Y. M. Crystal Structure and Magnetic Properties of an Ionic C_{60} Complex with Decamethylcobaltocene: $(Cp^*_2Co)_2C_{60}(C_6H_4Cl_2, C_6H_5CN)_2$. Singlet-Triplet Transitions in the C_{60}^{2-} Anion. Inorg. Chem., **2003**, 42, 3706-3708.

(375.) Chancellor, C. J.; Olmstead, M. M.; Balch, A. L. Formation of Crystalline Polymers from the Reaction of Amine-Functionalized C_{60} with Silver Salts. Inorg. Chem., **2009**, 48, 1339-1345.